

ACKNOWLEDGEMENTS

The author wishes to express his gratitude to Professor Putcha Venkateswarlu who guided this work to completion and contributed uncountable suggestions, and criticism during the course of the investigation. Thanks are also due to Professor J. Mahanty for his encouragement during the course of this work.

Sincere thanks go to my colleagues and friends M/s A.L. Verma, A.N. Garg, V.N. Sarin and J.P. Srivastava for their help and encouragement.

The author would also like to thank Drs. H.D. Bist, P.A. Narayana, S.D. Pandey and V.S. Tomar for their helpful suggestions.

The author is thankful to the Department of Physics, Indian Institute of Technology, Delhi for permitting the use of their Raman spectrophotometer. The help of Mr. H.K. Sehgal in taking the Raman spectra is gratefully acknowledged.

Thanks are due to Director, Indian Institute of Technology, Kanpur for his interest in this work.

Last but not the least, the author is thankful to his wife, Nirmala for her forbearance and understanding during the tenure of the work.

The typing of thesis by Mr. R.D. Tripathi is highly appreciated.

CONTENTS

			Page
PREFACE			v
CHAPTER	I	Introduction	1
CHAPTER	II	Experimental Details	29
CHAPTER	III	Vibrational Spectra and Molecular Conformation of Trimethylacetone	35
CHAPTER	IV	Vibrational Spectra and Molecular Conformation of 2,2-dimethoxypropane	66
CHAPTER	V	Vibrational Spectra and Rotational Isomerism of 1,1,1-trimethoxyethane	96
CHAPTER	VI	Vibrational Spectra and Rotational Isomerism of Triethylamine	128

PREFACE

The structural determination of simple molecules from their vibrational spectra has been of considerable interest for the past several decades. In recent years, however, these studies have been extended to some relatively more complex molecules. They are mainly helpful in determining the gross structure of the molecule viz. the symmetry of the molecule and the relative orientations of the different groups present in it.

For certain polyatomic molecules different configurations are possible due to the internal rotation of some group about a single bond. Generally trans and gauche configurations are found as the stable ones for the molecules having C-C linkage with $sp^3 - sp^3$ hybridization. However, relatively little is reported in the literature on the structural stability of the molecules having C-N and C-O linkages with $sp^3 - sp^3$ hybridization. It would be interesting to make a systematic study of the molecules with different linkages and see how far the vibrational analysis of these molecules could be helpful in ascertaining their structure.

The purpose of the present study is two fold: firstly to determine the structure of the molecules with C-C and C-O linkages taking into consideration the various factors determining their structural stability. Secondly to see whether a similar approach is adequate in determining the structure of the molecules possessing C-N linkage.

For the present work four molecules with different linkages were chosen and a systematic study of their vibrational spectra was made. To facilitate the analysis, the choice of the molecules was made such that they could be expected to have some order of symmetry. The molecules studied are trimethylacetone, 2,2-dimethoxypropane, 1,1,1-trimethoxyethane and triethylamine. These molecules may be assumed to be derived from acetone, dimethoxymethane, trimethoxymethane and trimethylamine respectively which have been well studied from structural point of view. The point group symmetries and relative orientations of the different groups in them are already well established which further simplifies the vibrational analysis of the molecules presently studied.

Theoretical details regarding the analysis of infrared and Raman spectra are given in Chapter I. The various factors contributing to the structural stability of the molecules are described. The general features of the spectra in liquid, vapour and solid phases and their application in identifying the rotational isomers is discussed. The effect of the variation of temperature and polarity of solvents on the intensity of infrared bands arising from different conformers of the molecule is also discussed.

Experimental techniques for observing the infrared and Raman spectra are given in Chapter II. The procedure for recording the infrared spectra in liquid, vapour and solid phases is discussed. This chapter also deals with the method of observation of the Raman spectrum and determination of Raman depolarization ratios.

Chapter III describes the infrared and Raman spectra obtained for trimethylacetone. On the basis of steric considerations, the structure of the molecule should be the one in which methyl group is staggered with respect to the other three C-C bonds, that is, the molecule should have C_{3v} symmetry. The observed data are found to be consistent with the proposed structure.


Chapter IV deals with the infrared and Raman spectra of 2,2-dimethoxypropane. Four spectroscopically distinct molecular conformations (Trans-Trans (TT), Trans-Gauche (TG), Gauche-Gauche (GG) and Gauche-Gauche' (GG')) and their relative stabilities are discussed. The vibrational data are consistent with the one and the same configuration of the molecule in all the three (liquid, vapour and solid) phases. The analysis of the gaseous infrared band contours favours a GG configuration (C_2 symmetry) in which the two O-CH₃ bonds are twisted in opposite directions by small angles from the bond positions in TT configuration. The analysis also reveals that the molecule is an approximate symmetric top.

In Chapter V the infrared and Raman spectra of 1,1,1-trimethoxyethane molecule is described. This molecule could exist in seven spectroscopically distinguishable configurations. All these forms are discussed from the point of view of structural stability and three low energy conformations (Trans-Gauche-Gauche (TGG), Trans-Gauche-Gauche' (TGG'), and Gauche-Gauche-Gauche (GGG)) are selected on the basis of steric considerations. The data are consistent with the coexistence of two rotational isomers in liquid phase but favour a single configuration in

vapour as well as in solid phase. The vibrational analysis reveals that the form with relatively higher concentration should possess C_3 symmetry (GGG configuration). The presence of rotational isomers is also favoured by the solvent effect and temperature variation studies.

Chapter VI reports the infrared and Raman spectra of triethylamine. The possible configurations for this molecule were predicted assuming that the trans and gauche forms with respect to lone pair of nitrogen atom exist about C-N bonds. Of the seven spectroscopically distinct configurations three (Trans-Gauche-Gauche (TGG), Trans-Gauche-Gauche' (TGG') and Gauche-Gauche-Gauche (GGG)) were considered as the low energy configurations. The liquid and solid phase spectra could be explained by taking into consideration the presence of atleast two rotational isomers. However, in vapour phase it is not clear whether the molecule exists as a mixture of two rotational isomers or assumes a single configuration. The shape of the infrared band contours in vapour phase closely resembles the one expected for TGG' configuration. The presence of rotational isomers is also established by the solvent effect and temperature variation studies in liquid phase.

References are numbered consequently at the end of every Chapter. Figures and Tables are given at the end of each Chapter. The Chapters III - VI have been written in a way suitable for publication, so the repetition of certain statements has become unavoidable.


Kamal Kumar

CHAPTER I

INTRODUCTION

The vibrational spectra of the molecules have been of considerable importance in obtaining information regarding their structure. This is done by assigning various plausible structures to the molecules and then fitting the observed spectrum with the expected ones corresponding to the various configurations. One then sees which of these plausible configurations leads to the best fit of the observed spectrum. The study of infrared or Raman spectrum of a molecule alone may not be very conclusive. Therefore, a combined study of these spectra is always desirable.

The infrared absorption spectra of the molecules arise due to the transitions between the vibrational and rotational energy levels. Its systematic study started with the publication of the infrared spectra of 135 organic compounds in 1905 by Coblentz¹ who showed that the spectra-structure correlations with the infrared spectra were possible. Since then infrared spectrum has been of immense importance in obtaining structural information regarding the molecules.

In Raman effect, the molecules of the sample interact with the photons of the exciting radiation and the scattering of the photons takes place. The energy of the scattered photons may be increased or decreased relative to the exciting photon. This increment is quantized and correspond to the energy difference in the vibrational and rotational energy levels of the molecule.

Although both the infrared and Raman spectra depend on the vibrational and rotational energy levels of the molecule still they are not exactly the same as the selection rules and the relative intensities of the bands may differ in the two cases. For a vibration to be infrared active the dipole moment of the molecule must change during the vibration whereas, for a vibration to be Raman active there must be a change in the "induced" dipole moment resulting from the change in the polarizability of the molecule during the vibration.

As the number and activity of the vibrational modes of a polyatomic molecule are dependent on the symmetry of the molecule, the vibrational spectra are quite helpful in determining the overall symmetry of the molecule. This type of analysis is very helpful in the case of molecules exhibiting rotational isomerism which may exist in several configurations having close energies and are difficult to separate.

Normal Modes of Vibration

For a non-linear molecule there are $3N-6$ fundamental vibrations or normal modes whereas, for linear molecules there are $3N-5$ fundamental vibrations. This is because of the simple reason that for non-linear molecules six coordinates are required to specify the translation and rotation of the molecule (three each for translation and rotation) but for linear molecules only five coordinates are required to specify the translation and rotation (three for translation and two for rotation). In a normal mode of vibration the motion of the atoms is simple harmonic in nature and the frequency with which they vibrate is same. The atoms also vibrate in phase i.e. all the atoms pass through their equilibrium position and attain maximum amplitudes simultaneously in the case of non-degenerate vibrations.

Number of Normal Modes of Vibration

The number of fundamental modes of vibration belonging to various types may be easily calculated² using the following formula and character table

$$N_i = \frac{1}{N_g} \sum_{n_e} n_e \chi_i(R) \quad (1.1)$$

Where N_i is the number of fundamental vibrations of type i , n_e is the number of elements in each class, N_g is the total number of elements in the group and $\chi_i(R)$ denotes the character in the character table for the i type of vibration and operation R . χ is expressed as

$$\chi(R) = (U_R - 2) (1 + 2 \cos \phi) \text{ for proper rotation}$$

and $\chi(R) = (U_R) (-1 + 2 \cos \phi) \text{ for improper rotation}$

Here U_R denotes the number of atoms remaining unchanged by a symmetry operation. ϕ is the angle of rotation for the symmetry operations.

Activity of the normal modes of vibration.

The activity of a normal mode of vibration may be predicted from the character table of the point group to which the molecule belongs.

A vibrational specie is said to be infrared active if one or more of the three components of translation (T_x , T_y , T_z) are listed in the row of that specie in the character table. This is because of the reason that the dipole moment is also a vector and it may be seen that it also transforms by a symmetry operation in the same way as the translation vector. The direction of the listed translation also tells the direction of the change of the dipole moment for that type of vibration. In a

similar way the components of polarizability which change during a vibration are given in the row for Raman active species. The character table for C_{3v} point group is given as an example.

C_{3v}	I	$2C_3(z)$	$3C_2$	
a_1	1	1	1	T_z $\alpha_{xx} + \alpha_{yy}, \alpha_{zz}$
a_2	1	1	-1	R_z
e	2	-1	0	$(T_x, T_y); (\alpha_{xx} - \alpha_{yy}, \alpha_{xy}),$ $(R_x, R_y) (\alpha_{yz}, \alpha_{xz})$

It can be seen from the character table that it is only the a_1 and e vibrations which will be active in the infrared and Raman spectra, whereas the a_2 vibrations will be forbidden in both the spectra.

The mathematical expressions for determining the vibration types which would be infrared or Raman active are given below:

Infrared Activity

The vibration types which are infrared active can be determined² by the following formula

$$N_i(M) = \frac{1}{N_g} \sum n_e \chi_M(R) \chi_i(R) \quad (1.2)$$

where n_e is the number of elements in each class, N_g is the number of elements in the group, $\chi_i(R)$ is the character in the character table for type i vibration, $\chi_M(R)$ is the character of the dipole moment for the

operation R and is given by,

$$\chi_M(R) = \pm 1 + 2 \cos \phi$$

where ϕ is the angle of rotation during operation R. The character $\chi_M(R)$ for a given class is linear combination of the characters of the vibration types of that class. Only those type of vibrations whose characters are contained in $\chi_M(R)$ are infrared active.

Raman Activity

The vibration types which are Raman active can be determined² by the following formula

$$N_i(\alpha) = \frac{1}{N_g} \sum n_e \chi_\alpha(R) \chi_i(R) \quad (1.3)$$

This equation is similar to the equation for calculation of the infrared activity except that here $\chi_M(R)$ has been replaced by $\chi_\alpha(R)$ which is given as

$$\chi_\alpha(R) = 2 \pm 2 \cos \phi + 2 \cos 2 \phi$$

The + and - signs are for proper and improper rotation. Here also $\chi_\alpha(R)$ is a linear combination of the $\chi_i(R)$ values. $N_i(\alpha)$ denotes the number of times the character of the vibration type appears in $\chi_\alpha(R)$. Only those types of vibrations whose characters are contained in $\chi_\alpha(R)$ are Raman active.

Overtone and combination Bands

In addition to the fundamentals the infrared and Raman spectra may contain overtone and combination bands. Generally, these bands are weaker

in intensity than the fundamentals and in Raman spectrum they are very few in number.

The normal mode of vibration is observed both in the infrared and Raman spectra corresponding to the selection rule $\Delta \nu_i = \pm 1$. However, the transitions for which one $\Delta \nu_i > 1$ or for which several $\Delta \nu_i \neq 0$ (overtone and combination bands respectively) may also occur. The overtone and combination bands for which $|\Delta \nu_i| = 2$ or $\sum |\Delta \nu_i| = 2$ are called binary combinations, those for which $|\Delta \nu_i| = 3$ or $\sum |\Delta \nu_i| = 3$ are called ternary combinations; and so on.

A combination band for which the lower state is the ground state is also called a summation band. In case the vibration ν_i is singly excited in the initial (lower) state and a transition takes place to a state in which the vibration $\nu_j (> \nu_i)$ is singly excited, the frequency of infrared absorption or the shift in Raman spectrum is equal to $\nu_j - \nu_i$ and this is called a difference band.

A somewhat different type of difference band is that for which one and the same low frequency vibration is excited in the upper and lower state in addition to some other vibrations in upper state, which is written as $\nu_j + \nu_i - \nu_i$, is also called hot band. Here ν_i is excited by one quantum both in the upper and lower state but ν_j is excited only in the upper state. Due to the coupling of vibrations the band $\nu_j + \nu_i - \nu_i$ will not exactly coincide with ν_j but will be slightly displaced and hence separately observable.

The combination bands which can be infrared or Raman active may be determined by evaluating the direct products of the characters of the

vibration types to which ν_i and ν_j belong. If the character of the product belongs to any of the allowed species the combination is said to be allowed. In case the product does not have the character of any particular specie, it may contain more than one component and hence the reduction formula (1.2) is used where $\chi_M(R)$ is replaced by the character of the direct product and $N_i(M)$ is replaced by $N_i(P)$ (P denoting the product) which is the number of times $\chi_i(R)$ appears in $\chi_P(R)$. If any of the components in which the product reduces is allowed, the combination band is allowed.

The overtones which can be infrared or Raman active may be determined by using separate formulas for non-degenerate or degenerate vibrations. For non-degenerate vibrations the character of the (n-1)th overtone is determined by employing the equation

$$\chi_i^n(R) = [\chi_i(R)]^n \quad (1.4)$$

For doubly degenerate vibrations, the following equation is employed

$$\chi_j^n(R) = \frac{1}{2} [\chi_j^{n-1}(R) \chi_j(R) + \chi_j(R^n)] \quad (1.5)$$

where $\chi_j(R^n)$ is the character corresponding to the operation R performed n times in succession.

Here again the direct product is evaluated to obtain the activity of overtones.

The reduction formula is again employed and if any of the components contained in the product is allowed the overtone is allowed.

Group Frequencies

It has been observed for variety of molecules that a characteristic infrared or Raman band of a group is found to occur at about the same frequency irrespective of the type of the molecule in which the group is present. This constancy of the group frequencies is due to the constancy of the bond force constant in different molecules. The constancy of the force constants holds good so long as the environments in the different molecules are somewhat similar. Small changes in the frequencies could be observed if the environment is changed.

Stretching Vibrations

The stretching vibrations associated with X-H bonds have the highest frequency. Though there is not appreciable difference between the X-H and X-Y bond force constants, the reduced mass of the X-H bond is much lower than the other bonds. The symbol ν is used to denote the stretching vibration frequencies.

Bending Vibrations

The bending vibrations are associated with smaller force constants than stretching vibrations and hence are observed at lower frequencies. Various notations are employed by spectroscopists to denote the bending vibrations: δ for deformation involving change of the bond angle; τ for the twisting frequencies; and γ for out-of-plane deformation frequencies.

Interaction of Vibrations

The vibrations associated with a bond between two atoms with a large mass difference can be treated satisfactorily as a separable group

frequency. In cases when the masses and force constants are approximately the same in the molecule, it is of no use talking of group frequencies. Due to the coupling of vibrations a resonance between two vibrations occurs with the resultant representing the inphase and out-of-phase combinations of the individual vibrations. The frequencies of these coupled vibrations fall both below and above the frequency of the single group. Coupling may also occur between two identical groups in the same molecule. It is not necessary that the atoms have to be very near if coupling is to occur, it could as well be present when the groups are separated by several atoms. It is thus clear that the concept of group frequency is true only when there is least interaction between the characteristic vibration of the given group with other vibrations of the molecule.

Fermi Resonance

It is possible that two vibrational level belonging to two different vibrations have nearly the same energy. This would lead to resonance between vibrations and energy levels will be perturbed. As this was first recognized by Fermi³, it is called as Fermi resonance. This resonance can occur only between vibrations of the same symmetry if their unperturbed frequencies are nearly alike. Due to the resonance the frequency and the intensity of the two bands get perturbed and they appear well separated. For close resonance, the intensity of the bands is approximately equal to the average of the unperturbed intensities. In case the unperturbed frequencies are not very much alike, the resonance may not change the frequency appreciably but intensity of the weaker band may be enhanced.

Effect of Mass

The frequency of the vibration is altered if the changes in the mass distribution in a part of the molecule are made. The effect of the heavy atom on the frequency of vibration is to decrease the frequency. Mass effects are sometimes employed to confirm the assignment of the bands.

Electrical Effects

The frequency is affected by change in the electronic distribution of a bond as the force constant of the bond is altered by this process. The electrical effects could be external or internal in nature. The dielectric constant of a solvent, hydrogen bonding and the crystalline field are the examples of external influences. The internal influences may be due to the electronegativities of nearby groups in the molecule. The electronegativity effects include both resonance and inductive interactions. The band position and its intensity are altered by the electron-donating or electron withdrawing power of the substituents.

Intramolecular and Intermolecular Interactions

The vibrational group frequencies and band intensities are affected by the intramolecular interactions. The important intramolecular interactions are mass effects, electrical effects, hydrogen bonding, symmetry, conjugation, bond angle strain, field effects and vibrational coupling effects. Different structural problems could be studied due the effect of intramolecular interactions on the vibrational frequencies.

The intermolecular interactions usually involve weaker electrical forces than intramolecular interactions with the exception of hydrogen bonding. If hydrogen bonding is present, sometimes new bands are observed which are ascribed to associated molecules. The effect of intermolecular interactions in crystalline state is to influence the structure and the intensities of the absorption bands. The frequencies of vibration may not be greatly affected. The splitting of bands in solid state spectra is observed due to crystal field effects.

Rotational Isomerism

The rotational isomers are possible for a molecule if there is an internal rotation about one or more single bonds in the molecule. The internal rotation results in various conformations which may be of comparable stability. Sometimes, the energy barrier hindering the rotation about the bond is not large and there may be transformation from one form to the other and a dynamic equilibrium is achieved. The barrier heights may be large, comparable or small as compared to kT where k is the Boltzmann factor and T the absolute temperature. If the barrier height is large as compared to kT each configuration may be obtained by ignoring the possibility of other equilibrium configuration. On the other hand when barrier height is comparable with kT , the relative stability of the isomers may change with temperature. In the case where the barrier height is smaller than kT there is no hindered rotation and it corresponds to free rotation. The relative abundance of the conformations is also dependent on the physical environment. Generally, only one conformation having lower energy gets stabilized in the solid phase. However, in some

cases the solid phase may contain even more than one conformation⁴ or even an entirely new (different than the one present in fluid phase) conformation of the molecule⁵.

Solvent Effects

The shifts in the frequencies are observed on passing from one solvent to another. This shift is usually small unless hydrogen bonding is involved. The changes in the frequency could be attributed to the dielectric constant and refractive index of the medium.

The solvent effect studies are, sometimes very helpful in determining the relative polarities of the different conformations of the molecule. The intensity of the more polar form of the molecule decreases considerably in non polar solvents, whereas just the reverse happens in polar solvents^{4,6}.

Effect of Temperature Variation

The intensity of the bands originating from ground state viz. fundamentals, overtone and summation tones is expected to remain constant but the intensity of other bands may vary with the change in temperature. These bands are related with the transitions between the excited states viz. hot or difference bands. The change in the intensity of these bands is proportional to $e^{-\frac{1}{kT}}$ therefore, there is a decrease in their intensity with the lowering of the temperature due to the depopulation of excited states.

In addition to the bands associated with excited states, the bands arising due to the similar type of vibration of different isomers

of a molecule may also show an intensity variation with temperature. It is because of the reason that here also the relative abundance of the isomers is dependent on the temperature function $e^{-\frac{1}{kT}}$.

Intensity of Infrared and Raman Bands

The intensity of IR band is proportional to the square of the transition moment (or change in dipole moment) of the vibration giving rise to that band. In crystalline solids, the band intensity is also dependent on the relative directions of the transition moment and the electric field vector of the incident radiation. The component of the transition moment in the direction of electric vector is equal to the transition moment multiplied by $\cos \phi$ where ϕ is the angle between them. The absorbance is proportional to the square of this quantity.

The intensity of the Raman lines is proportional to the square of the induced dipole moment. The absolute intensity determination of Raman lines is even more difficult than the one in infrared absorption.

Factors governing the structural stability of the molecules

There are various factors which determine the structural stability of the molecules. One of the important factors is the steric considerations according to which no two atoms can approach a distance closer than the sum of their vander Wall radii which greatly limits the number of possible configurations. For oxygenated molecules, however, besides the steric effects the lone pair interactions of the oxygen atoms¹² also play an important role in determining their stable configurations.

of a molecule may also show an intensity variation with temperature. It is because of the reason that here also the relative abundance of the isomers is dependent on the temperature function $e^{-\frac{1}{kT}}$.

Intensity of Infrared and Raman Bands

The intensity of IR band is proportional to the square of the transition moment (or change in dipole moment) of the vibration giving rise to that band. In crystalline solids, the band intensity is also dependent on the relative directions of the transition moment and the electric field vector of the incident radiation. The component of the transition moment in the direction of electric vector is equal to the transition moment multiplied by $\cos \phi$ where ϕ is the angle between them. The absorbance is proportional to the square of this quantity.

The intensity of the Raman lines is proportional to the square of the induced dipole moment. The absolute intensity determination of Raman lines is even more difficult than the one in infrared absorption.

Factors governing the structural stability of the molecules

There are various factors which determine the structural stability of the molecules. One of the important factors is the steric considerations according to which no two atoms can approach a distance closer than the sum of their vander Wall radii which greatly limits the number of possible configurations. For oxygenated molecules, however, besides the steric effects the lone pair interactions of the oxygen atoms¹² also play an important role in determining their stable configurations.

The Infrared Spectra in the Three Phases

The infrared spectra in the three phases viz. liquid, vapour and solid have been studied for a large number of molecules. The intensity of the bands may be different in the three phases but still if the spectra are showing an overall similarity it may be taken as an indication for the constancy of the structure of the molecule. Because of the absence of rotational structure, the spectra in liquid and solution are sharper as compared to the vapour phase. So far as the information is based only on the band frequencies of the spectra, it is not very much important which phase of the compound is studied. Sometimes, however, the study of the vapour and solid phase spectra is very important, especially in the cases when the molecule may assume one or more than one configuration out of the several possible ones.

What follows is a brief discussion of the characteristics and applications of the infrared spectra in vapour and solid phases.

The Vapour Phase

The shape of the bands occurring in vapour spectra is very much dependent upon the distribution of the energy over all rotational levels. If the molecules possess relatively large rotational constants the rotational fine structure is resolved and clearly separated rotational bands may appear. However, for molecules with smaller rotational constants these bands may not be resolved and what the spectrometer would record is only a band envelope. The study of these band shapes is sometimes very helpful in assigning fundamentals and in differentiating among the various configurations of the molecules. In the following discussion, we

shall deal with the band shapes and PR separations as predicted for various molecules. The P and R branches are observed corresponding to the $\Delta J = -1$ and $\Delta J = +1$ transitions respectively and lie on either side of the Q branch ($\Delta J = 0$ transition).

Before going into the details of the calculations we shall first define the various types of molecules and discuss the notations used in the calculations.

The molecules may be divided into four categories depending upon the relative values of the three moments of inertia I_A , I_B and I_C about the three axes passing through the centre of gravity of the molecule. These three moments of inertia are commonly denoted as

$$I_A \leq I_B \leq I_C.$$

- a) Linear molecule : For a linear molecule $I_A = 0$ whereas $I_B = I_C$.
- b) Spherical top molecule : If all the three moments of inertia are equal that is, $I_A = I_B = I_C$ the molecule is referred as spherical top.
- c) Symmetric top molecule : If the two moments of inertia are equal and third is nonzero, the molecule is called symmetric top. Two possibilities exist for such a combination:

$$I_A = I_B < I_C \quad \text{and} \quad I_A < I_B = I_C$$

In the former case the molecule is said to be oblate symmetric top and in the latter prolate symmetric top.

- d) In case all the three moments of inertia are unequal that is,

$$I_A \neq I_B \neq I_C$$

the molecule is said to be asymmetric top.

The molecular parameters required for the calculations are either functions or simple ratios of the rotational constants (the rotational constants are related to moments of inertia by the relations $A = h/(8\pi^2 c I_A)$, $B = h/(8\pi^2 c I_B)$ and $C = h/(8\pi^2 c I_C)$).

The frequently used parameters are K , β , ρ^* and $S(\beta)$. They are defined as

$$K = \frac{(2B - A - C)}{(A - C)}$$

$$\beta = \frac{A}{B} - 1 \text{ for prolate and } \beta = \frac{C}{B} - 1 \text{ for oblate molecules}$$

$$\rho^* = \frac{A - C}{B}$$

The molecule is referred as oblate type for $K = +1$ and for all values of β in the range $-\frac{1}{2} \leq \beta < 0$, whereas it is considered as prolate type for $K = -1$ and for all values of β in the range $0 < \beta < \infty$. The constant ρ^* may have all values between 0 and ∞ for prolate asymmetric top molecules but it can not exceed unity for oblate molecules. The constants ρ^* and β are identical for symmetric top molecules. The parameter $S(\beta)$ is defined as

$$\log S(\beta) = \frac{0.721}{(\beta + 4)^{1.13}} \quad (1.6)$$

The constant $S(\beta)$ may have a fixed value or lie in a specific interval depending upon the type of the molecule.

PR separation of symmetric top molecules: The PQR structure of the bands is governed by two factors: the intensity of the Q branch and the PR separation^{7,8}.

The intensity of the Q branch appears to be closely related to β and the absolute temperature, whereas, the PR separation is apparently dependent on β , B and the absolute temperature.

Gerhard and Dennison⁷ have shown that for parallel bands

$$\frac{I_Q}{L} = \frac{[\log(\sqrt{\beta} + \sqrt{\beta+1}) - \sqrt{\beta/(\beta+1)}]}{\beta \sqrt{\beta/(\beta+1)}}, \beta > 0 \quad (1.7)$$

where I_Q refers to the intensity of the Q branch and L to the total intensity of the band. For parallel bands I_Q reaches a maximum for $\beta = -\frac{1}{2}$. An increase in I_Q is there for the decrease in β in the region $\infty > \beta > 0$. For negative values of β , I_Q increases rapidly and reaches maximum for $\beta = -\frac{1}{2}$. For the two limiting cases $\beta = 0$ (spherical top molecule) and $\beta = \infty$ (linear molecule), I_Q is zero and $1/3$ of the total intensity of the band.

For perpendicular bands the intensity of the Q branch should be of comparable intensity relative to the P and R branches when

$\beta \approx -\frac{1}{2}$. I_Q increases with the increase in β and equals $1/3$ of the total intensity of the band for $\beta = 0$ (there is no distinction between parallel and perpendicular bands for $\beta = 0$). The intensity of the Q branch increases rapidly for positive values of β and all branches become broader with their maxima lower. For very large values of β , the PQR structure of the band disappears and the shape of the band is like gauss error curve.

The second factor determining the total structure of the band is the PR separation. According to Gerhard and Dennison⁷ the PR separation of the parallel bands may be given as

$$\Delta \nu(\text{PR}) = 5 S(\beta) \left(\frac{2BT}{9}\right)^{\frac{1}{2}} \quad (1.8)$$

where T is the absolute temperature and other parameters have been already defined.

It may be seen from the above formula that for $\beta = 0$ the molecule is a spherical top and the PR separation is given as

$$\Delta \nu(\text{PR}) = 10 \left(\frac{BT}{9}\right)^{\frac{1}{2}} \quad (1.9)$$

The parallel and perpendicular bands would not be distinguishable in this case.

For $\beta = \infty$ the molecule is linear and the PR spacing is given as,

$$\Delta \nu(\text{PR}) = 5 \left(\frac{2BT}{9}\right)^{\frac{1}{2}} \text{ cm}^{-1} \quad (1.10)$$

In both the spherical top and linear molecules the PR separation of parallel and perpendicular type bands will be equal. According to Gerhard and Dennison⁷ the PR separation of the perpendicular band is given by the relation

$$\Delta \nu(\text{PR}) = 10 \hat{\chi} \left(\frac{BT}{9}\right)^{\frac{1}{2}} \text{ cm}^{-1} \quad (1.11)$$

where $2\hat{\chi}$ refers to the distance between those points of the envelope where the absorption coefficient of the P and R branches are maximum.

Theoretical band envelopes have been drawn by Gerhard and Demmison⁷ for the values of $\beta = -\frac{1}{2}, -\frac{1}{3}, \frac{1}{2}, 1$ and 4 . It is possible to calculate the PR separation for these values of β from the given figures but for other values an interpolation is to be performed.

Seth-Paul and Dijkstra⁹ have suggested the formula

$$\Delta \nu (\perp \text{PR}) = (\beta + 1)^{\frac{1}{2}} \Delta \nu (\parallel \text{PR}) \quad (1.12)$$

for the range $-\frac{1}{2} \leq \beta \leq 3/4$ and this relation may be used as a substitute for the interpolation technique.

PR separation of asymmetric top molecules: The calculations of Gerhard and Demmison were extended to asymmetric top molecules by Badger and Zumwalt¹⁰. The band envelopes were drawn for different combinations of molecular parameters $\rho^* = \frac{1}{3}, \frac{1}{2}, \frac{3}{4}$ and $\frac{5}{4}$ and $\kappa = -\frac{1}{2}, 0$ and $+\frac{1}{2}$. The PR separations of A, B and C type contours could be calculated by estimating $\hat{\chi}$ values from the figures and then substituting in formula (1.11) for symmetric top molecules. Though this method is quite convenient for large number of molecules, the main difficulty is experienced when the ρ^* and κ values lie beyond the range for which the band envelopes are drawn. Laborious interpolation may be required for calculating the $\hat{\chi}$ values and hence the branch separations. In addition to this for certain molecules $\rho^* > 5/4$ which interferes with the interpolation.

In order to overcome these limitations Seth-Paul and Dijkstra⁹ worked out a procedure and gave the formula

$$\Delta \nu (\text{PR}) = 10 \tilde{\chi} \left(\frac{BT}{9} \right)^{\frac{1}{2}} \text{ cm}^{-1} \quad (1.13)$$

where $\tilde{\chi}$ is either a number, a constant ratio of rotational constants or

a function of molecular parameters and

$$\tilde{B} = \frac{BC}{B+C} \quad \text{for prolate asymmetric top molecules}$$

$$\text{and } \tilde{B} = \frac{AB}{A+B} \quad \text{for oblate asymmetric top molecules}$$

The agreement between the calculated and observed values was quite satisfactory for a large number of molecules.

The branch separation of the parallel bands is given as

$$\Delta \nu(\text{PR}) = 10 \, S(\tilde{\rho}) \left(\frac{\tilde{B}T}{9} \right)^{\frac{1}{2}} \text{ cm}^{-1} \quad (1.14)$$

for $\rho^* \leq 3/4$ and $-1 \leq K \leq +1$.

The B type contours may show two sharp Q branches separated by a central minimum for certain values of ρ^* . The central gap is due to the reason that the selection rules do not allow Q branch to appear near the the centre of the band. Theoretical calculation of the band envelopes show that the separation between the two Q branches increases with the increase in the value of ρ^* . When ρ^* approaches unity there is no clear PQR structure due to the overlapping of the P and R branches, the decrease in the intensity of Q branch and the simultaneous broadening of all branches. From an analysis of several observed $\Delta \nu(\text{QQ})$ values of oblate molecules Seth-Paul and De Meyer¹¹ gave the following relation

$$\Delta \nu(\text{QQ}) = \frac{1}{3} \rho^* S_B \sqrt{2} \quad \text{for } \frac{1}{3} < \rho^* \leq \frac{1}{2} \quad (1.15)$$

$$\text{and } \Delta \nu(\text{QQ}) = \frac{2}{3} \rho^{*2} S_B \sqrt{2} \quad \text{for } \rho^* \geq \frac{1}{2} \quad (1.16)$$

where S_B is the calculated PR separation of the corresponding type B (\perp) band.

Marked differences are sometimes observed between the expected and observed PR spacings. Various factors may be responsible for such a behaviour viz. change of rotational constants in going from the ground to the excited state, varying coriolis coupling constants, dipole moment not changing parallel to one axis of inertia thus giving rise to hybrid bands.

Seth-Paul and De Meyer¹² found a better agreement between the expected and observed PR spacings by using the formula

$$\Delta \nu(\text{PR}) \text{ type } \alpha\beta = \left[(\tilde{\chi} \text{tg } \alpha + 1) / (\text{tg } \alpha + 1) \right] S_\alpha \text{ cm}^{-1} \quad (1.17)$$

where S_α denotes the PR spacing for pure α type band, α being the angle between the direction of the oscillating dipole and the major (α) axis of inertia with respect to the other (β) axis $\tilde{\chi}$ is either a number, a constant ratio or a function of several molecular constants depending on the value of K and p^* .

For simplicity it would be assumed that the change of electric vector is parallel to the bonds for symmetrical stretching modes and normal to this direction for asymmetrical stretching modes and similarly for symmetrical and asymmetrical deformation modes. For instance in $X - \text{CH}_3$ group, the dipole is assumed to oscillate parallel to $C - X$ bond for the $\nu(\text{CX})$, $\nu_{\text{sym}}(\text{CH}_3)$ and $\delta_{\text{sym}}(\text{CH}_3)$ modes. On the other hand, the dipole moment change is taken perpendicular to this direction for $\nu_{\text{asym}}(\text{CH}_3)$ and $\delta_{\text{asym}}(\text{CH}_3)$ modes.

The hybrid bands are very commonly observed in the spectra of molecules possessing C_s symmetry.

The Solid Phase

The solid state spectrum may be quite different from the fluid phase spectra. The changes in the crystalline spectra may be due to following causes:

- a) The removal of degeneracy : The degenerate bands may split in the crystalline phase due to the reduction of the molecular symmetry at the lattice site. This type of splitting is called site group splitting.
- b) Resonance Interaction : No site group splitting occurs for non-degenerate vibrations. However, these vibrations may split due to the resonance interaction between inequivalent molecules in the unit cell. This splitting known as factor group splitting may always be small in magnitude. This fact is borne out experimentally as the modes generally show either less than the expected number of components or, in many cases, do not show any resolvable splitting.
- c) Lattice Vibrations : The crystalline spectra may show some new bands. These new bands called lattice vibrations are associated with the crystal field and are not directly concerned with the internal modes of the molecules. They arise due to the motion of the molecules relative to one another in a crystal. The lattice vibrations usually occur at much lower frequencies ($< 650 \text{ cm}^{-1}$) as compared to intramolecular vibrations (motion of the atoms within a molecule). In addition to the lattice vibrations the combination of the fundamental frequencies and

crystal lattice frequencies may also appear in the crystalline phase.

d) The changes due to rotational isomerism : The solid state spectra may sometimes be much simpler than the fluid phase spectra if different isomers are present in the fluid phase as only one conformation with lower energy gets stabilized in the solid state.

e) The change in force constants : In addition to the change in the number of observed bands, the shift in the frequencies is also observed which means that there is a change in the force constants when the temperature is lowered.

In liquid and vapour phases the interaction of radiation takes place with the normal modes of the molecule whereas, in solid state it is the normal modes of the unit cell which interact with the radiation. The normal modes of a unit cell consist of the normal modes of the individual molecules present in the cell. These normal modes would be in as many different phases as the number of molecules per unit cell.

The Assignment of Bands

The assignment of the observed infrared and Raman spectra is somewhat difficult especially in the complex molecules where many bands may appear due to the large number of fundamental modes of vibration. Several techniques are employed in order to assign the spectra viz. selection rules, polarization data, vapour phase band contours, isotope effect. These techniques are discussed in the following text.

a) Selection rules : The selection rules, which are responsible for the appearance or nonappearance of a band in the vibrational

spectrum of a molecule, are very useful in the cases where the activity of the modes is different in the infrared and Raman spectra. If the point group symmetry of the molecule is already known, the number of infrared and Raman active vibrations could be easily calculated.

b) Vapour phase infrared band contours : The shape of the infrared band contours is sometimes very helpful in making vibrational assignments. If the symmetry of the molecule and its moments of inertia are known, the band shapes and PR separations are predicted. These predicted values are then compared with the experimental values.

c) Depolarization ratios : In Raman effect the scattered light is observed at right angles to the direction of the incident beam which may be polarized or unpolarized.

The direction of the induced dipole moment P always coincides with the direction of the electric vector E producing it for the molecules whose polarizability ellipsoid is a sphere irrespective of whether the incident light is polarized or not. However, for the cases where the polarizability ellipsoid is not a sphere, the direction of E and P will coincide only when E is in the direction of one of the axes of the polarizability ellipsoid. If the sample containing such molecules with all orientations is irradiated, the direction of P is not restricted to the plane at right angles to the beam, even though it cannot take all orientations with respect to it with equal probability.

It may be shown that any vibration which is antisymmetric or degenerate with respect to any other symmetry element should give rise to Raman line with the maximum degree of depolarization ($\rho = 6/7$ or $3/4$)

depending upon whether the incident light is unpolarized or linearly polarized respectively).

The degree of depolarization ρ is defined as $\rho = \frac{I_{\perp}}{I_{\parallel}}$ where I_{\perp} is the intensity of the scattered light polarized perpendicular to the xy plane (the plane containing the direction of observation) and I_{\parallel} is the intensity of the light polarized parallel to this plane. The direction of propagation of incident radiation being the z axis.

Born¹³ has shown, by averaging over all directions of the polarizability ellipsoid, that the depolarization ratio for the natural incident light is given by the relation

$$\rho_n = \frac{I_{\perp}}{I_{\parallel}} = \frac{6(\alpha^a)^2}{45(\alpha^s)^2 + 7(\alpha^a)^2} \quad (1.18)$$

where α^s and α^a are the isotropic and completely anisotropic part of the polarizability respectively.

The equation (1.18) is true for the Rayleigh scattering and for Raman scattering under identical conditions the depolarization ratio is given as

$$\rho_n = \frac{6(\alpha^{a'})^2}{45(\alpha^{s'})^2 + 7(\alpha^{a'})^2} \quad (1.19)$$

the primes representing the derivatives.

The maximum value of equation (1.19) is 6/7 which is obtained when $\alpha^{s'} = 0$. A Raman line is said to be depolarized if the depolarization ratio is 6/7. It is only the Raman lines arising due to totally

symmetric vibrations which can have a degree of depolarization lower than the maximum value.

If the incident light is linearly polarized the depolarization ratio ρ_i is related¹⁴ to ρ_n as

$$\rho_i = \frac{\rho_n}{2 - \rho_n} \quad (1.20)$$

The maximum value in this case is $3/4$, so the totally symmetric vibrations should have a degree of depolarization less than $3/4$ and thus may be distinguished from others.

d) Isotope effect : The shift in the frequencies by altering the mass is useful in the assignment of bands. The larger the difference in mass the greater will be the shift in the frequencies. The deuterium substitution is very commonly employed to identify the bands associated with hydrogen atoms.

REFERENCES

1. W.W. Coblentz, "Investigations of Infrared Spectra", Part I: Infrared Absorption Spectra, Carnegie Institute Publications (Bull. No. 35), Washington, D.C., 1905.
2. A.G. Meister, F.F. Cleveland and M.J. Murray, Am. J. Phys., 11, 239 (1943).
3. E. Fermi, Z. Physik., 71, 250 (1931).
4. P. Klaeboe, D. Jones, and E.R. Lippincott, Spectrochim. Acta, 23, 2957 (1967).
5. H. Lee and J.K. Wilmshurst, Spectrochim. Acta, 23, 347 (1967).
6. G.A. Crowder and B.R. Cook, J. Mol. Spectry., 25, 133 (1968).
7. S.L. Gerhard and D.M. Dennison, Phys. Rev., 43, 197 (1933).
8. E. Teller, Handb. Jahrb. Chem. Phys., 9, 43 (1934).
9. W.A. Seth-Paul and G. Dijkstra, Spectrochim. Acta, 23, 2861 (1967).
10. R.M. Badger and L.R. Zumwalt, J. Chem. Phys., 6, 711 (1938).
11. W.A. Seth-Paul and H. De Meyer, Spectrochim. Acta, 25, 1671 (1969).
12. W.A. Seth-Paul and H. De Meyer, J. Mol. Struct., 3, 11 (1969).
13. M. Born, "Optik", Edwards Brothers, Ann Arbor, Michigan, 1943.
14. G. Herzberg, "Infrared and Raman Spectra of Polyatomic Molecules", Van Nostrand, New York, 1945.

GENERAL REFERENCES

1. M. Davies, "Infrared Spectroscopy and Molecular Structure", Elsevier (1963).
2. S.I. Mizushima, "Structure of Molecules and Internal Rotation", Academic Press (1959).
3. G.M. Barrow, "Introduction to Molecular Spectroscopy", McGraw-Hill (1962).
4. J.H. Hibben, "The Raman Effect and its Chemical Applications" Reinhold (1939).
5. S. Bhagvantam, "Scattering of Light and Raman Effect" Chemical Publishing Co. (1942).
6. E.B. Wilson, J.C. Decius and P.C. Cross, "Molecular Vibrations", McGraw-Hill (1955).
7. L.I. Maklakov, V.N. Nikitin and A.V. Purkins, Optics and Spectroscopy, 15, 178 (1963).
8. T.S. Hermann and S.R. Harvey, Appl. Spectry., 23, 435 (1969).
9. T.S. Hermann, S.R. Harvey and C.N. Honts, Appl. Spectry., 23, 451 (1969).
10. T.S. Hermann, Appl. Spectry., 23, 461 (1969).
11. M.Ito and T. Shigeoka, Spectrochim. Acta, 22, 1029 (1966).
12. N.B. Colthup, L.H. Daly and S.E. Wiberley "Introduction to Infrared and Raman Spectroscopy" Academic Press, New York (1964)

CHAPTER II

EXPERIMENTAL DETAILS

The infrared spectra were recorded in the region $4000\text{--}250\text{ cm}^{-1}$ with the help of Perkin-Elmer model 521 spectrophotometer which uses the optical null principle with two diffraction gratings as the dispersing means. The first grating is used in the first and second orders, whereas the second grating is used only in first order, the other orders being suppressed by employing interference filters. The source of infrared radiation is a Nerst glower. The instrument has a resolution of 0.3 cm^{-1} at 1000 cm^{-1} and automatically records the infrared transmittance of the sample as a function of frequency of the incident radiation. The abscissa and ordinate of the chart papers are linear in cm^{-1} and % transmittance (0 - 100) respectively.

For recording high resolution spectra the slit was kept as narrow as possible and the amplifier gain was increased to compensate for the loss in power at the detector. Scanning rate was also considerably slowed down as compared to the survey runs.

The infrared spectra of pure liquids and solutions were studied employing fixed cells of thickness .025 and 0.5 mm fitted with CsBr windows. The liquid was also sometimes, studied by sandwiching a small quantity of it between two CsBr plates. When the spectra of the solutions were studied, the solution was kept in the sample cell and

the solvent in the reference cell, in order to compensate for the absorption due to the solvent molecules in the solution. However, if the concentration of the solution is high the compensation is not exact and some information due to the overlapping of the bands is lost. Solvents such as carbon tetrachloride, chloroform, acetone and carbon disulphide were employed.

Gas cells of 2,5 and 10 cm path lengths fitted with CsBr windows were employed to study the gas phase infrared spectra of the molecules. Most of the spectra were recorded at room temperature but a few weak bands were studied at elevated temperatures as well (the temperature of the cell was raised by using heating tape). Wherever found necessary the pressure of the gas was lowered than the saturated vapour pressure at room temperature.

The spectra of solids were recorded by depositing a thin film of the solid on a CsBr plate cooled by conduction from liquid nitrogen reservoir and put in a cell (Fig. 2.1) fitted with CsBr windows. The cell used was of Wagner-Hornig type¹. The deposited film was allowed to anneal in the infrared beam and the spectra were recorded when the peaks reached their maximum sharpness.

The instrument was calibrated against the standard lines of CO_2 , H_2O , HCl and Indene. The frequencies for calibration were taken from the references (2) and (3). The band positions for the sharp bands could be located to an accuracy of 2 cm^{-1} . However, for the broad bands the uncertainty may be as large as $\pm 10 \text{ cm}^{-1}$.

The Raman spectra of the liquid were recorded photoelectrically with a Coderg model PH-1 Raman spectrophotometer equipped with a Spectra-Physics Model 125 He-Ne 50 mw laser with output at 6328 Å. The instrument employs two monochromators having 600 and 300 mm focal lengths latter acting as a filter to get rid of stray light and eliminate ghosts. The plane grating has a ruling of 1200 lines/mm, blazed at 7500 Å. The maximum resolution of the instrument is $.5 \text{ cm}^{-1}$.

The Raman depolarization data were determined employing a half wave plate in the path of the incident radiation. This half wave plate was used to rotate the plane of polarization of the incident light. Band intensity ratios were measured using incident light polarized parallel and perpendicular to the slit which is taken vertical. This could be affected by rotation of the half wave plate by 45° . Intensity ratios were obtained by comparing the relative band areas. The measured intensity ratio R is not simply equal to depolarization ratio ρ_s but is a function of f and is given by the relation⁴

$$R = \rho_s [(1+f)/(f+\rho_s)]$$

where f is defined as the ratio of the efficiency of monochromator and detector system for horizontally polarized light to that for vertically polarized light. This ratio can be easily measured and for the limiting value of $f = 1$, it has the value $R = .86$.

It has been found that accurate depolarization ratios are not obtained using coaxial or right angle laser excitation from samples contained in multipass capillary cells. This is mainly due to the fact

that the inherent directional polarization of the laser beam becomes disoriented when reflected from the walls of the tube. Therefore, theoretical band ratios cannot be expected and only qualitative data can be obtained.

All the Raman spectra were recorded employing a sample holder having a volume of 1 cc. The slit width and the photomultiplier voltage were varied for various recordings.

The calibration of the instrument was checked against the known lines of CCl_4 , C_6H_6 and $(\text{CH}_3)_2\text{CO}$ and the observed frequencies were corrected. The Raman frequencies should be accurate to $\pm 2 \text{ cm}^{-1}$ for reasonably sharp peaks.

REFERENCES

1. E.L. Wagner and D.F. Hornig, J. Chem. Phys., 18, 296 (1950).
2. IUPAC "Tables of wave numbers for the calibration of infrared spectrometers", Butterworth, London (1961).
3. R.N. Jones, N.B.W. Jonathan, M.A. Mackenzie and A. Nadeau, Spectrochim. Acta, 17, 77 (1961).
4. H.H. Claassen, H. Selig and J. Shamir, Appl. Spectry., 23, 8 (1969).

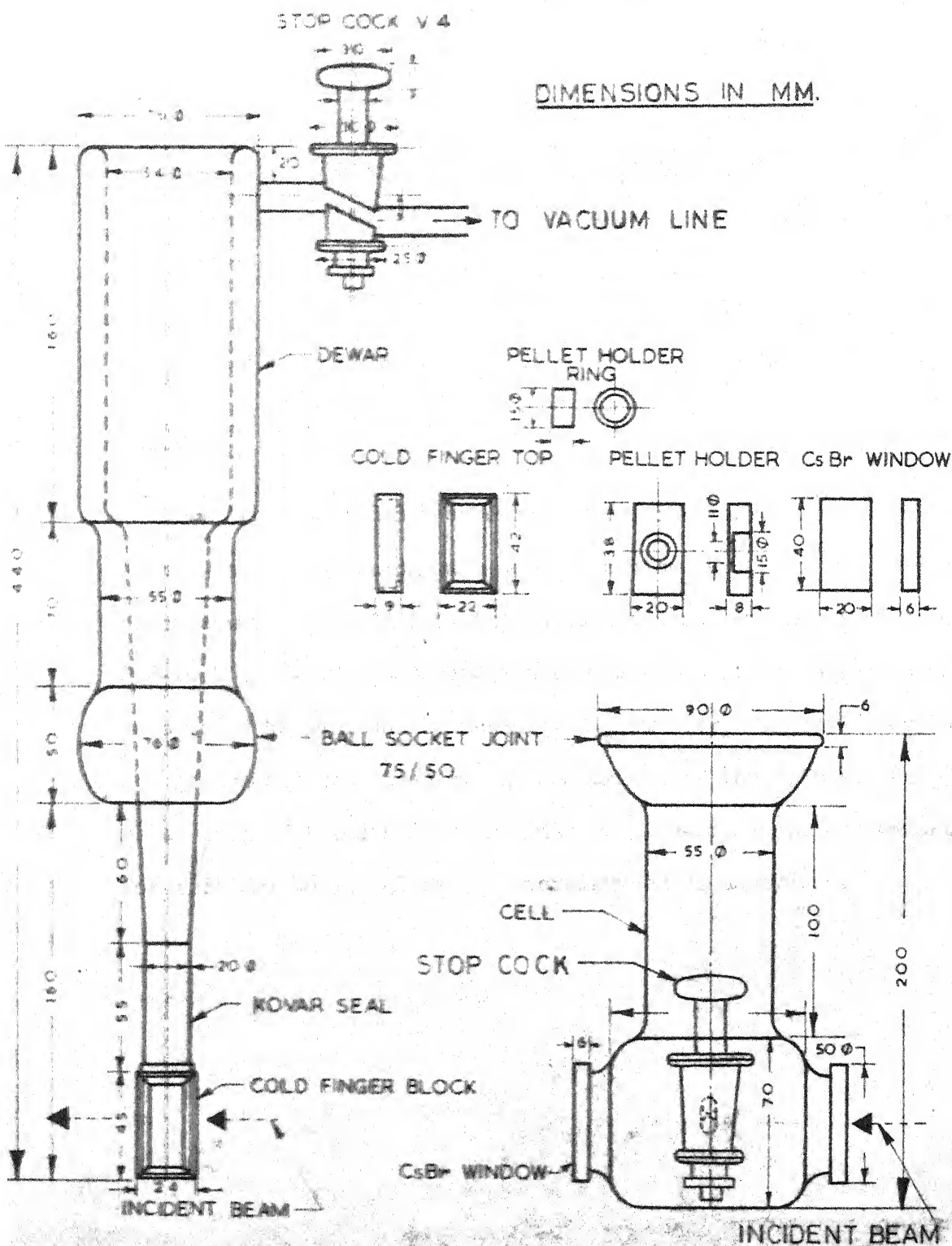


Fig. 2-1 LOW TEMPERATURE CELL

CHAPTER III

VIBRATIONAL SPECTRA AND MOLECULAR
CONFORMATION OF TRIMETHYLACETONITRILE

ABSTRACT

The laser-Raman spectrum of trimethylacetone in liquid state was obtained along with depolarization data, and the infrared spectra were recorded both in liquid and vapour phases in the region 250-4000 cm^{-1} . A satisfactory interpretation of the experimental data could be achieved by assuming C_{3v} symmetry for the molecule. The assignment was aided by the comparison of the infrared and Raman data of trimethylacetone with the data and assignments for tertiary butyl halides and tertiary butyl acetylene.

INTRODUCTION

The trimethylacetone nitrile (TMA) molecule has been of considerable interest from the structural point of view. Livingston and Rao¹ determined the structural parameters by electron diffraction technique assuming C_{3v} symmetry for the molecule. Lide and coworkers² studied the microwave spectra of four isotopic species of TMA and determined the parameters involving heavy atom skeleton. Reliable structural information may be found from the microwave data. However, it is difficult from the microwave data to distinguish between the C_{3v} and C_3 symmetries which are the probable ones for this molecule. The vibrational spectrum has been of considerable importance in the structural assessment of $(CH_3)_3CX$ ($X = F, Cl, Br$ and I) type of molecules^{3,4}. So it was felt that the study of the vibrational spectrum would throw some more light on the structure of this molecule. The vibrational spectrum of this molecule has so far not been extensively studied except that a few infrared bands have been reported in the literature^{5,7}. In the present investigation, the infrared spectra in the liquid and vapour phases and the laser-Raman spectrum in liquid phase are reported and the results are discussed.

EXPERIMENTAL

The sample used for recording the infrared and Raman spectra was commercially obtained and was distilled before use.

The infrared spectrum of the liquid was studied in a cell having fixed spacer .025 mm thick. The spectrum in the vapour phase was

recorded using 5 cm and 10 cm gas cells at room and elevated temperatures. The infrared spectrum of the liquid is shown in Fig. 3.1 and that of the vapour in Fig. 3.2.

The Raman spectrum of liquid was recorded at room temperature and is shown in Fig. 3.3.

The results are listed in Table 3.2 together with the vibrational frequency assignments.

DISCUSSION

The possibility of the internal rotation of CH_3 groups about each of the three C-C bonds allows several configurations for the TMA molecule. However, the restriction that only staggered conformation about C-C bond is possible, permits only one configuration for this molecule in which the methyl group is staggered with respect to the other three C-C bonds (Fig. 3.4). This configuration of the molecule possesses C_{3v} point group symmetry. Under this symmetry it has, $9a_1$ species, $13e$ species and $4a_2$ species. The a_1 and e vibrations are active both in infrared and Raman spectra while the a_2 vibrations are inactive in both the spectra. The type a_1 modes give rise to parallel type bands in the infrared spectrum and polarized lines in the Raman spectrum. The e type modes give rise to depolarized lines in the Raman spectrum and perpendicular type bands in the infrared absorption. The fundamental vibrations of TMA molecule are described in Table 3.1.

The moments of inertia of TMA have been calculated to be $I_a = 110.0$ a.m.u. - \AA^2 and $I_b = I_c = 185.8$ a.m.u. - \AA^2 by taking $d_{\text{C-C}} = 1.536 \text{ \AA}$,

$d_{C-C} = 1.478 \text{ \AA}$, $d_{C \equiv N} = 1.159 \text{ \AA}$ and all angles tetrahedral. Using these values of I_a and I_b the β value and PR separations for parallel and perpendicular bands were calculated^{8,9}. They were found to be $\beta = .689$, $\Delta \nu (\parallel PR) \approx 17 \text{ cm}^{-1}$ and $\Delta \nu (\perp PR) \approx 19 \text{ cm}^{-1}$. The parallel bands are, therefore, expected to have strong and sharp Q branch with P and R branches on either side separated by about 17 cm^{-1} . While the perpendicular bands are expected to show strong but broad Q branch with P and R branches appearing as shoulders with a separation of about 19 cm^{-1} .

The frequencies of the fundamentals are given in Table 3.3

A close examination of the bands shows that the band contours are essentially of two kinds; (1) Bands that show a strong and sharp Q branch with broad P and R branches. These bands have been designated as parallel type, (2) The bands with a strong but broad Q branch and weaker humps or peaks on either side which correspond to the P and R branches. These bands are of perpendicular type. Some bands show only broad maxima without any structure.

Of the 22 active fundamental modes of vibration of TMA 14 are due to the three CH_3 groups present in the molecule. Ten of these methyl group vibrations are the well known internal vibrations of methyl group, the remaining four are of external type. The eight remaining vibrations are concerned with the heavy atom skeleton and are called skeletal vibrations.

To proceed with the assignment of bands, we shall first dispose of the bands due to internal vibrations of methyl group. There are several

bands in the region $2900-3000\text{ cm}^{-1}$ in which the CH stretching vibrations are expected to fall. Some of these bands may be due to the overtones of the bending vibrations and hence a detailed and unambiguous assignment of fundamentals is not possible for the CH stretching modes. Lide and coworkers³ assigned the bands at 3010 and 2985 cm^{-1} to the three degenerate and two non-degenerate vibrations respectively in the infrared spectrum of tertiary butyl fluoride. A similar type of assignment was made by them for other t-butyl halides as well. However, the assignment of the CH stretching modes by Evans and Lo is somewhat different for t-butyl chloride⁴. The two e type vibrations of t-butyl chloride have been assigned at 2993 and 2981 cm^{-1} , whereas the third one is placed at 2937 cm^{-1} . The a_1 modes are assigned to the 2981 and 2937 cm^{-1} bands. The assignment by Evans and Lo seem to be more reasonable and accurate and we shall assign the CH stretching modes of TMA accordingly. The liquid phase spectrum shows two bands at 2980 and 2940 cm^{-1} and the corresponding bands in vapour phase ir appear to show perpendicular and parallel type shapes respectively. Very near to the Q branch of perpendicular type band, there is a sharp peak at 2991 cm^{-1} . It is quite probable that the two e modes are not resolved in liquid state but split up in vapour phase. We shall therefore assign the two modes ν_{14} and ν_{15} in vapour phase at 2991 and 2987 cm^{-1} respectively and in the liquid to the same band at 2980 cm^{-1} . The corresponding Raman band is observed at 2988 cm^{-1} and is depolarized. The above assignments leave three modes unassigned. Two of them are of a_1 type and the third one is of e type. One of these modes ν_1 has been placed at 2948 and 2933 cm^{-1} in infrared and Raman spectrum respectively. There are two more strong infrared bands

at 2922 and 2888 cm^{-1} which need attention. The corresponding Raman bands are observed at 2912 and 2878 cm^{-1} and are of medium and weak intensity respectively. Both of these Raman bands are polarized. These two bands are believed to arise due to Fermi resonance of $\nu_{\text{sym.CH}_3}$ with $(\delta_{\text{asym.CH}_3} + \delta_{\text{sym.CH}_3})$. The intensity of the infrared bands suggests that the two bands arise due to nearly equal contribution from the fundamental ν_2 and the summation tone $\nu_4 + \nu_5$. However, Raman data gives an indication that the higher frequency component is mainly due to $\nu_{\text{sym.CH}_3}$ as the intensity of this component is higher than the low frequency one. The higher frequency component in both the spectra has therefore, been assigned to $\nu_{\text{sym.CH}_3}$ vibrations ν_2 and ν_{16} .

It has been observed in t-butyl halides³ that the $\delta_{\text{sym.CH}_3}$ shows no splitting due to coupling of vibrations, whereas the $\delta_{\text{asym.CH}_3}$ splits up because of the coupling of modes. However, a splitting of a_1 and e modes was found for isobutane by Evans and Bernstein¹⁰. The higher frequency component of the pair of bands at 1371 and 1394 cm^{-1} was assigned to the a_1 mode of the $\delta_{\text{sym.CH}_3}$ and the lower one to the e species of $\delta_{\text{sym.CH}_3}$. We have observed four infrared bands in the region of CH_3 deformation modes. Two of these bands at 1486 and 1468 cm^{-1} are clearly due to the $\delta_{\text{asym.CH}_3}$ vibrations. The infrared band contour reveals that the band at 1468 cm^{-1} is of perpendicular type. No Raman counterpart is available for the 1486 cm^{-1} infrared band but a depolarized band is observed at 1466 cm^{-1} corresponding to the 1468 cm^{-1} infrared band. The assignment is then straight forward and the bands at 1486 and 1468 cm^{-1} have been assigned to the ν_4 and, ν_{18} and ν_{17}

respectively. The Raman spectrum shows one more band at 1455 cm^{-1} adjoining to 1466 cm^{-1} band. This may be due to one of the modes ν_{17} and ν_{18} which are probably overlapping in infrared but split up in Raman spectrum. In the region of the symmetric CH_3 deformation, two bands are seen at 1405 and 1376 cm^{-1} . The P branch of the 1405 cm^{-1} band is probably overlapped by the R branch of 1376 cm^{-1} band. The infrared band contours are of parallel and perpendicular type for 1405 and 1376 cm^{-1} bands respectively and suggest them to be assigned to ν_5 and ν_{19} respectively. The assignments are further aided by analogy with Isobutane¹⁰. No Raman bands could be observed for both of these bands. Contrary to the observation in t-butyl halides, the $\delta_{\text{sym. CH}_3}$ vibration shows a splitting indicating that there is enough coupling to separate the a_1 and e modes of vibration.

There are two strong infrared bands at 1212 and 1245 cm^{-1} in the liquid phase spectrum. The band at 1245 cm^{-1} splits into two components at 1251 and 1257 cm^{-1} in the vapour spectrum. Corresponding to the liquid state bands two Raman bands are observed at 1209 and 1245 cm^{-1} . The one at 1209 cm^{-1} is depolarized but 1245 cm^{-1} band seems to be polarized. The infrared band contours seem to be of perpendicular and parallel type for the 1216 and 1251 cm^{-1} vapour phase bands. The assignment of 1216 cm^{-1} band to the asymmetric C-CH_3 stretching vibration ν_{20} is quite straight forward and there seems to be no ambiguity regarding this assignment. The C-CH_3 stretching mode for TMA is at somewhat higher frequency as compared to the t-butyl halides where the corresponding mode is found in the range $1100 - 1150\text{ cm}^{-1}$ ³. The assignment of the

1251 and 1257 cm^{-1} bands is somewhat ambiguous. Sheppard¹¹ assigned the band at 1245 cm^{-1} in the Raman spectrum of t-butyl acetylene to the symmetric C-C \equiv stretching mode. His assignment was based on the results of calculations of Sutherland and Simpson¹² who showed that the pair of frequencies at 1250 and 1200 cm^{-1} are probably due to C-C stretching modes of vibration. The possibility of placing CH_3 rocking mode at 1245 cm^{-1} was also discussed. The results of t-butyl halides also favour the above assignment as no CH_3 rocking modes were assigned in that region. We, therefore, place the C-C \equiv stretching mode ν_6 at 1251 cm^{-1} . The adjacent band at 1257 cm^{-1} arises probably due to Fermi resonance between the fundamental $\nu_{\text{C-C}\equiv}$ and the combination $2\nu_{26} + \nu_7$. The symmetric C-C stretching vibration ν_8 called as the breathing frequency of the C_5 skeletal has been attributed to the parallel type infrared band at 685 cm^{-1} and very strong polarized Raman band at 686 cm^{-1} . The above assignment is analogous to the t-butyl acetylene where the corresponding mode has been placed at 690 cm^{-1} in the Raman spectrum¹¹. This vibration is again at somewhat lower frequency than the corresponding mode in t-butyl halides where the similar mode is found in the range of 750-820 cm^{-1} ³. We thus see that the splitting between the skeletal asymmetric and symmetric stretching vibrations is much larger in TMA than the separation between the corresponding modes in t-butyl halides.

The methyl rocking modes may interact with the skeletal modes of the same symmetry specie, making an exact assignment of the three active vibrations somewhat difficult. What follows is an approximate

description of these vibrations. The Raman spectrum in the liquid phase shows three bands at 1032 (vw), 940 (m) and 873 (m) cm^{-1} which may correspond to the three rocking modes. As the Raman bands at 1032 and 940 cm^{-1} are depolarized and their infrared counterparts at 1038 and 937 cm^{-1} respectively seem to be perpendicular type in nature, they have been selected for the ρ_{CH_3} modes ν_{21} and ν_{22} respectively. The remaining Raman band at 873 cm^{-1} (highly polarized) and the 876 cm^{-1} parallel type infrared band may be assigned to the vibration ν_7 . However, the assignment of 876 cm^{-1} band is somewhat ambiguous and may be reversed with the 1251 cm^{-1} band assignment as pointed out earlier.

The four skeletal bending modes are yet to be assigned. By analogy with t-butyl fluoride, three out of these four vibrations may fall in the region 330-470 cm^{-1} . However, only two bands are observed in the infrared and Raman spectra of liquid. The vapour phase spectrum shows a band with Q branch at 365 cm^{-1} which probably corresponds to the 378 cm^{-1} liquid state band. The other liquid state band at 361 cm^{-1} is probably overlapped by the P branch of the 365 cm^{-1} band. The Raman bands at 366 and 378 cm^{-1} are depolarized and polarized respectively. As only two bands are observed and three modes have to be assigned, it may be thought that the two degenerate modes $\rho_{\text{C}_3\text{C}}$ and δ_{ccc} are overlapped as these vibrations are of somewhat similar nature. We, therefore, assign the $\rho_{\text{C}_3\text{C}}$ and δ_{ccc} modes to 361 cm^{-1} infrared and 366 cm^{-1} Raman bands respectively. The symmetric δ_{ccc} mode may then be placed at 378 cm^{-1} in the liquid infrared and Raman spectra. By looking at t-butyl halides we find that the assignment of asymmetric

and symmetric bending modes is reversed for TMA, as symmetric mode is assigned at higher frequency than the asymmetric one. However, a similar type of behaviour was found for isobutane, where the asymmetric and symmetric bending modes were assigned at 367 and 426 cm^{-1} respectively¹⁰. Lucier and coworkers⁷ have assigned the δ_{ccc} vibration at 573 cm^{-1} in liquid phase. But this assignment does not seem to be very reasonable as the frequency is quite high for the δ_{ccc} modes. By looking at t-butyl halides³ we see that in no case it was found higher than about 460 cm^{-1} , the highest bending frequency being of t-butyl fluoride at 461 cm^{-1} .

The depolarized Raman band at 195 cm^{-1} (very strong) must be ascribed to some skeletal bending vibration as no other vibration could give rise to such a strong band in this region. Moller *et al.*⁶ reported an infrared band at 183 cm^{-1} describing it as skeletal vibration of specie e. The only possible assignment for this band is C-C \equiv N bending mode ν_{26} .

The assignment of the C \equiv N stretching vibration ν_3 at 2249 and 2240 cm^{-1} infrared and Raman bands respectively is very definite as the origin of such a band is characteristic of nitriles.

All other bands could be satisfactorily interpreted as combinations or overtones of the fundamentals discussed above. Their assignments have been included in Table 3.2 and will not be discussed here in detail except for the band at 1142 cm^{-1} in the infrared spectrum. The Raman band corresponding to this infrared band is not available which favours its assignment as the summation tone as they are usually not observed in

the Raman spectrum. Its assignment as a summation tone is further aided by the fact that a summation tone must be observed corresponding to the difference tone at 765 cm^{-1} ($\nu_{22} - \nu_{26}$). An alternate explanation for this band would have been that it arises due to the CH_3 rocking vibration (ν_{12}) when the symmetry of the molecule is C_3 and not C_{3v} (the a_2 species become active under C_3 symmetry). This explanation does not seem to be very reasonable as none of the structurally similar $(\text{CH}_3)_3 \text{CX}$ ($X = \text{F}, \text{Cl}, \text{Br}$ and I) type molecules needed any explanation on the basis of C_3 symmetry. Furthermore, the explanation of the band as a summation tone is quite satisfactory and hence the need of interpreting the band on the basis of lower symmetry C_3 does not arise.

As all the infrared and Raman bands could be satisfactorily explained on the basis of C_{3v} symmetry, the proposed structure of the molecule seems to be the correct one, that is, the molecule possesses a structure in which the methyl group is staggered with respect to the other three C-C bonds. The projections of the trimethylacetone on the planes containing the ab and bc inertial axes are shown in Fig. 3.5.

REFERENCES

1. R.L. Livingston and C.N.R. Rao, J. Amer. Chem. Soc., 81, 3584 (1959).
2. L.J. Nugent, D.E. Mann and D.R. Lide, JR., J. Chem. Phys., 36, 965 (1962).
3. D.E. Mann, N. Acquista and D.R. Lide, JR., J. Mol. Spectry., 2, 575 (1958).
4. J.C. Evans and G.Y.S.Lo. , J. Am. Chem. Soc., 88, 2118 (1966).
5. E. Augdahl and P. Klaboe, Spectrochim. Acta, 19, 1665 (1963).
6. K.D. Moller, A.R. De Meo, D.R. Smith and L.H. London, J. Chem. Phys., 47, 2609 (1967).
7. T.J. Lucier, E.C. Tuazon and F.F. Bentley, Spectrochim. Acta, 24, 771 (1968).
8. S.L. Gerhard and D.M. Dennison, Phys. Rev., 43, 197 (1933).
9. W.A. Seth-Paul and G. Dijkstra, Spectrochim. Acta, 23, 2861 (1967).
10. J.C. Evans and H.J. Bernstein, Can. J. Chem., 33, 1792 (1955).
11. N. Sheppard, J. Chem. Phys., 17, 455 (1949).
12. G.B.B.M. Sutherland and D.M. Simpson, J. Chem. Phys., 15, 153 (1947).

TABLE 3.1

Description, Symmetry and Activity of the Normal Modes*
of Trimethylacetonitrile Molecule Under Point Group C_{3v} .

Approximate description	a_1 (ir and Raman active)	a_2 (ir and Raman inactive)	e (ir and Raman active)
C-H asym. st.	ν_1	ν_{10}	ν_{14}, ν_{15}
C-H sym. st.	ν_2		ν_{16}
C \equiv N st.	ν_3		
CH ₃ asym. def.	ν_4	ν_{11}	ν_{17}, ν_{18}
CH ₃ sym. def.	ν_5		ν_{19}
C-C \equiv st.	ν_6		
CH ₃ rock.	ν_7	ν_{12}	ν_{21}, ν_{22}
C-C st.	ν_8		ν_{20}
< CCC def.	ν_9		ν_{23}
C ₃ C rock.			ν_{24}
CH ₃ tors.		ν_{13}	ν_{25}
C-C \equiv N bend.			ν_{26}

Abbreviations : st. = stretching, def. = deformation, rock. = rocking,
tors. = torsion, bend. = bending, sym. = symmetric,
asym. = asymmetric.

*The notation system of Herzberg was adopted (G. Herzberg,

"Infrared and Raman Spectra of Polyatomic Molecules", D. Van Nostrand,
New York (1945)).

TABLE 3.2

Observed Infrared and Raman Spectra of Trimethylacetoneitrile

Infrared			Raman effect					
Vapour			Liquid		in liquid			Assignment
(cm ⁻¹)	Int.	Type	(cm ⁻¹)	Int.	(cm ⁻¹)	Int.	Depol.	
1	2	3	4	5	6	7	8	9
					195	vs	dp	ν_{26}
355	w	⊥	361	w	366	w	dp	ν_{23}, ν_{24}
365			378	m	378	w	p?	ν_9
376								
597	vw		573	vw	585	vw	p?	3x ν_{26}
676	m							ν_8
685			687	m	686	vs	p	
694								
765	w		773	w	760	vw	p	$\nu_{22} - \nu_{26}$
865	vw							ν_7
876			873	w	873	m	p	
887								
926	w	⊥						ν_{22}
937			938	m	940	m	dp	
948								
1026	vw	⊥						ν_{21}
1038			1037	w	1032	vw	dp	
1049								
1142	vw		1148	w				$\nu_{22}^+ \nu_{26}$
1204	s	⊥						ν_{20}
1216			1212	s	1209	m	dp	
1223								

Contd.

Table 3.2 (contd.)

1	2	3	4	5	6	7	8	9
1244								
1251	s	11	1245	s	1245	vw	p	\checkmark_6
1257	s							$2x \checkmark_{26} + \checkmark_7 (F.R.)$
1265								
1367								
1376	s	17	1372	s				\checkmark_{19}
1386								
1405	m	11	1403	m				\checkmark_5
1415								
1456								
1468	s	L	1464	s	1455	m	dp	$\checkmark_{17}, \checkmark_{18}$
1477					1466			
1486	s	11	1480	s				\checkmark_4
1495								
			1627	vw				$\checkmark_8 + \checkmark_{22}$
			1722	vw				$\checkmark_{19} + \checkmark_{23}$
1807	vw		1802	vw				$\checkmark_8 + \checkmark_{22} + \checkmark_{26}$
1898	vw		1894	vw				$\checkmark_8 + \checkmark_{20}$
			1972	vw				$\checkmark_{21} + \checkmark_{22}$
			2186	vw				$\checkmark_{21} + \checkmark_{22} + \checkmark_{26}$
2249	w	?	2236	s	2240	m	p	\checkmark_3
2258								
2307	vw		2307	vw				$\checkmark_{19} + \checkmark_{22}$
2406	vw		2406	vw				$\checkmark_{17} + \checkmark_{22}$
	vw		2423	vw				$\checkmark_4 + \checkmark_{22}$
	vw		2477	vw				$\checkmark_{17} + \checkmark_{21}$

Contd.

Table 3.2 (contd.)

1	2	3	4	5	6	7	8	9
2587	vw		2574	vw				$\checkmark_{19} + \checkmark_{20}$
2616	vw		2610	vw				$\checkmark_{18} + \checkmark_{22} + \checkmark_{26}$
2738	vw		2730	vw	2728	vw	p	$2x \checkmark_{19}$
			2761	vw				$\checkmark_5 + \checkmark_{19}$
2799	sh		2798	sh	2795	vw	p	$\checkmark_{19} + \checkmark_{20} + \checkmark_{26}$
2817	sh		2813	sh				$2x \checkmark_5$
2837	sh		2832	sh				$\checkmark_{18} + \checkmark_{19}$
2870								
2888	s	11?	2878	s	2878	w	p	$\checkmark_4 + \checkmark_5$ (F.R.)
2898								
					2893	w	p	$\checkmark_4 + \checkmark_{21} + \checkmark_{23}$
2914								
2922	s	11?	2913	s	2912	m	p	$\checkmark_2, \checkmark_{16}$
2933								
2942								
2948	s	11?	2940	s	2933	m	p	\checkmark_1
2960								
					2960	w	p	$2x \checkmark_4$
2981								
2987	vs	1	2980	vs	2988	m	dp	$\checkmark_{14}, \checkmark_{15}$
2991	s							
3000								
3121	w		3106	w				$\checkmark_3 + \checkmark_8 + \checkmark_{26}$
3200	w		3190	vw				$\checkmark_9 + \checkmark_{18} + \checkmark_{19}$
3242	w		3242	w				$\checkmark_4 + \checkmark_9 + \checkmark_{19}$

Contd.

Table 3.2 (contd.)

1	2	3	4	5	6	7	8	9
3350	w		3345	w				$\nu_9 + \nu_{21} + \nu_{22}$
			3475	w				$\nu_4 + \nu_{21} + \nu_{22}$
			3780	vw				$\nu_4 + \nu_6 + \nu_{21}$

Abbreviations : w = weak, m = medium, s = strong, vw = very weak,

vs = very strong, sh = shoulder, p = polarized,

dp = depolarized, F.R. = Fermi Resonance.

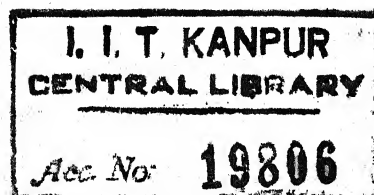


TABLE 3.3

Fundamentals of Trimethylacetonitrile

Species	Type	ir work		Raman effect in liquid (cm ⁻¹)
		Liquid (cm ⁻¹)	Vapour (cm ⁻¹)	
1	2	3	4	5
a ₁	ν_1	2940	2948	2933
	ν_2	2913	2922	2912
	ν_3	2236	2249	2240
	ν_4	1480	1486	
	ν_5	1403	1405	
	ν_6	1245	1251	1245
	ν_7	873	876	873
	ν_8	687	685	686
	ν_9	378	365	378
a ₂	ν_{10}	-	-	-
	ν_{11}	-	-	-
	ν_{12}	-	-	-
	ν_{13}	-	-	-

contd.

table 3.3 (contd.)

1	2	3	4	5
	✓ 14	2980	2991	2988
	✓ 15	2980	2987	2988
	✓ 16	2913	2922	2912
	✓ 17	1464	1468	1466
	✓ 18	1464	1468	1455
	✓ 19	1372	1376	
e	✓ 20	1212	1216	1209
	✓ 21	1037	1038	1032
	✓ 22	938	937	940
	✓ 23	361	355	366
	✓ 24	361	355	366
	✓ 25			
	✓ 26			195

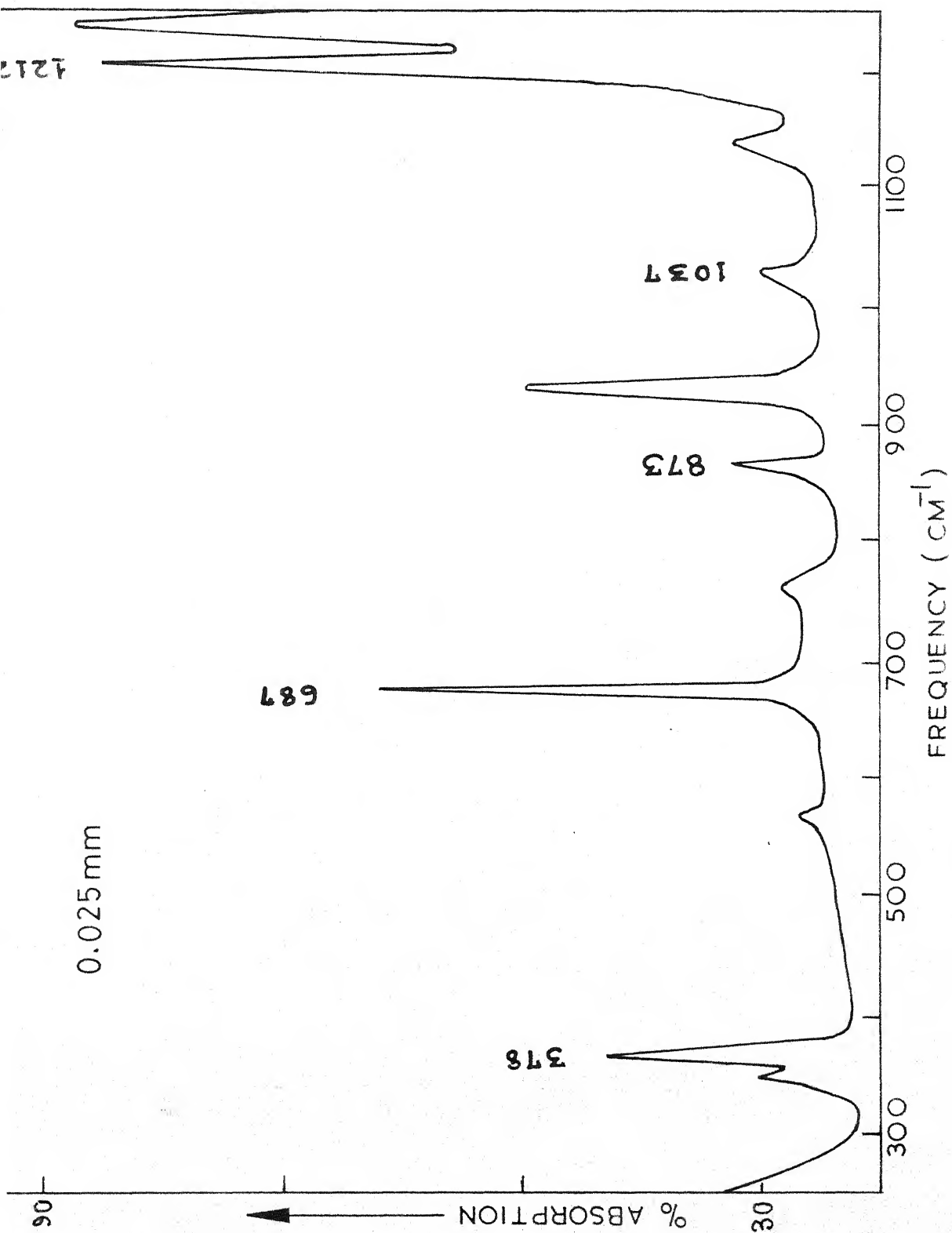
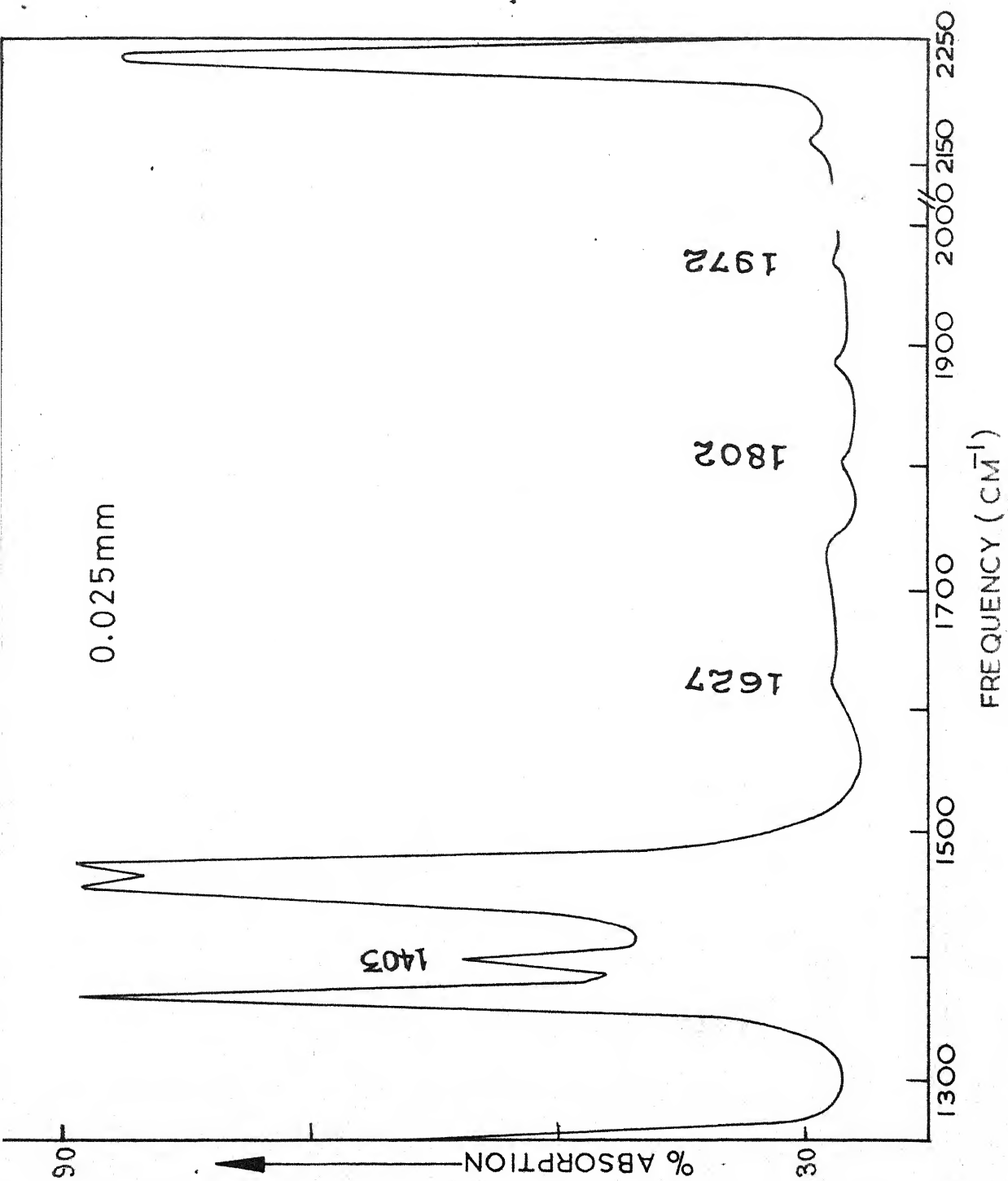
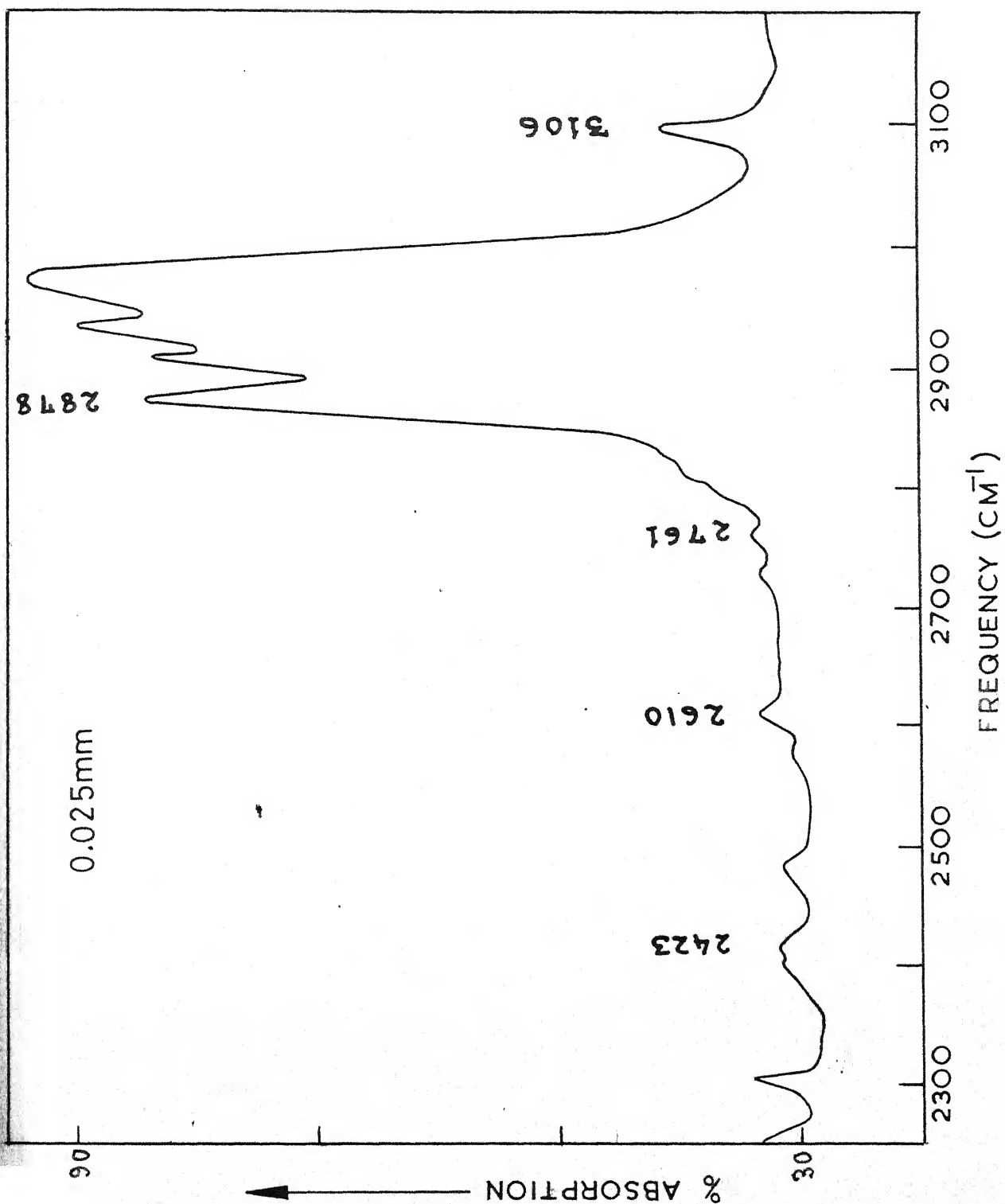


Fig. 3.1(a). The infrared spectrum of liquid trimethylacetone nitrile in the region 250-1200 cm^{-1} .





0.025mm

3242

3475

3780

3200

3400

3600

3800

4000

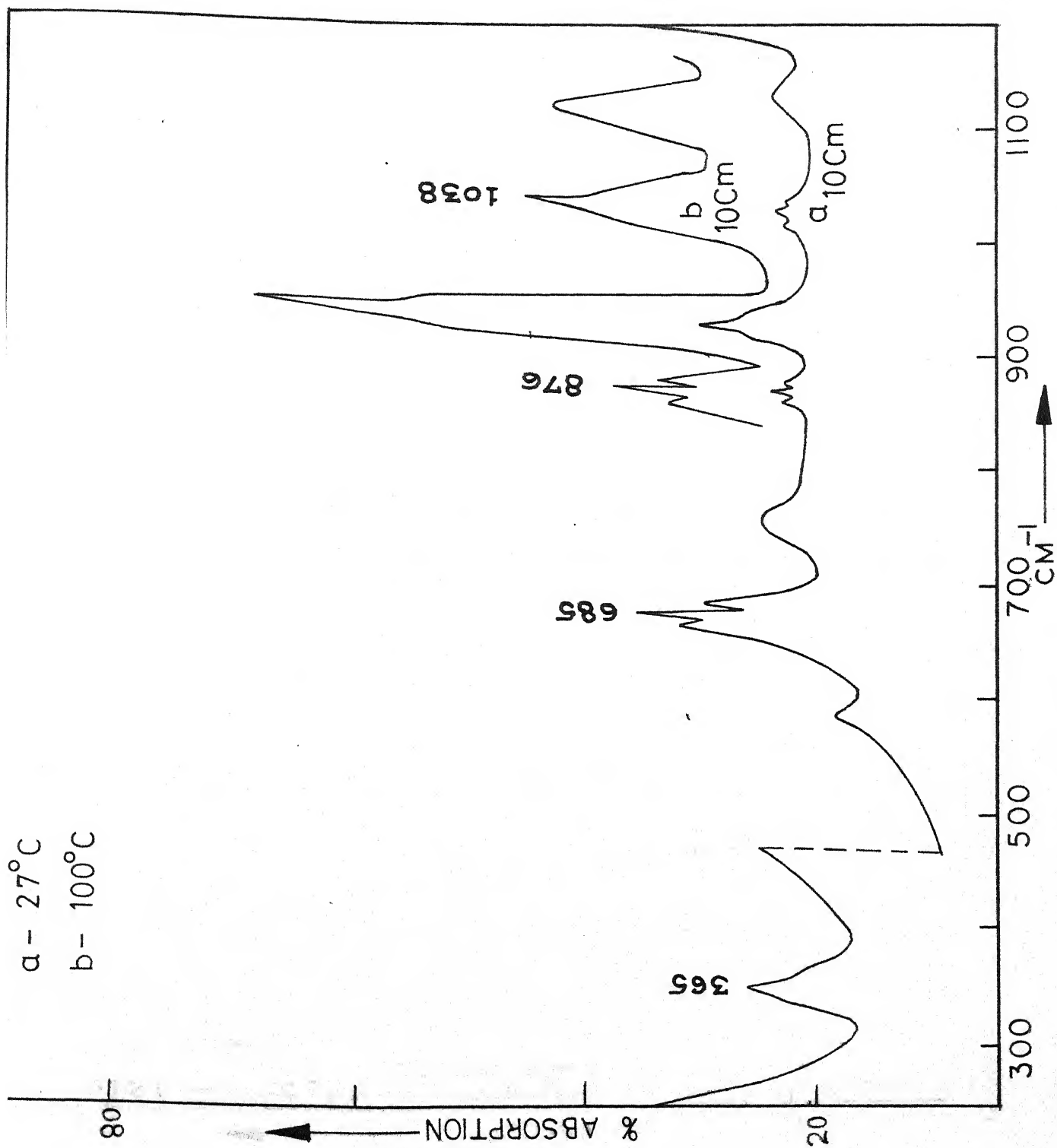
FREQUENCY (CM⁻¹)

% ABSORPTION



90

30



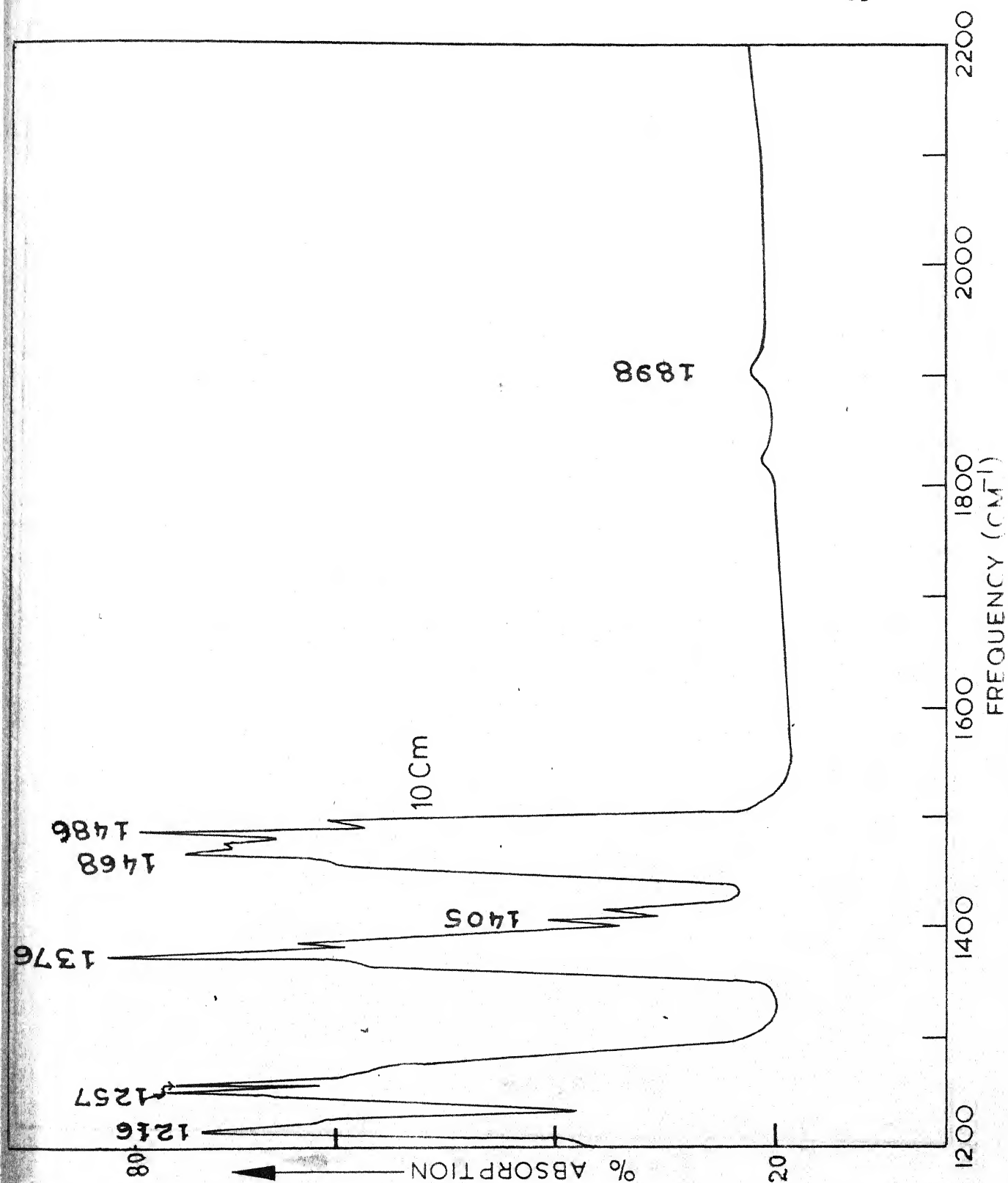


Fig. 5.2(b). The infrared spectrum of gaseous trimethylacetoneitrile in the region 1200-2200 cm^{-1} .

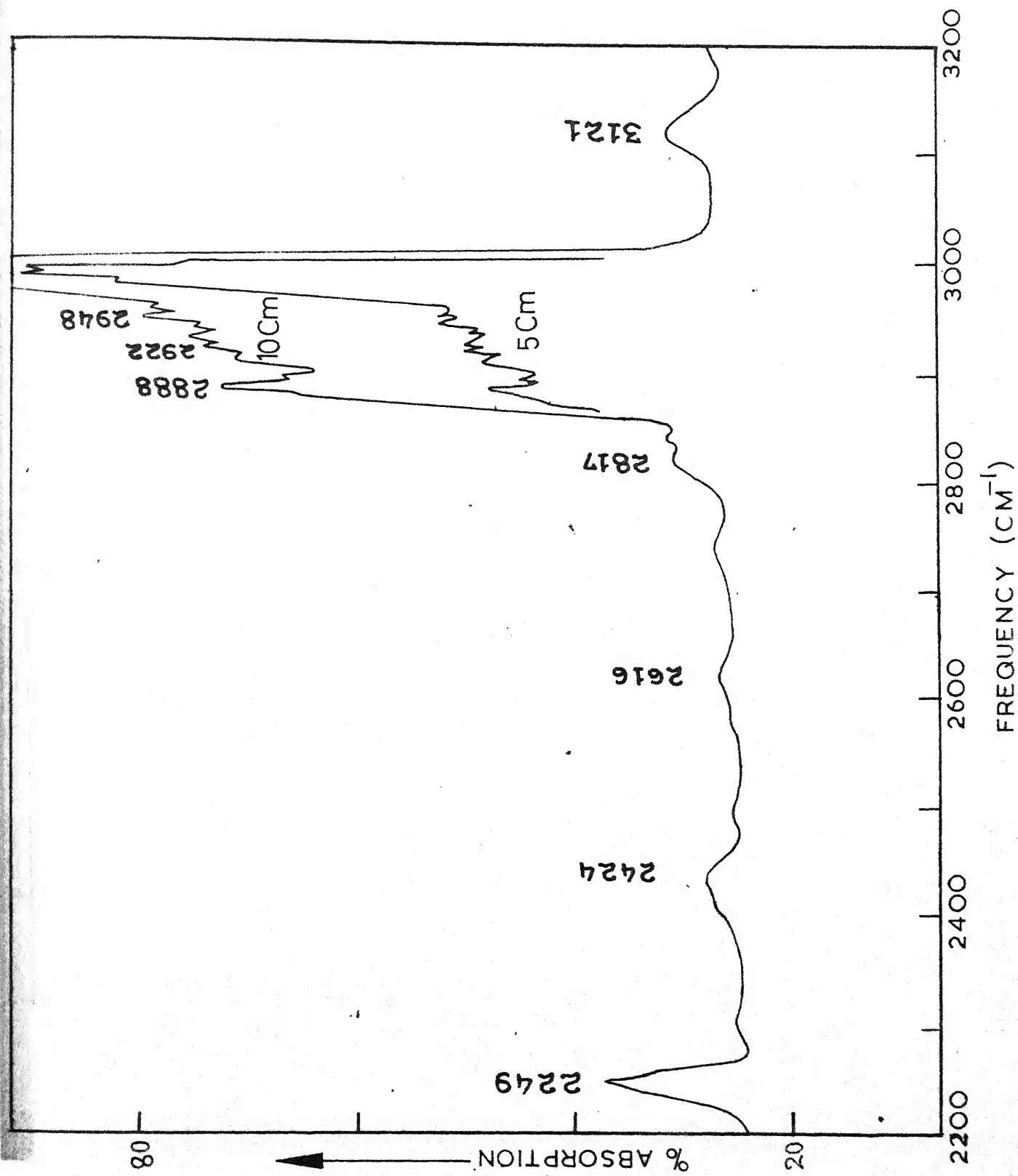


Fig.3.2(e). The infrared spectrum of gaseous trimethylacetone nitrile in the region 2200-3200 cm^{-1} .

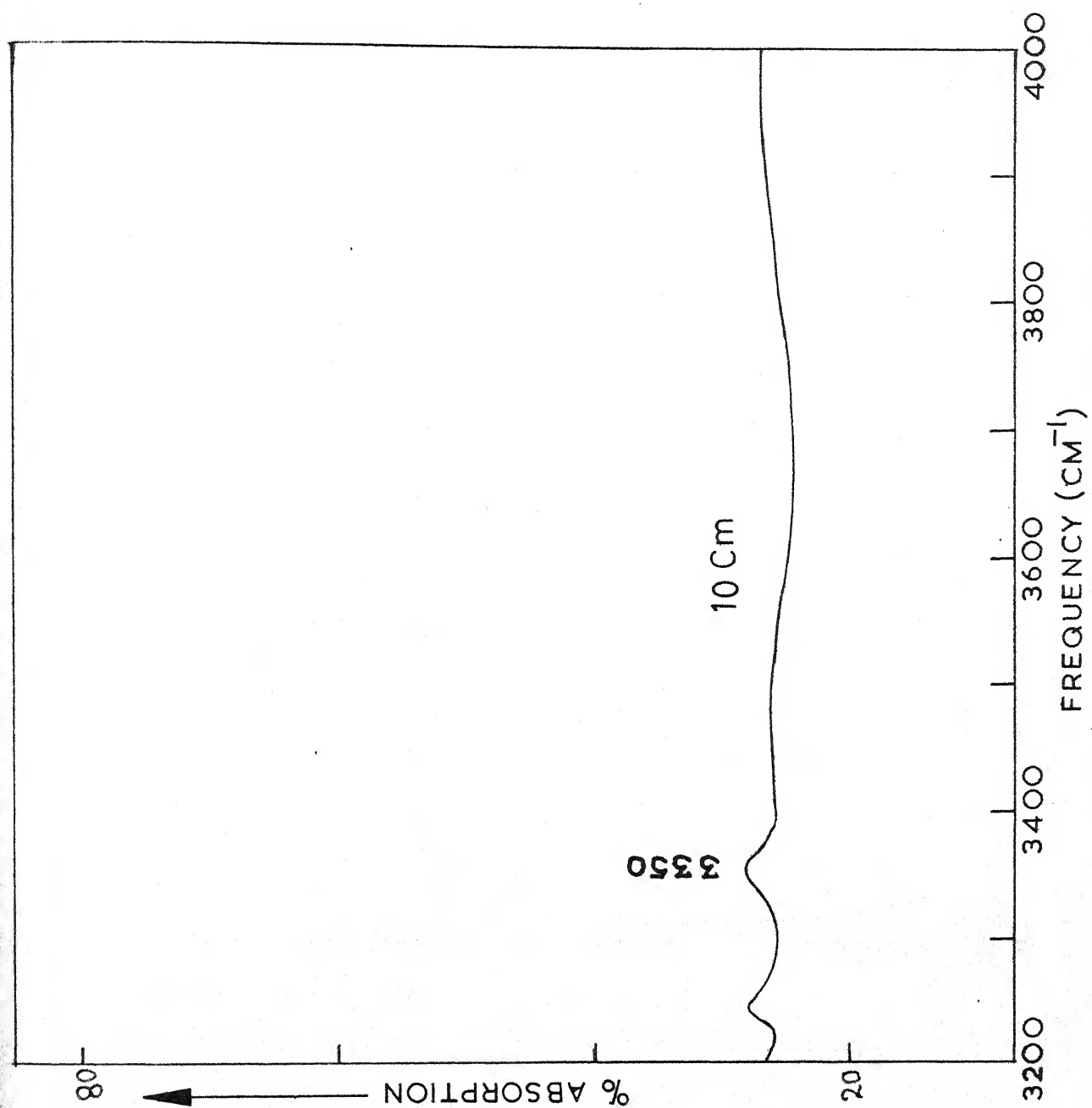


Fig. 3.2(d). The infrared spectrum of gaseous trimethylacetoneitrile in region 3200-4000 cm⁻¹.

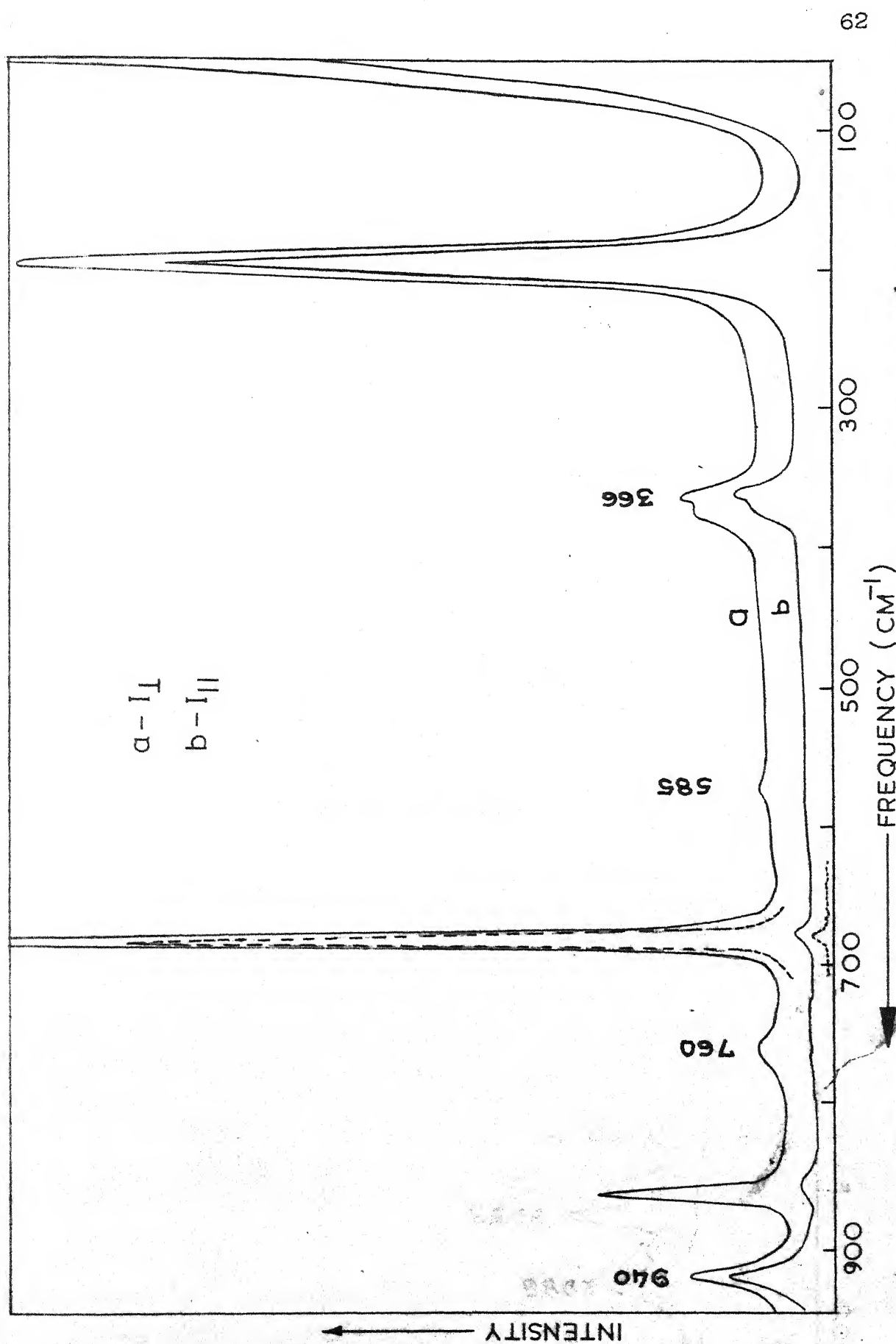


Fig. 3.3(a). The Raman spectrum of liquid trimethylacetone in the region 50-950 cm^{-1} : I_{\perp} and I_{\parallel} denote whether the plane of polarization of incident light is \perp or \parallel to the slit respectively.

$a-I_{\perp}$
 $b-I_{\parallel}$

INTENSITY

2240

2933

2988

2878

2728

1455

1209

1032

a
 b

FREQUENCY (cm⁻¹)

Fig. 3.5(b). The Raman spectrum of liquid trinitrolylacetone in the region 950-3050 cm⁻¹.

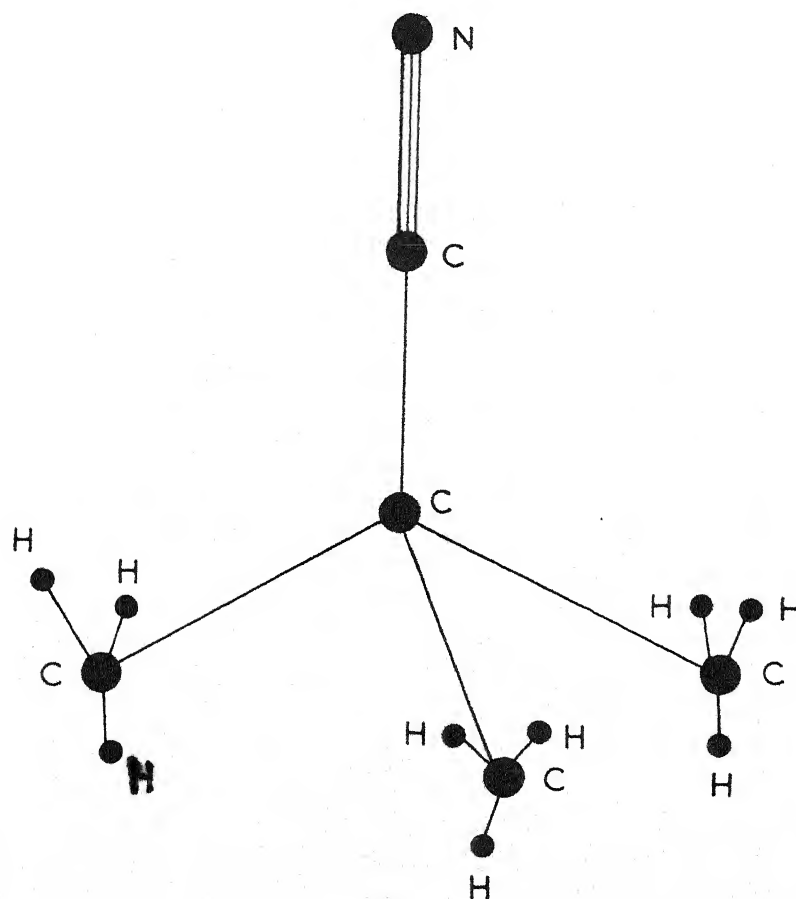


Fig. 3.4. The schematic structure of trimethylacetone nitrile molecule.

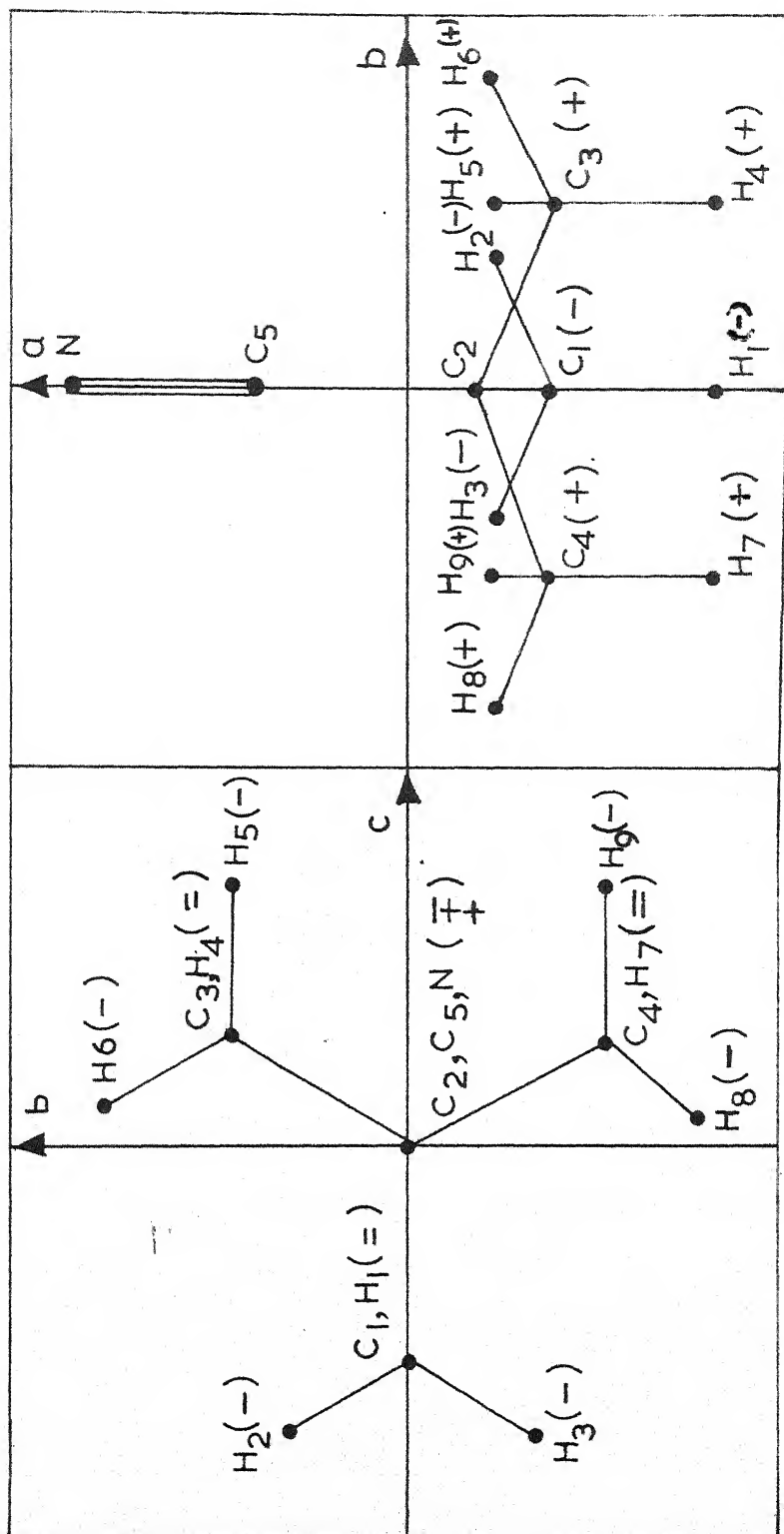


Fig. 3.5. The projections of the trimethylacetone molecule on the planes containing the ab and bc axes (+ and - signs indicate the atoms above and below the plane of the paper respectively).

INTRODUCTION

Several papers concerning the structural determination of methoxy compounds have appeared in literature¹⁻⁴. Wilmshurst¹ and Nukada² studied the vibrational spectra of dimethoxy methane and assigned the spectral data on the basis of only one conformation having C_2 point symmetry. The spectra of trimethoxy and tetramethoxy methanes were studied by Lee and Wilmshurst³. The presence of rotational isomers was established in trimethoxy methane, whereas the data for tetramethoxy methane are consistent with the assumption of only one geometric structure. The methoxy substituted ethanes (methyl ethyl ether, 1,2-dimethoxy ethane, 1,1,1-trimethoxy ethane) have recently been studied^{4,5} and the existence of at least two rotational isomers claimed. Snyder and Zerbi⁴ examined the spectra of methyl isopropyl ether (a methoxy substituted propane) and carried out force constant calculations. Their interpretation of the data is compatible with the existence of two rotational isomers in liquid state, while in solid state the molecular form having C_{1a} structure gets stabilized⁴. It was felt that it would be of interest to investigate the infrared and Raman spectra of higher substituted methoxy propane, the 2,2-dimethoxy propane (DMP) in which both the hydrogen atoms of the CH_2 group of propane have been replaced by OCH_3 groups. To our knowledge, no structural determinations have been attempted for this molecule. This molecule is expected to exist in several molecular conformation due to the internal rotation about each of the two $C-OCH_3$ bonds.

In the present investigation the Raman spectrum of pure liquid and the infrared spectra of solid, liquid and gaseous DMP have been studied. The data are found to be consistent with the assumption of only one molecular model having C_2 symmetry. A vibrational assignment consistent with the Raman depolarization data and vapour phase infrared band contours has been made.

EXPERIMENTAL

The sample used for recording the infrared and Raman spectra was commercially obtained and was distilled prior to use.

The liquid phase infrared spectrum was recorded by sandwiching a small quantity of the compound between two CsBr plates. The vapour phase spectrum was investigated using 5 cm gas cell. The solid phase spectrum was recorded with the help of a low temperature cell. The initial deposit was properly annealed and then the spectrum was recorded. The visual inspection indicated that the films were crystalline. The details of the instruments used and experimental procedure are given in Chapter II.

The liquid, vapour and solid phase spectra are shown in Figs. 4.1, 4.2 and 4.3 respectively. The Raman spectrum of liquid is shown in Fig. 4.4.

The complete set of infrared and Raman data is given in Table 4.3.

DISCUSSION

The possibility of rotational isomerism, due to internal rotation about each of the two C-OMe bonds, allows nine conformations for 2,2-dimethoxy propane of which only four TT, TG, GG and GG' are spectroscopically distinct (Fig. 4.5). The first letter designates whether the $C_5-O_2-C_2-O_1$ chain has the trans (T) or gauche (G) configuration and the second letter indicates whether the $C_1-O_1-C_2-O_2$ chain has the trans (T) or one of the two nonequivalent gauche (G and G') configurations. The numbering of atoms is shown in Fig. 4.6. However, the important assumption that the primary interaction affecting the stability of any particular configuration is the steric effect involving the methyl groups, reduces the number of isomers to three TG, TT and GG. Further the overall similarity in the infrared spectra of liquid, vapour and solid phases suggests that the molecule exists in a single configuration in all the three phases. If now the secondary interaction affecting the stability of the isomers is considered as lone pair interactions, this leads to GG as the stable conformation for the molecule.

The rotational constants A, B and C were calculated for the GG form (the expected value of dihedral angle $(\theta) = 120^\circ$), assuming $r_{C-H} = 1.09 \text{ \AA}$, $r_{C-O} = 1.44 \text{ \AA}$, $r_{C-C} = 1.54 \text{ \AA}$ and all angles tetrahedral. The values of rotational constants and asymmetry parameter ($K = \frac{2B-A-C}{A-C}$) are shown in Table 4.1 and indicate that the molecule is highly asymmetric ($K = -0.428$) for $\theta = 120^\circ$. Three distinct A, B and C type of band contours may, therefore, be expected for this

structure. The A type band contours should have a very strong Q branch and PR spacing* of $\sim 12 \text{ cm}^{-1}$, the B type band contours should have a PQQR type structure with PR spacing of $\sim 10 \text{ cm}^{-1}$ and C type band contours should appear with a strong Q branch and PR spacing of $\sim 19 \text{ cm}^{-1}$. However, the observed vapour phase infrared band contours are mainly of two types in nature and resemble very closely to that of parallel and perpendicular type of bands expected for symmetric top molecules. So, the proposed structure seems to be improbable.

The calculations for the rotational constants and asymmetry parameter were then carried out for various values of dihedral angle (θ) ranging from 0 to 180° . The plot of A, B, C and K vs. θ as shown in Fig. 4.7 indicates that the molecule is an approximate symmetric top for $\theta \sim 0^\circ$ and 90° . As is clear from the graph the molecule is nearly an oblate symmetric top for $\theta \sim 90^\circ$. This structure of the molecule is expected to give rise to perpendicular type of bands with well separated P and R branches having sharper but weak Q branch. The parallel type of contours should also have well separated P and R branches with pronounced Q branch. The observed infrared gas contours are of somewhat different in nature and appear as: (1) The bands with a strong and broad Q branch having unresolved weaker humps on either side which correspond to P and R branches. (2) The bands having resolved P and R branches with strong and sharper Q branch than those of first

*The PR spacings were calculated using the formulas given by R.M. Badger and L.R. Zumwalt, J. Chem. Phys., 6, 711 (1938) and W.A. Seth-Paul and G. Dijkstra Spectrochim. Acta, 23, 2861 (1967).

type. This difference in the expected and observed shapes of band contours rules out the possibility of this structure.

One is then left with the other possible configuration of the molecule with $\theta = 0^\circ$. As pointed out earlier, the lone pair interactions of oxygen atoms are likely to twist the two O-CH₃ bonds, thus making the configuration with θ exactly equal to 0° unstable. Since no structural data are available for DMP the angle of twist is not known a priori, but the plot in Fig. 4.7 suggests that this has to be very small ($\theta \sim 10^\circ$) if the molecule is to have an approximate symmetric top structure. The shapes and PR separations of the bands may then be calculated for TT conformation and used for assignment purposes. The calculations* for this configuration show that the parallel bands should appear with P and R branches closer than the perpendicular bands ($\Delta \nu(\text{PR})_{\parallel} \approx 13 \text{ cm}^{-1}$, $\Delta \nu(\text{PR})_{\perp} \approx 20 \text{ cm}^{-1}$) and show a more distinct central peak. The observed shapes of the band contours closely resemble these calculated ones which clearly indicates that the molecule assumes a structure very near to TT conformation.

For this twisted TT conformation (GG) the molecule can have at the most two fold symmetry axis as an element of symmetry and hence belongs to the C₂ point group. Under this symmetry the fundamental modes of vibration divide as

$$\Gamma_{\text{vib}} = 26 \underline{a} + 25 \underline{b}$$

*The PR spacings were calculated using the formulas given by S.L. Gerhard and D.M. Dennison, Phys. Rev., 43, 197 (1933) and W.A. Seth-Paul and G. Dijkstra, Spectrochim. Acta, 23, 2861 (1967).

all vibrations being active in both the infrared and Raman, with the type a modes being polarized in the latter. The a type modes should give rise to perpendicular bands in infrared vapour whereas, type b modes may arise as parallel or perpendicular bands.

The following assignments have been carried out on the basis of C_2 symmetry for the molecule.

ASSIGNMENT OF FUNDAMENTALS

C-H Stretchings

The twelve active C-H stretching vibrations are expected to fall in the region $2800-3050\text{ cm}^{-1}$. Several overtones and combination bands of the CH_3 bending modes may also lie in this region and appear with enhanced intensity due to the Fermi resonance with the nearby C-H stretching fundamentals. An unambiguous assignment of the C-H stretching modes is, therefore, a bit difficult. The infrared bands concerned with the ν_{CH_3} modes are expected to be weaker than those arising due to the ν_{OCH_3} vibrations⁶. Therefore, the strong infrared band at 2991 cm^{-1} in liquid and the corresponding depolarized 2994 cm^{-1} Raman band have been associated with the four ν_{OCH_3} modes ν_1 , ν_2 , ν_{27} and ν_{28} . The corresponding gaseous band contour seems to be of parallel type in nature with its central peak at 3002 cm^{-1} . The sharp peak at 2999 cm^{-1} in gaseous infrared on the lower frequency side of the Q branch at 3002 cm^{-1} , is probably a hot band. The relatively weak infrared band at 2954 cm^{-1} may then be attributed to the $\nu_{\text{asym.CH}_3}$ vibrations ν_3 , ν_4 , ν_{29} and ν_{30} . Its Raman counterpart appears as

polarized Raman band at 2944 cm^{-1} . The perpendicular band at 2837 cm^{-1} in gaseous infrared and the polarized Raman band at 2830 cm^{-1} may be assigned to the $\nu_{\text{sym.OCH}_3}$ vibrations ν_6 and ν_{32} by correlation with other oxygenated compounds⁴. The $\nu_{\text{sym.CH}_3}$ vibrations ν_5 and ν_{31} have been placed at 2908 cm^{-1} in the infrared spectrum of liquid. The corresponding Raman band is not well resolved and appears as a broad shoulder whose center may be approximately taken at 2910 cm^{-1} .

CH₃ Deformations

The twelve modes conventionally described as CH₃ deformations may occur in the region $1350\text{--}1500\text{ cm}^{-1}$. As the symmetric CH₃ deformation modes of methoxy group also generally lie above 1400 cm^{-1} ²⁻⁴, the region $1400\text{--}1500\text{ cm}^{-1}$ may contain the bands arising due to $\delta_{\text{sym.OCH}_3}$, $\delta_{\text{asym.OCH}_3}$ and $\delta_{\text{asym.CH}_3}$ vibrations. Four bands have been observed in this region in solid and vapour spectra of DMP but liquid spectrum shows only three bands. Since the two methoxy groups are sufficiently separated from each other, the deformation modes of one group may not be much coupled with the other. Thus $\delta_{\text{sym.OCH}_3}$ and $\delta_{\text{asym.OCH}_3}$ modes of both the groups should have nearly the same frequency as the corresponding modes of the individual methoxy groups. Therefore, the bands at 1480 and 1476 cm^{-1} appearing as shoulders in both infrared and Raman respectively have been attributed to the $\delta_{\text{asym.OCH}_3}$ vibrations ν_7 , ν_8 , ν_{33} and ν_{34} . The above assignments have been made in analogy with dimethoxy and trimethoxy methanes^{2,3}. The $\delta_{\text{sym.OCH}_3}$ modes ν_{11} and ν_{37} may be associated with the 1436 cm^{-1} infrared band in the liquid phase. No Raman counterpart is available for this infrared band. The

remaining two bands at 1458 and 1468 cm^{-1} in infrared spectrum of solid may then be assigned to the $\delta_{\text{asym.CH}_3}$ modes ν_9 , ν_{10} , and ν_{35} , ν_{36} respectively. The $\delta_{\text{sym.CH}_3}$ modes may be safely placed at 1374 and 1379 cm^{-1} in infrared spectrum of liquid. The higher frequency component has been ascribed to $\delta_{\text{sym.CH}_3}$ mode ν_{12} and the low frequency one to ν_{38} by analogy with propane where the corresponding modes were found at 1385 and 1370 cm^{-1} respectively⁷. This splitting of symmetric and asymmetric modes is probably due to the interaction between the modes of the individual methyl groups.

CH₃ Rockings

The ρ_{OCH_3} vibrations, highly mixed with the skeletal modes generally fall in the complex region 1150 - 1250 cm^{-1} , which may also contain bands associated with ρ_{CH_3} , $\nu_{\text{C-C}}$ and $\nu_{\text{C-O}}$ modes. This makes the assignment of the individual modes somewhat difficult. The four solid phase infrared bands at 1287, 1264, 1241 and 1215 cm^{-1} may be taken for the ρ_{OCH_3} vibrations. The Raman spectrum shows two depolarised bands at 1265 and 1221 cm^{-1} corresponding to the 1264 and 1215 cm^{-1} infrared bands and they are probably associated with the b type ρ_{OCH_3} vibrations ν_{39} and ν_{40} respectively. The ir band in vapour phase with its centre at 1222 cm^{-1} appears to be of perpendicular type in nature whereas, the other band at 1260 cm^{-1} does not show any clear structure. The remaining two infrared bands without any Raman counterparts are then assigned to the ρ_{OCH_3} modes ν_{13} and ν_{14} . The liquid and vapour spectra do not clearly indicate any band corresponding to the 1241 cm^{-1} solid state band, probably because of the broadness of the

bands. But this band separates out in solid state due to the sharpening of the bands at low temperatures.

The solid phase infrared bands at 1192 and 1174 cm^{-1} have been attributed to the ρ_{CH_3} vibrations ν_{41} and ν_{15} respectively in analogy with propane⁷. The 1192 cm^{-1} band is absent in fluid phase spectra. The ρ_{CH_3} vibration ν_{44} has been assigned to the 926 cm^{-1} infrared band showing perpendicular behaviour in vapour phase. Its Raman counterpart appears as depolarized band at 934 cm^{-1} . The remaining mode ν_{18} may be ascribed to the 990 cm^{-1} infrared band with its Raman counterpart at 996 cm^{-1} . The vapour phase contour seems to be of perpendicular type with its Q branch at 985 cm^{-1} . This completes the assignment of eight rocking modes associated with CH_3 and OCH_3 groups.

Skeletal Modes

Once the assignment of CH_3 rockings is over, it is easy to pick out the skeletal modes. The $\nu_{\text{O-CH}_3}$ modes may not be sufficiently split due to the smaller coupling of individual stretchings of the O-CH_3 bonds. Therefore, they have been assigned coincidentally to the strong and broad 1056 cm^{-1} infrared band with Raman counterpart at 1056 cm^{-1} . However, the solid spectrum shows two bands at 1044 and 1052 cm^{-1} , the latter appearing as shoulder and may correspond to a and b vibrations of $\nu_{\text{O-CH}_3}$. The gaseous infrared band seems to be of perpendicular type with its Q branch at 1066 cm^{-1} . The four stretching modes of $\begin{array}{c} \text{C} & & \text{C} \\ & \diagdown & / \\ & \text{C} & \\ & / & \diagdown \\ \text{O} & & \text{O} \end{array}$ skeleton cannot be specifically assigned to individual bands as they will be highly mixed due to their close

proximity. What follows is an approximate description of these vibrations. Four prominent bands are available which may be associated with these vibrations. The depolarized Raman bands at 1148 and 835 cm^{-1} corresponding to the 1145 and 828 cm^{-1} infrared bands have been selected for the \underline{b} type vibrations ν_{42} and ν_{45} respectively. The lower frequency band shows parallel type nature in gaseous infrared, whereas the higher one does not indicate any clear structure. Now it is natural to assign the two polarized Raman bands at 1082 and 735 cm^{-1} to the symmetric stretching modes ν_{16} and ν_{19} respectively. The corresponding infrared bands appear as perpendicular type in vapour spectrum with central peaks at 1086 and 727 cm^{-1} respectively.

As the two COC bending modes are likely to fall quite near to each other due to smaller coupling of individual COC bending modes, the modes ν_{20} and ν_{46} have been associated with the polarized and depolarized Raman bands at 582 and 550 cm^{-1} respectively. These bands show clear structure in gas phase and appear as perpendicular and parallel bands with Q branches at 576 and 546 cm^{-1} respectively. The polarized Raman band at 400 cm^{-1} and the corresponding perpendicular band in infrared at 395 cm^{-1} may be attributed to the δ_{CCC} mode ν_{21} in analogy with propane where the corresponding vibration has been placed at 375 cm^{-1} . The ρ_{CCO} modes ν_{47} and ν_{48} are located at 416 and 356 cm^{-1} respectively which appear as parallel and perpendicular bands in the vapour phase spectrum. The corresponding Raman bands are observed at 426 and 366 cm^{-1} , both being depolarized. The δ_{OCO} mode ν_{22} may be placed at 318 cm^{-1} in infrared spectrum of

liquid whose Raman counterpart is not available and the vapour phase spectrum indicates it to be probably of perpendicular type.

Torsional Modes

The torsional frequencies are expected to fall below 300 cm^{-1} and may appear as weak bands in infrared and Raman spectra. This region may also contain the difference tones of fundamentals discussed above. Therefore, the assignment of torsional modes is highly ambiguous. Two broad Raman bands are observed at 266 and 138 cm^{-1} and appear to be polarized and depolarized respectively. The higher frequency band with its infrared counterpart at 280 cm^{-1} has been tentatively selected for the twisting mode ν_{25} . The remaining 138 cm^{-1} band may be associated with $\text{CH}_3\text{-O}$ torsional modes ν_{26} and ν_{51} . As no other bands are available, the assignment of the remaining torsional modes could not be made.

Overtones and Combination Bands

In addition to the bands assigned above, there are some more bands in the spectra of DMP which have not been explained so far. These bands could be satisfactorily assigned as combinations or overtones of fundamentals discussed above. Their assignments do not need much discussion and have been listed in the Table 4.3.

REFERENCES

1. J.K. Wilmshurst, Can. J. Chem., 36, 285 (1958).
2. K. Nukada, Spectrochim. Acta, 18, 745 (1962). This paper may be referred for earlier references.
3. H. Lee and J.K. Wilmshurst, Spectrochim. Acta, 23, 347 (1967).
4. R.H. Snyder and G. Zerbi, Spectrochim. Acta, 23, 391 (1967).
5. K. Kumar: Chapter V of the present thesis.
6. B. Nolin and R.N. Jones, Can. J. Chem., 34, 1382 (1966).
7. J.H. Schachtschneider and R.G. Snyder, Spectrochim. Acta, 19, 117 (1963).

TABLE 4.1

The Molecular Parameters of the Three Configurations of 2,2-dimethoxy propane Corresponding to Dihedral Angle $\theta = 0^\circ$, 90° and 120° .

Species	$\theta = 0^\circ$	$\theta = 90^\circ$	$\theta = 120^\circ$
Ia (a.m.u. - $A^{\circ 2}$)	109.7	179.5	147.7
Ib (a.m.u. - $A^{\circ 2}$)	276.6	180.7	204.1
Ic (a.m.u. - $A^{\circ 2}$)	279.5	251.4	240.9
$\rho^* = \frac{A-C}{B}$	1.53	0.29	0.53
$K = \frac{2B-A-C}{A-C}$	-0.981	+0.954	-0.428
$\Delta \nu$ (PR) type	$\sim 13 \text{ cm}^{-1}$	$\sim 18 \text{ cm}^{-1}$	$\sim 19 \text{ cm}^{-1}$

TABLE 4.2

Description, Symmetry and Activity of the Normal
Modes of Vibration of 2,2-Dimethoxy Propane.

Approximate description			a	b
CH ₃ vibrations	OCH ₃ vibrations	Skeletal	(R(p) ,i.r.)	(R(dp) ,i.r.)
1	2	3	4	5
	C-H st. (asym.)		✓ ₁ , ✓ ₂	✓ ₂₇ , ✓ ₂₈
C-H st. (asym.)			✓ ₃ , ✓ ₄	✓ ₂₉ , ✓ ₃₀
C-H st. (sym.)			✓ ₅	✓ ₃₁
	C-H st. (sym.)		✓ ₆	✓ ₃₂
	CH ₃ def. (asym.)		✓ ₇ , ✓ ₈	✓ ₃₃ , ✓ ₃₄
CH ₃ def. (asym.)			✓ ₉ , ✓ ₁₀	✓ ₃₅ , ✓ ₃₆
	CH ₃ def. (sym.)		✓ ₁₁	✓ ₃₇
CH ₃ def. (sym.)			✓ ₁₂	✓ ₃₈
	CH ₃ rock.		✓ ₁₃ , ✓ ₁₄	✓ ₃₉ , ✓ ₄₀
CH ₃ rock.			✓ ₁₅	✓ ₄₁
		C-O st.	✓ ₁₆	✓ ₄₅
		H ₃ C-O st.	✓ ₁₇	✓ ₄₃
CH ₃ rock.			✓ ₁₈	✓ ₄₄
		C-C st.	✓ ₁₉	✓ ₄₂
		COC bend.	✓ ₂₀	✓ ₄₆
		CCC bend.	✓ ₂₁	
		CCO rock.		✓ ₄₇ , ✓ ₄₈
		OCO bend.	✓ ₂₂	

Contd.

table 4.2 (contd.)

1	2	3	4	5
	CH ₃ tors.		✓ ₂₃	✓ ₄₉
CH ₃ tors.			✓ ₂₄	✓ ₅₀
		Skeletal twist.	✓ ₂₅	
		C-O tors	✓ ₂₆	✓ ₅₁

Abbreviations : st. = stretching, def. = deformation, rock. = rocking,
 bend. = bending, tors. = torsion, twist. = twisting,
 asym. = asymmetric, sym. = symmetric.

TABLE 4.3

Infrared and Raman Spectra of 2,2-Dimethoxy propane

Infrared Spectrum						Raman Spectrum			Assignment
Liquid		Vapour		Solid		Liquid			
cm ⁻¹	int.	cm ⁻¹	type	cm ⁻¹	int.	cm ⁻¹	int.	depol.	
1	2	3	4	5	6	7	8	9	10
						138	m,br	dp	$\checkmark_{26}, \checkmark_{51}$
280	vvw			280	vw	266	m,br	p	\checkmark_{25}
318	w	305 312 320	$\perp ?$	325	w				\checkmark_{22}
361	w	348 356 366	\perp	367	mw	366	w	dp	\checkmark_{48}
398	w	387 395 401	\perp	397	mw	400	m	p	\checkmark_{21}
422	mw	408 416 426	\parallel	426	mw	426	w	dp	\checkmark_{47}
548	m	536 546 553	\parallel	549	m	550	m	dp	\checkmark_{46}
580	mw	567 576 582	\perp	582	w	582	s	p	\checkmark_{20}
730	w	717 727 732	\perp	727	vw	735	vs	p	\checkmark_{19}
828	s	826 832 839	\parallel	828	s	835	m	dp	\checkmark_{45}

Contd.

Table 4.3 (contd.)

1	2	3	4	5	6	7	8	9	10
929	w	917 926 933	⊥	932	m	934	m	dp	✓ ₄₄
990	w	973 985 992	⊥	993	m	996	vw		✓ ₁₈
1056	vs	1057 1066 1072	⊥	1044 1052	vs	1056	w	dp	✓ ₁₇ , ✓ ₄₃
1081	s	-- 1086 1094	⊥?	1076	s	1082	m	p	✓ ₁₆
1116	sh			1114	vw				✓ ₂₀ + ✓ ₄₆
1145	ms	1146 1157 --	⊥?	1144	s	1148	w,br	dp	✓ ₄₂
1180	s	1180 1187 1192	⊥	1174	s	1194	w	p	✓ ₁₅
				1192	sh				✓ ₄₁
1217	s	1216 1222 1230	⊥	1215	s	1221	w	dp	✓ ₄₀
				1241	sh				✓ ₁₄
1262	m	1260		1264	s	1265	w	dp	✓ ₃₉
1283	sh			1287	sh				✓ ₁₃
1374	s	1368 1376		1373	s				✓ ₃₈
1379	sh	1383		1382	s				✓ ₁₂

Contd.

table 4.3 (contd.)

1	2	3	4	5	6	7	8	9	10
1436	sh	1439	sh	1434	w				γ_{11}, γ_{37}
		1451	sh	1458	sh				γ_9, γ_{10}
1463	m	1461 1469 1476	\perp	1468	s	1450	s,br	dp	γ_{35}, γ_{36}
1480	sh	1483	sh	1477	s	1476	sh		$\gamma_7, \gamma_8, \gamma_{33}, \gamma_{34}$
2827	s	2830 2837 2844	\perp	2832	s	2830	m	p	γ_6, γ_{32}
2888	sh			2873	sh				$2x \gamma_{11}$ (F.R.)
				2896	sh				$2x \gamma_9$ (F.R.)
2908	sh	2919	?	2907	sh	2910	sh,br	p	γ_5, γ_{31}
2942	m			2942	m				$2x \gamma_{35}$ (F.R.)
2954	m	2955	?	2956	s	2944	s	p	$\gamma_3, \gamma_4, \gamma_{29}, \gamma_{30}$
		2992 2999							$\gamma_{28}^+ \gamma_{48}^- \gamma_{48}$
2991	s	3002 3010	\parallel	2982	s	2994	m	dp	$\gamma_1, \gamma_2, \gamma_{27}, \gamma_{28}$
				2993	sh				$2x \gamma_{40} + \gamma_{46}$

Abrieiations : w = weak, m = medium, s = strong, vw = very weak,

vvw = very very weak, vs = very strong, mw = medium weak,

ms = medium strong, br = broad, sh = shoulder, p = polarized,

dp = depolarized and F.R. = Fermi resonance.

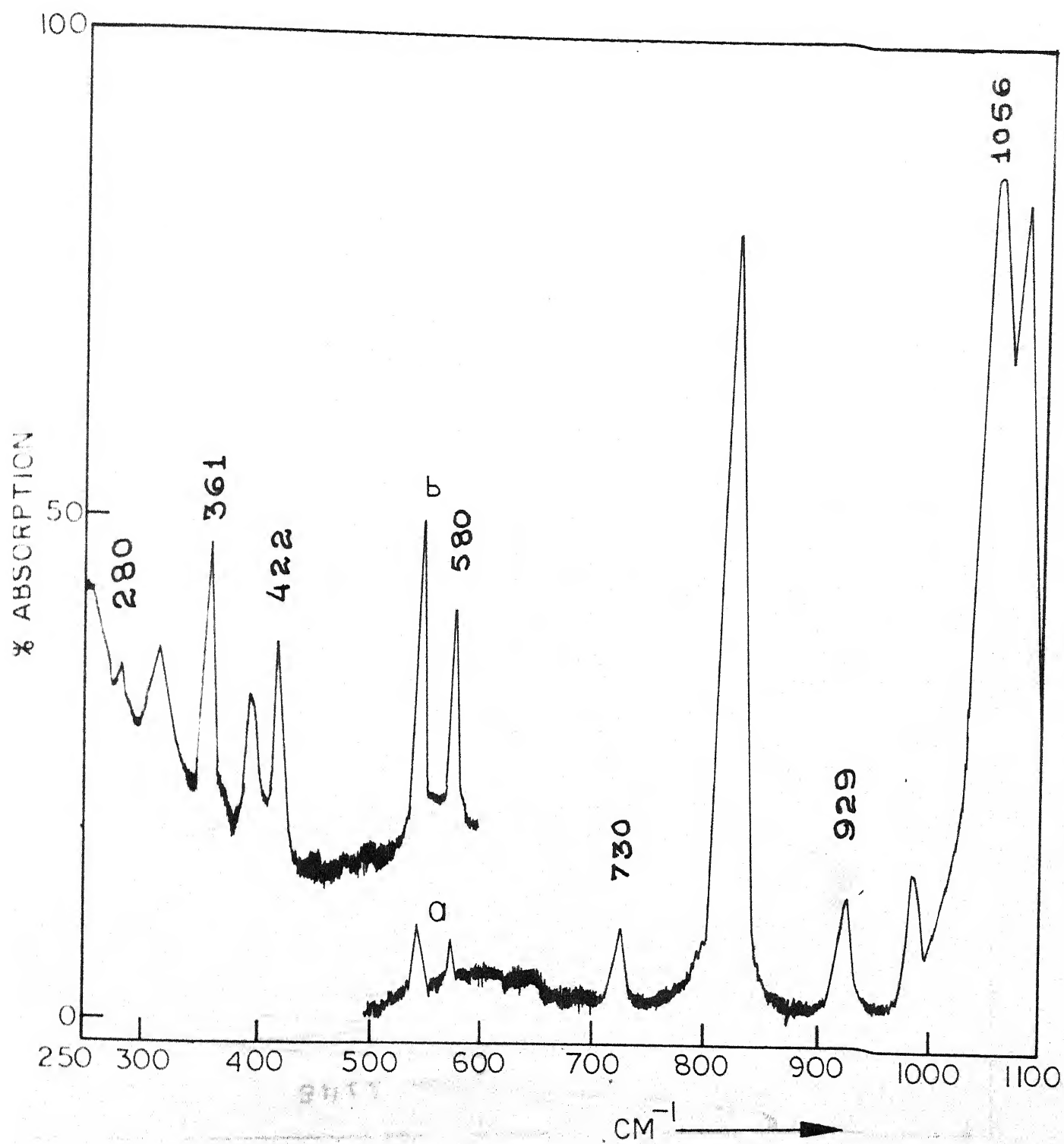


Fig.4.1(a). The infrared spectrum of liquid 2,2-dimethoxy propane in the region 250-1100: Thin film (the spectrum b is of thicker film than a).

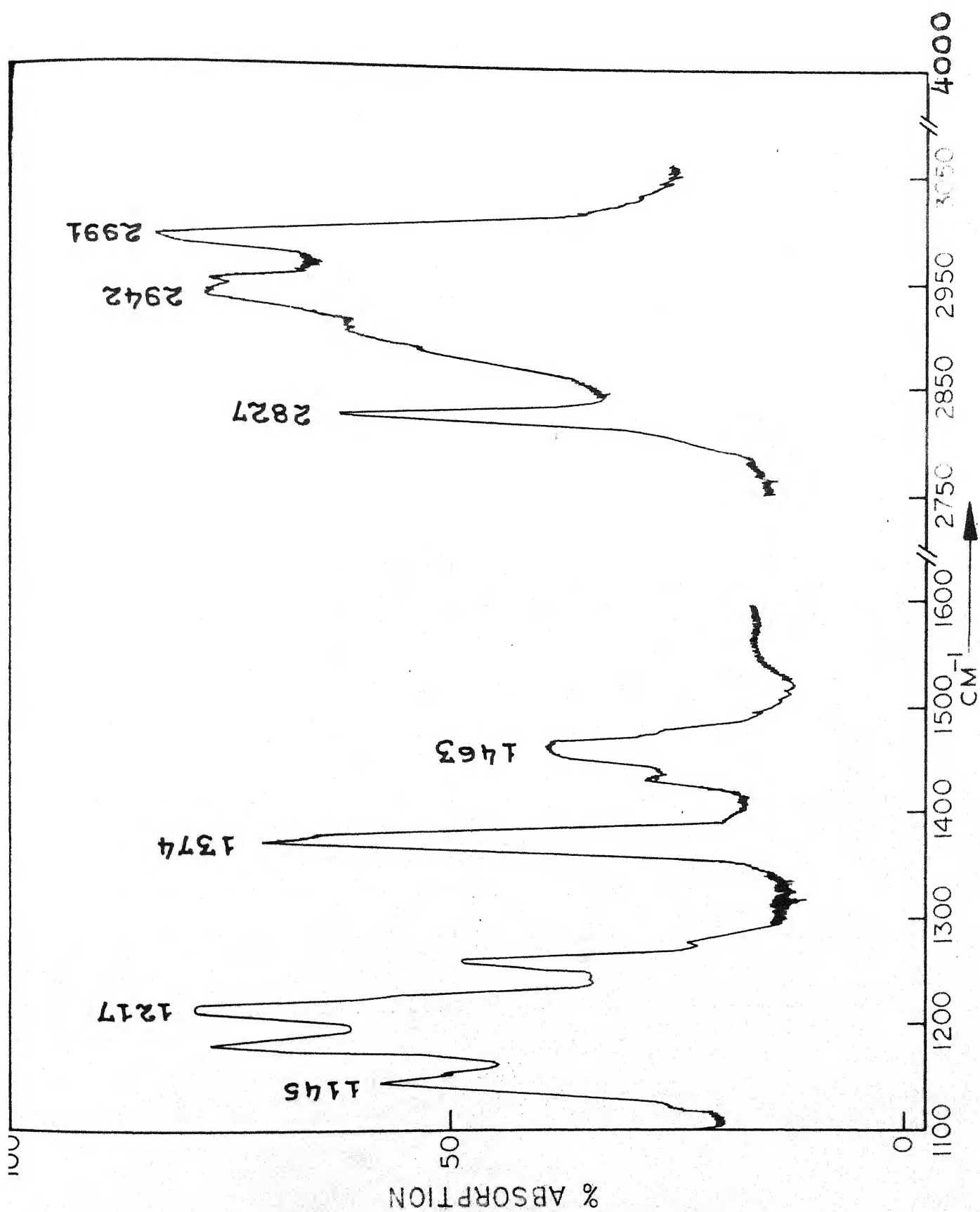


Fig.4.1(b). The infrared spectrum of liquid 2,2-dimethoxy propane in the region 1100-4000 cm^{-1} ; thin film.

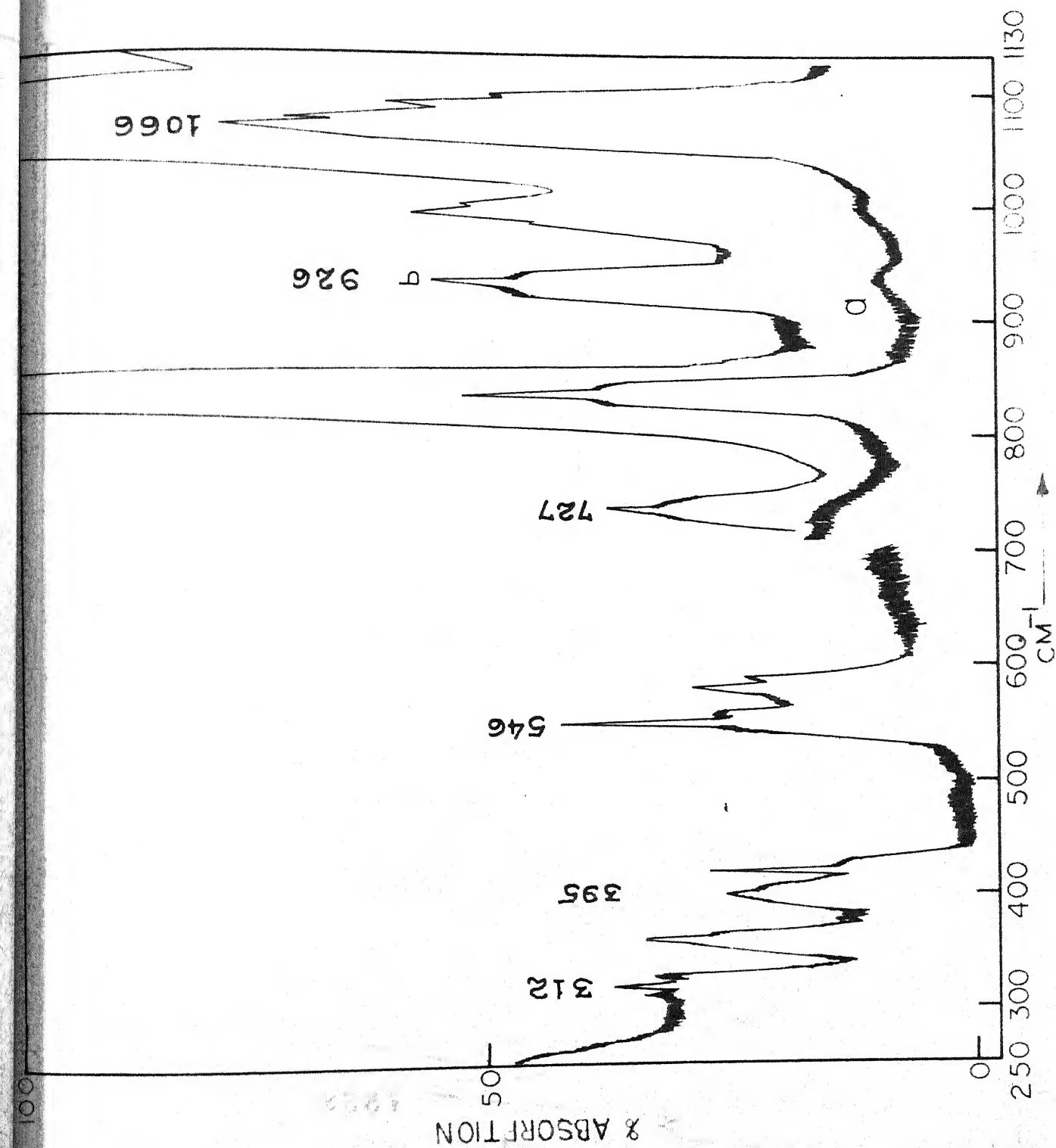


Fig.4.2(a). The infrared spectrum of gaseous 2,2-dimethoxy propane at room temperature in the region 250-1130 cm^{-1} . The letters *a* and *b* designate different pressures, latter being higher.

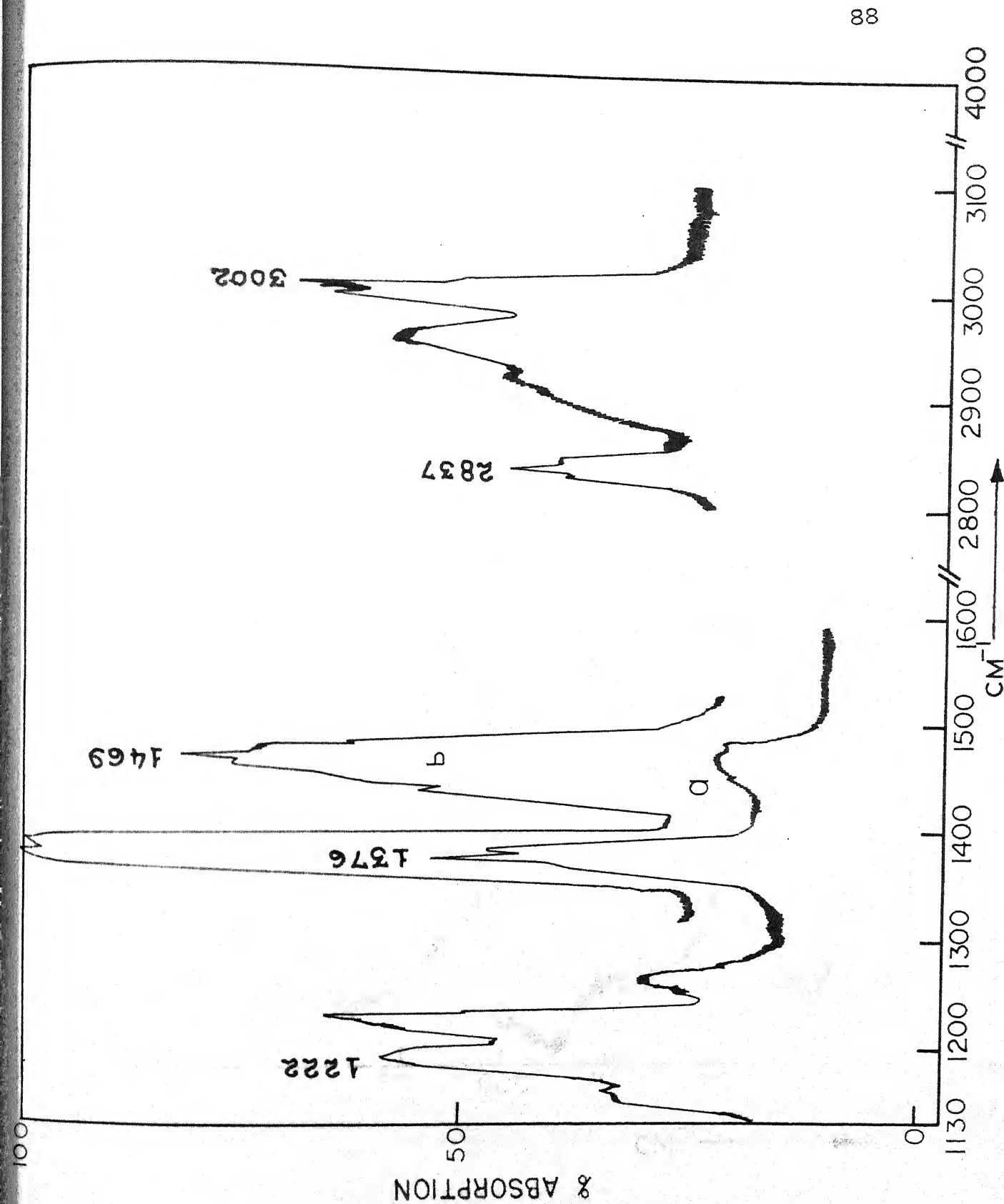


Fig. 4.2(b). The infrared spectrum of gaseous 2,2-dimethoxy propane at room temperature in the region 1130-4000 cm^{-1} . The letters a and b designate different pressures, latter being higher.

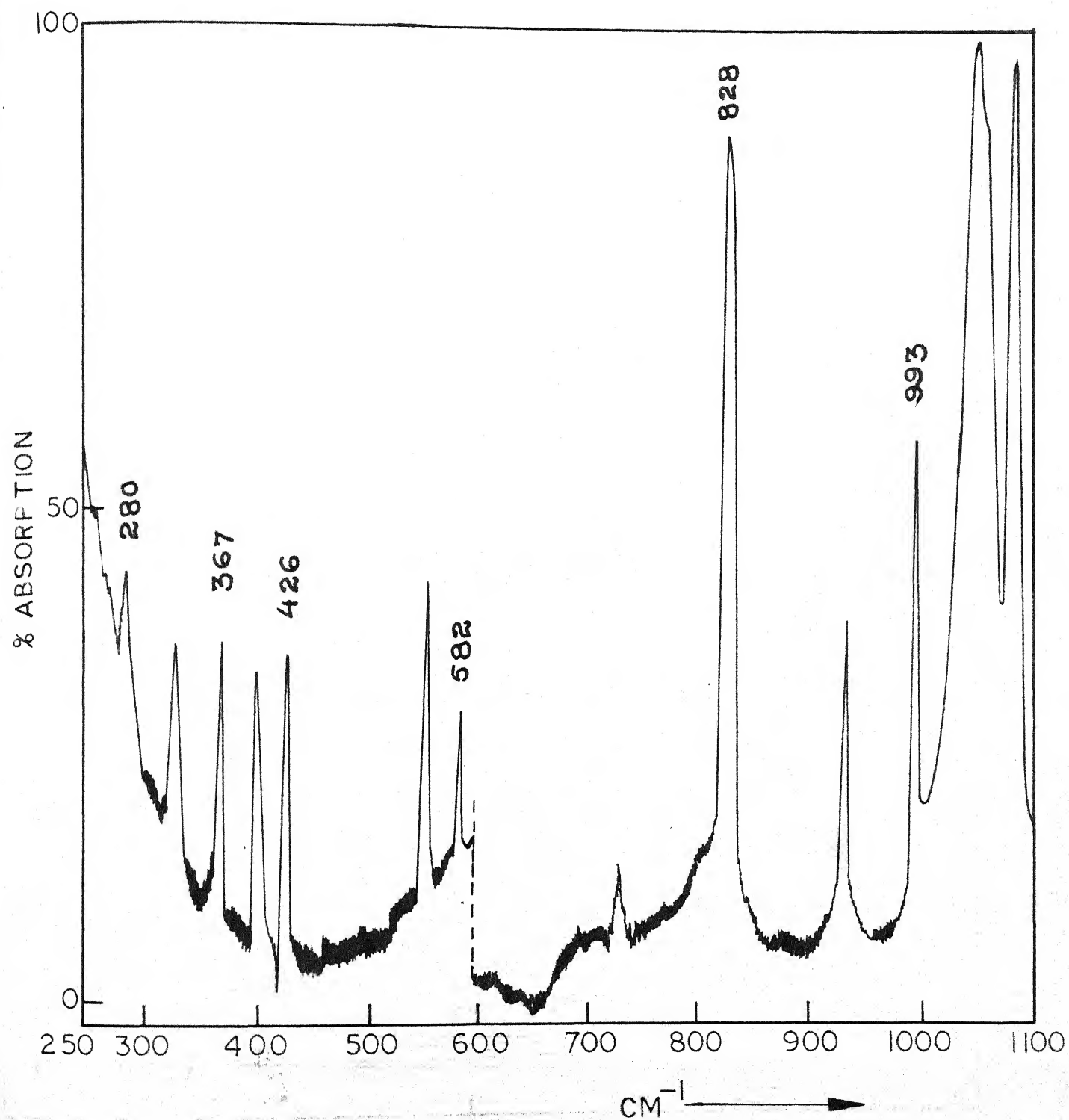


Fig.4.3(a). The infrared spectrum of solid 2,2-dimethoxy propane near liquid nitrogen temperature in the region 250-1100 cm⁻¹.

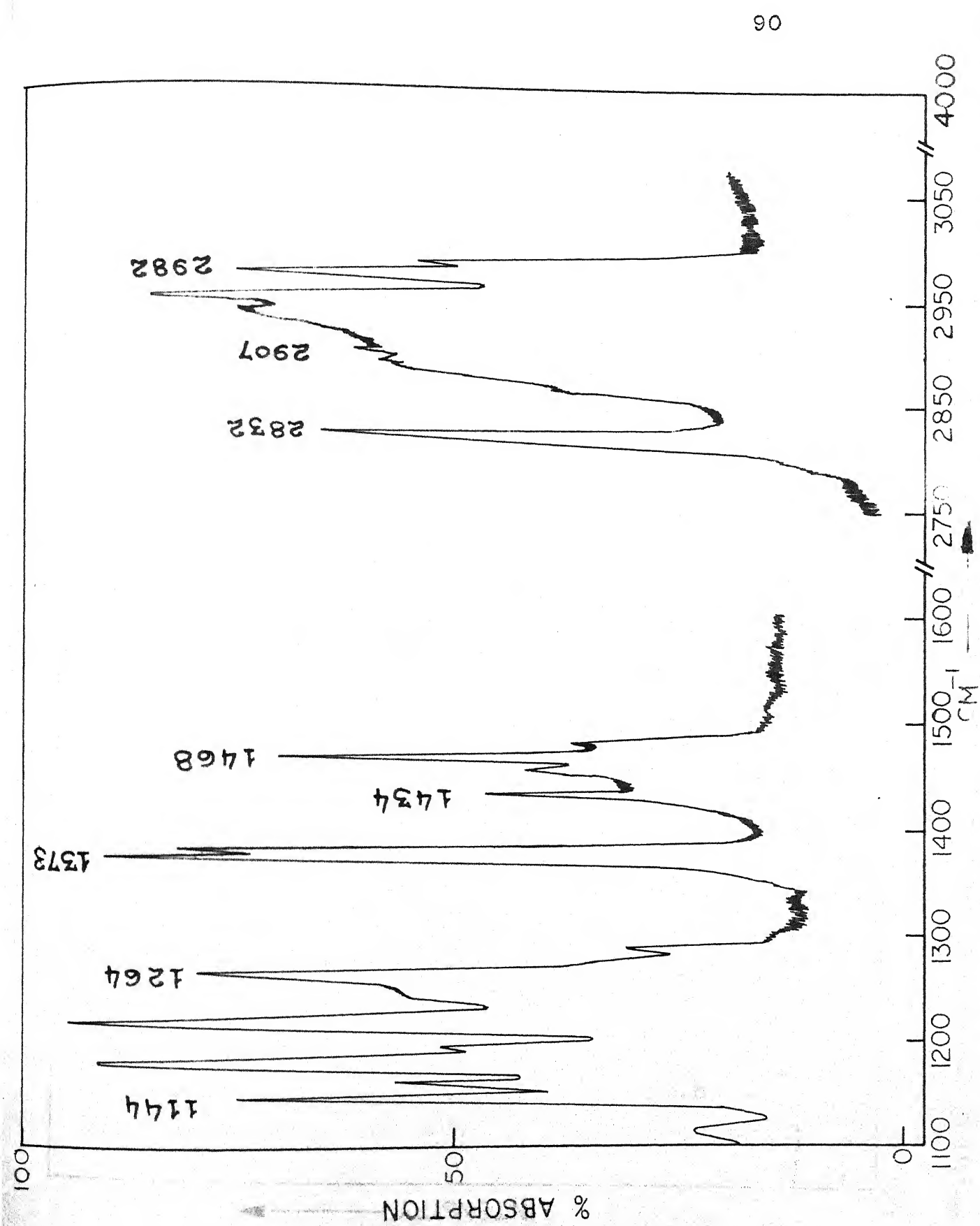


Fig. 4.3(b). The infrared spectrum of solid 2,2-dimethoxy propane near -126°C in the region $1100\text{--}4000\text{ cm}^{-1}$.

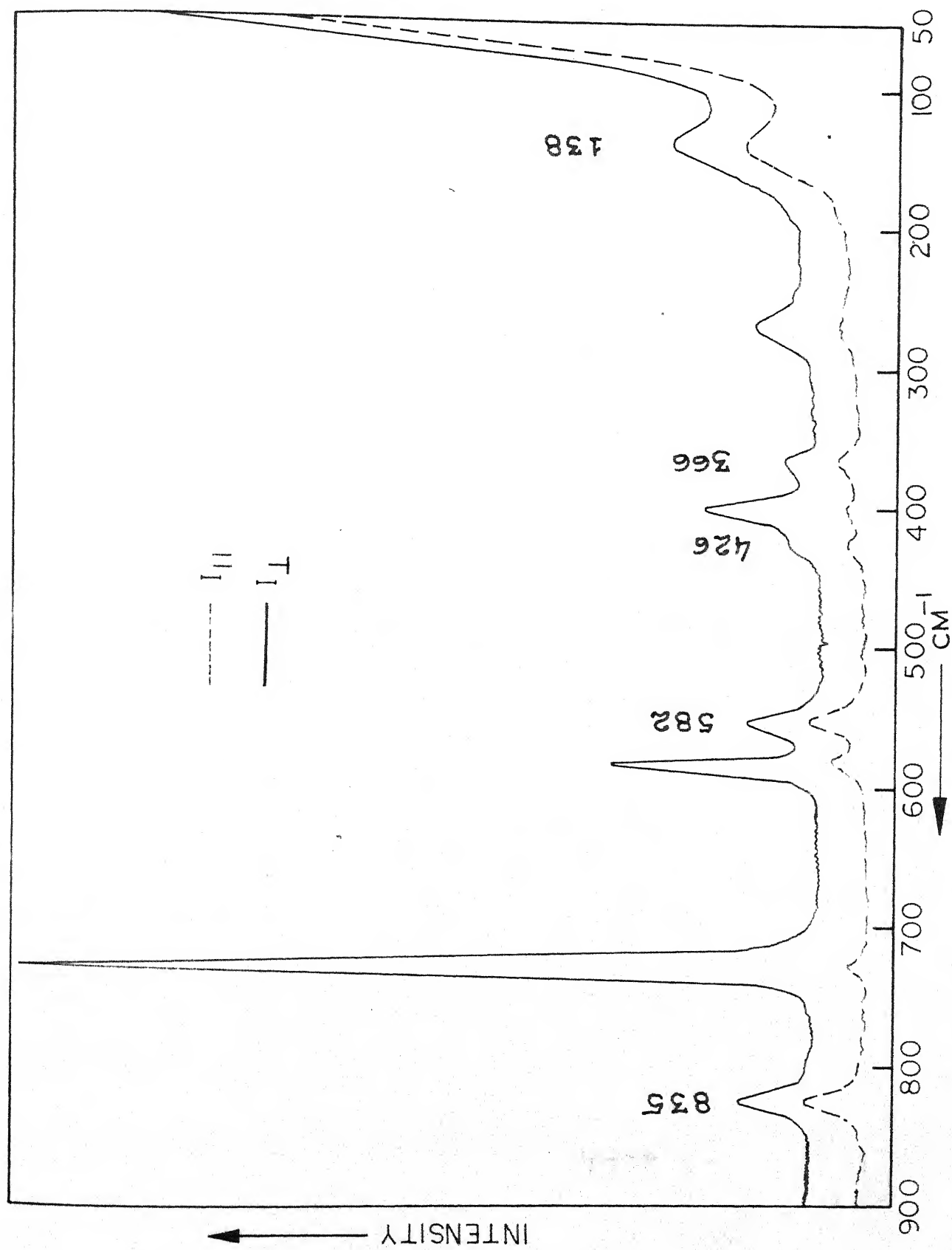


Fig. 4.4(a). The Raman spectrum of liquid 2,2-dimethoxy propane in the region 50-900 cm^{-1} .

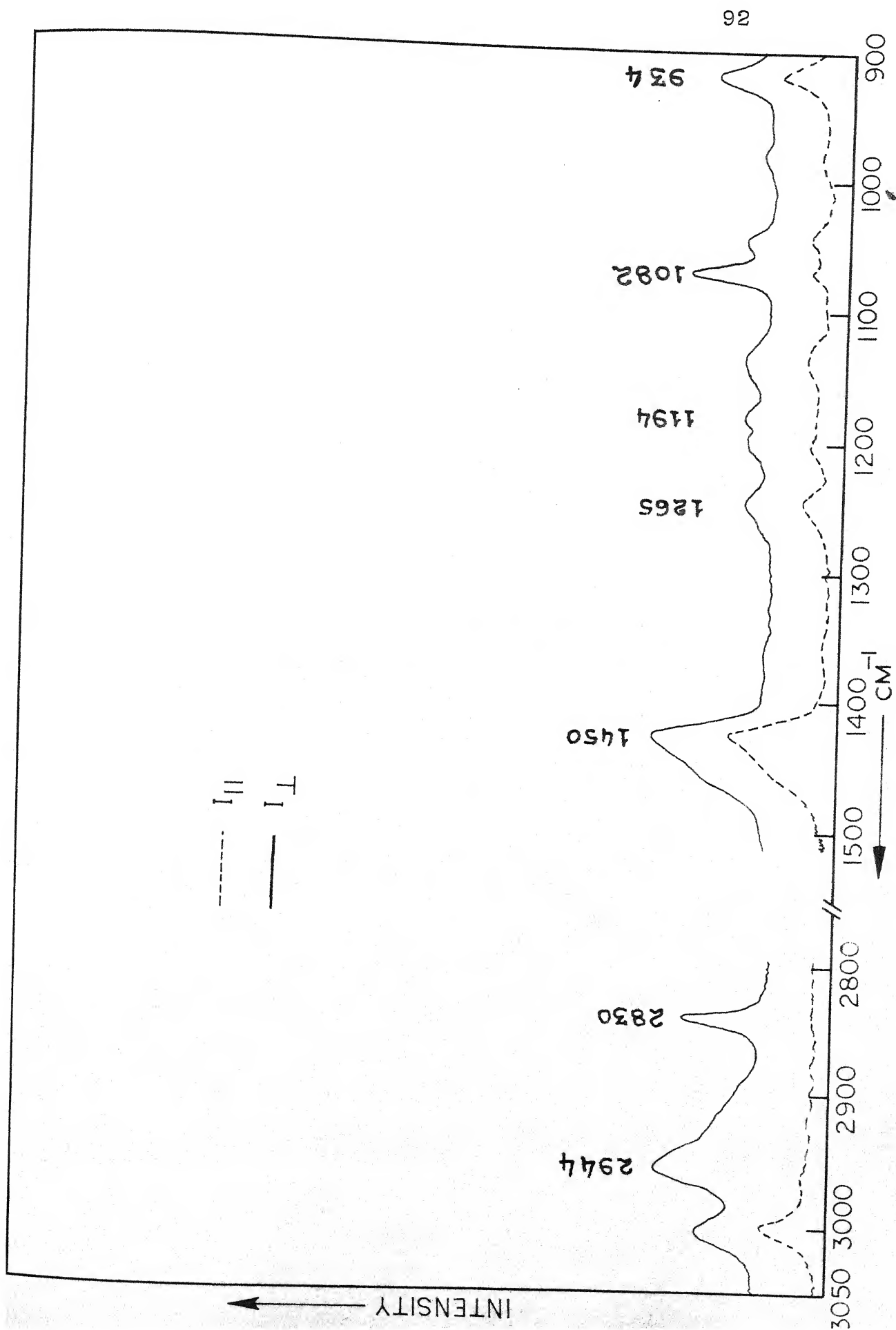


Fig. 4.4(b). The Raman spectrum of liquid 2,2-dimethoxy propane in the region 900-3050 cm⁻¹.

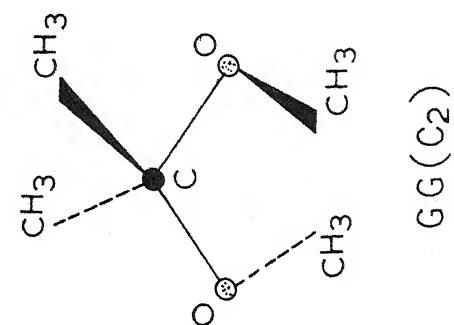
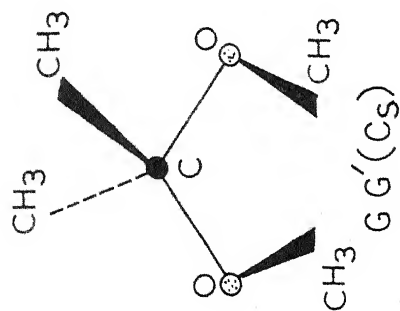
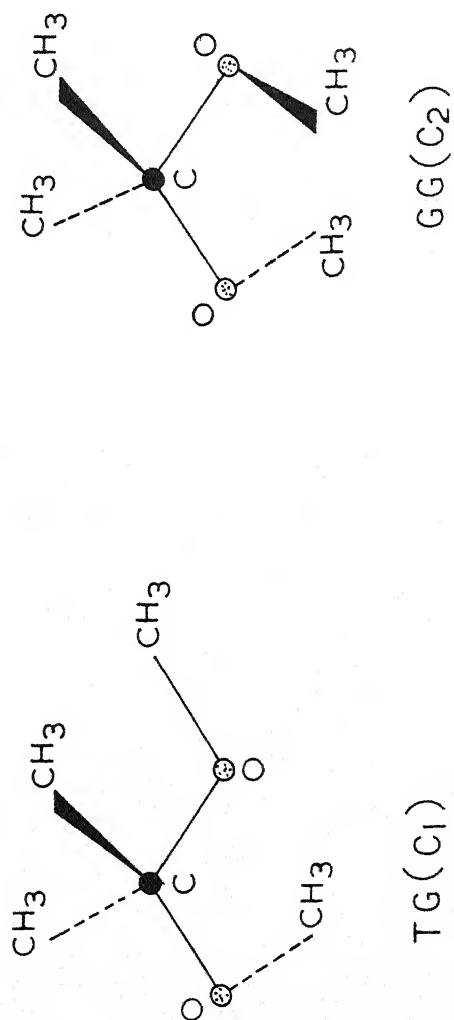
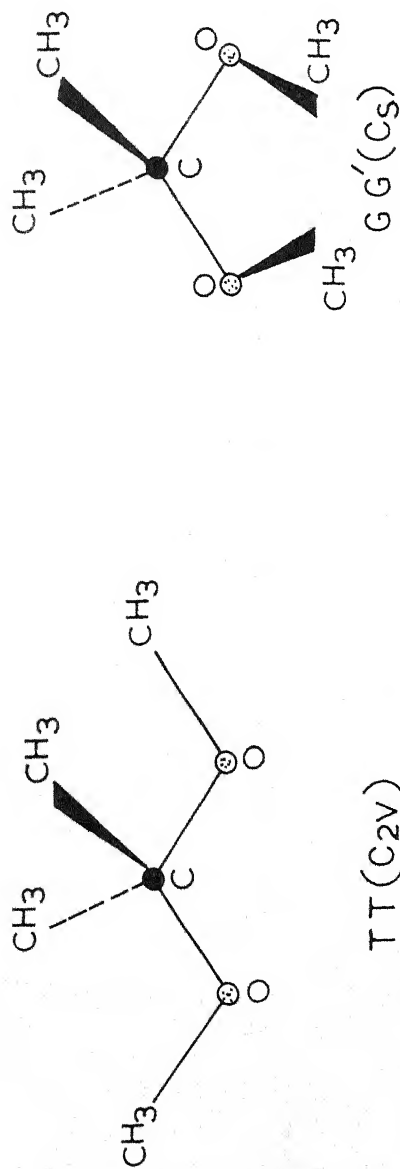


Fig.4.5. The possible structures, conformations and point groups of 2,2-dimethoxy propane molecule.

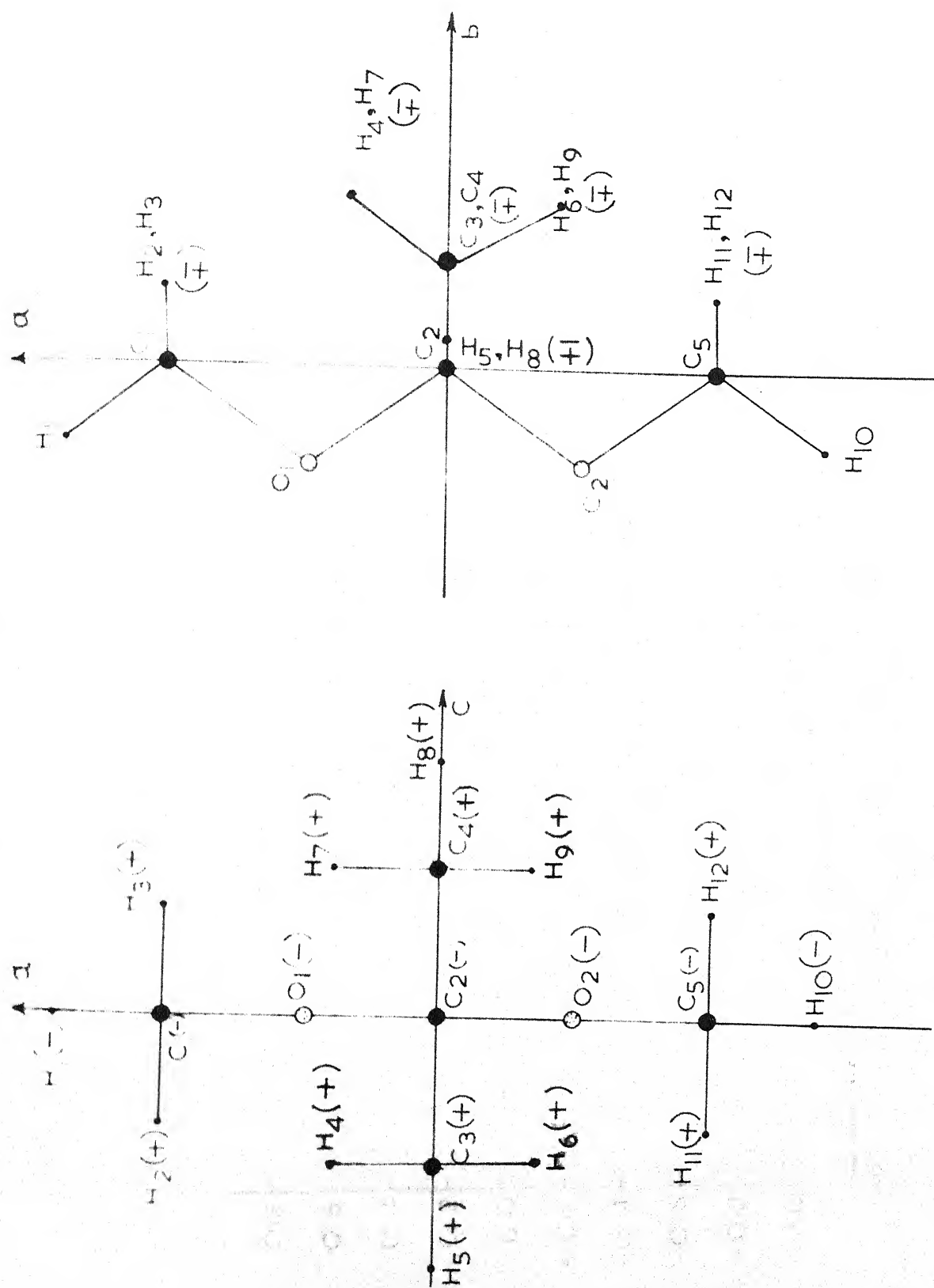


Fig.4.6. The projections of 2,2-dimethoxy propane molecule on the ab and ac planes of principal axes system for TT conformation.

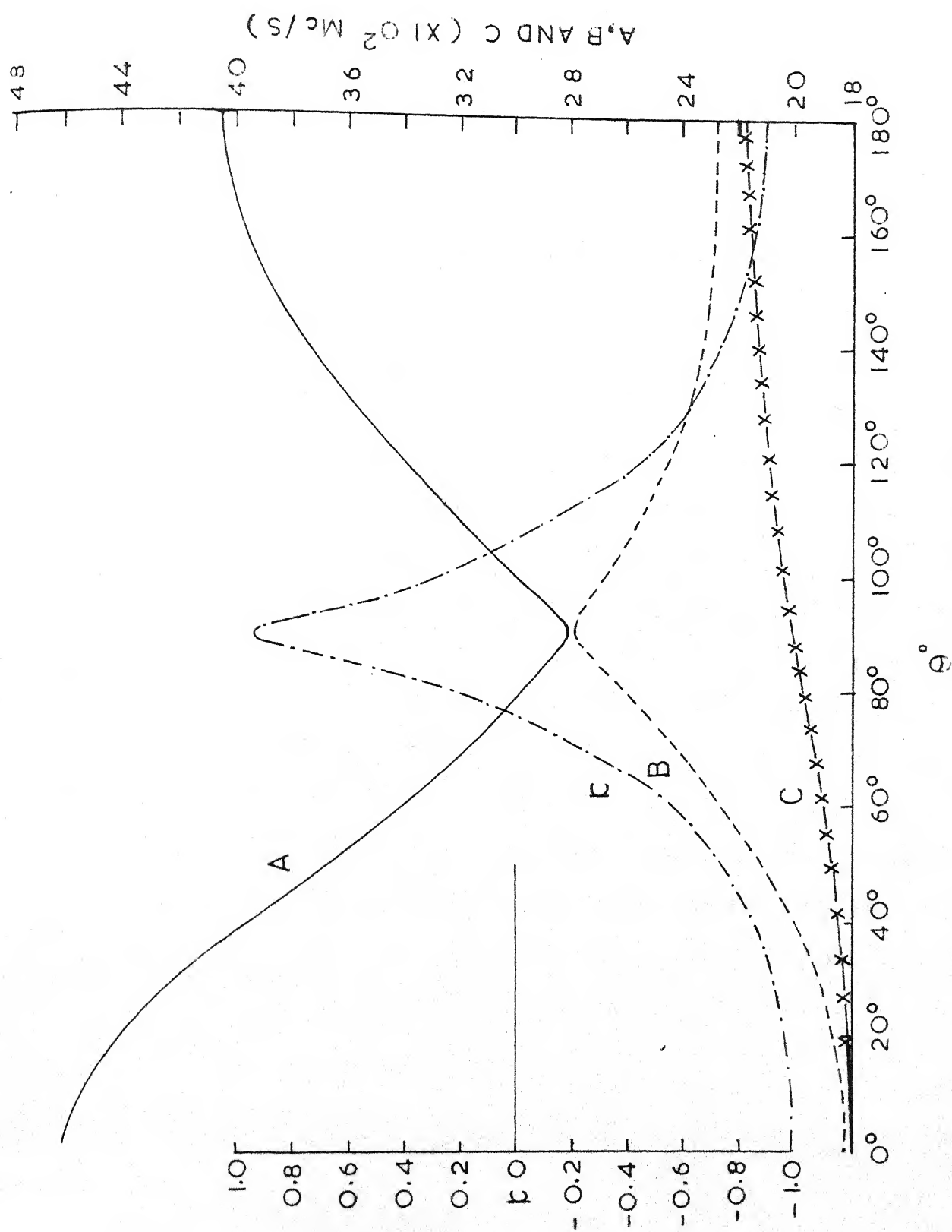


Fig.4.7. The rotational constants and asymmetry parameter as functions of the dihedral angle (θ).

CHAPTER V

VIBRATIONAL SPECTRA AND ROTATIONAL
ISOMERISM OF 1,1,1-TRIMETHOXY ETHANEABSTRACT

The liquid, vapour and solid state infrared spectra of 1,1,1-trimethoxy ethane were recorded in the region 250-4000 cm^{-1} . The laser-Raman spectrum with qualitative depolarization data was obtained for liquid only. The spectra show that there are at least two rotational isomers present in the liquid phase. The temperature dependence of the band intensities confirms the presence of rotational isomers. The solution spectra reveal that the less polar form is the more stable form in the liquid state. In vapour phase the molecule seems to possess a single configuration *Gauche-Gauche-Gauche* (GGG), other form(s) being almost absent. In solid state at low temperature the same configuration (GGG) gets stabilized. A vibrational assignment has been attempted for the observed infrared and Raman bands.

INTRODUCTION

The infrared spectrum of 1,1,1-trimethoxy ethane (TME) has been reported by Nukada in LiF and NaCl regions¹ and a partial assignment of the bands based on the solution spectra has been presented. The assignment is, however, by no means complete because of two reasons: Firstly the molecule is expected to exhibit rotational isomerism and therefore, the fluid phase spectrum may be quite complicated due to the presence of the bands associated with different isomers. Secondly, Nukada's investigations do not include Raman data and hence the structural information is not available. Though partial Raman spectrum of TME molecule has been reported by Braun and coworkers², no vibrational assignment was attempted by them. No other structural determinations seem to have been made for this molecule. Keeping in view the above mentioned facts, it was thought necessary to make a systematic study of the vibrational spectra of this molecule. We have studied the infrared spectra of this molecule in liquid, vapour and solid phases. The conformational equilibrium in this molecule is further studied in different solvents. The laser-Raman spectrum is photoelectrically recorded and qualitative depolarization ratios are determined in liquid phase.

The data are consistent with the co-existence of two rotational isomers in the liquid phase and only one isomer in the vapour and solid phases.

EXPERIMENTAL

The compound studied was a commercial material and was distilled prior to use.

The liquid phase spectrum was recorded by sandwiching a small quantity of the liquid between two CsBr plates. A part of the pure liquid phase spectrum and the spectra in CCl_4 and CHCl_3 solutions were studied using .025 mm thick fixed cell. The solid phase spectrum was recorded with the help of a low temperature cell. The initial deposit was properly annealed by warming and recooling of the film several times but no "crystalline peaks" appeared. Thus, in spite of annealing it seems that TME was completely or partially an amorphous glass. The infrared spectra of liquid, vapour and solid phases are shown in Figs. 5.1, 5.2 and 5.3 respectively.

The Raman spectrum of liquid only was recorded and is shown in Fig. 5.4.

The details of the instruments used and experimental procedure are given in Chapter II.

The infrared and Raman frequencies together with their assignments are listed in Table 5.3.

DISCUSSION

The 1,1,1-trimethoxy ethane (TME) molecule may, in principle exist in twenty seven configurations due to the internal rotation about

each of the three C-O Me bonds. However, several of them are spectroscopically indistinguishable. The spectroscopically distinct conformations are TTT, TTG, TGG, TGG', TG'G, GGG and GGG' (Fig. 5.5). The letters T and G denote the trans or gauche configurations about any C-O Me bond with respect to the CH₃ group. G' also denotes the gauche configuration but with rotation in the opposite sense to G. The steric interactions between the methyl groups do not favour TTT, TTG, TG'G and GGG' as the low energy conformations and hence these forms need not be considered seriously as the likely isomers. The TGG, TGG' and GGG forms could then be taken as the probable configurations of TME molecule.

The GGG form of the molecule belongs to C₃ point group symmetry and hence the fifty four fundamental modes will divide as

$$\Gamma_{\text{vib}} = 18 \underline{a} + 18 \underline{e}$$

both the a and e vibrations will be infrared and Raman active, the former appearing as polarized bands in the Raman spectrum. The calculations* of the Gerhard and Dennison³ parameter gives $\beta = - .362$ and hence the infrared vapour phase spectrum should show two types of bands, parallel type bands with a strong Q branch and a PR separation^{3,4} of $\sim 17 \text{ cm}^{-1}$ and perpendicular type bands with a medium weak Q branch and a PR spacing of $\sim 14 \text{ cm}^{-1}$.

The TGG configuration belongs to C₁ point group as there is no element of symmetry in this case. All the fifty four fundamental

*The calculation of the Gerhard and Dennison or Badger and Zumwalt parameters was done using the rotational constants given in Table 5.1 which were obtained assuming $r_{\text{C-O}} = 1.44 \text{ \AA}$, $r_{\text{C-C}} = 1.54 \text{ \AA}$ and all angles tetrahedral.

modes will be infrared and Raman active with all Raman bands being polarized. The calculation of the Badger and Zumwalt⁵ parameters gives $K = -0.165$ and $\rho^* = .514$ and hence the infrared spectrum of the gas should show three types of band contours, the A type contours having a medium Q branch with a PR spacing^{4,5} of $\sim 14 \text{ cm}^{-1}$, the B type contours having a PQQR type structure with a PR spacing of $\sim 10 \text{ cm}^{-1}$ and $\Delta \nu(QQ) \sim 2.5 \text{ cm}^{-1}$ and the C type bands having a strong Q branch with a PR spacing of $\sim 21 \text{ cm}^{-1}$.

The TGG' form should ideally have a plane of symmetry (C_s point group) and hence it should possess 30 \underline{a}' and 24 \underline{a}'' type of vibrations the latter appearing as depolarized bands in the Raman spectrum. However, the lone pair interactions of the oxygen atoms may twist the two OCH_3 groups in opposite senses and thus destroy the C_s symmetry of the molecule. The molecule would then belong to C_1 symmetry and all fifty four modes would be infrared and Raman active. All the Raman lines would appear as polarized bands. The Badger and Zumwalt parameters for this configuration are $K = -0.429$ and $\rho^* = .784$ and hence the infrared spectrum of the gas should exhibit three types of band contours; type A should have a strong Q branch with a PR separation^{4,5} of $\sim 14 \text{ cm}^{-1}$, type B bands should appear with a PR separation of $\sim 10 \text{ cm}^{-1}$ and possibly PQQR type structure having $\Delta \nu(QQ) \sim 6 \text{ cm}^{-1}$ and the C type contours should show a medium Q branch with $\sim 20 \text{ cm}^{-1}$ separation between P and R branches.

The description of vibrations under the different point group symmetries is given in Table 5.2.

A close study of the gaseous infrared band contours reveals that the shape of the band contours is essentially of the type expected for GGG configuration which indicates that this form of the molecule is predominant in the vapour phase.

The interpretation of the vibrational spectra of TME can be carried out only when the bands due to different isomers could be separated. The method which has been successfully employed for many compounds, is to observe the solid state spectrum, as only one of the isomers is expected to crystallize in the lattice. The solid phase spectrum is not very much different from fluid phase spectra in the region of CH_3 group vibrations except for a few changes in the intensity of bands. However, in the skeletal frequency region certain bands disappear on solidification. The bands appearing at 480 and 745 cm^{-1} in the liquid phase are not observed in the solid state spectrum. This behaviour indicates that more than one rotational isomers are present in the liquid state and one of them gets stabilized in the solid state at low temperatures.

It may be seen by comparing the liquid and vapour phase spectra that the band corresponding to the liquid state band at 480 cm^{-1} is missing in the vapour phase spectrum. However, it is difficult to predict whether the band corresponding to the weak shoulder at 745 cm^{-1} in the liquid phase is present or absent in the vapour phase as the band to which it appears as a shoulder in liquid phase is very weak and further, it gets broadened in the vapour phase. The disappearance of the 480 cm^{-1} band probably indicates that the concentration of one

rotational isomer decreases considerably upon vapourization, almost to the point of being negligible.

The temperature dependence of the pair of bands at 480 and 516 cm^{-1} in liquid phase demonstrates convincingly that TME molecule exists as a mixture of at least two rotational isomers in the liquid phase. As the temperature is lowered the intensity of the low frequency component of the doublet increases markedly. This behaviour indicates that these bands are due to two different conformations of the molecule.

In order to determine the relative polarities of the two forms, infrared spectra of TME in carbon tetrachloride and chloroform solutions were studied. The pair of bands at 516 and 480 cm^{-1} was chosen for this purpose. Relative intensity of this pair $\left\{ \frac{I_{516}}{I_{480}} \right\}$ decreases considerably in carbon tetrachloride solution, whereas an increase in the relative intensity is observed in chloroform solution. This means that the band at 516 cm^{-1} is due to more polar form of the molecule. The fact that 516 cm^{-1} band is present in the solid state spectrum suggests that the more polar form is the one present in the solid state.

The point group symmetry of TME will be C_3 if it assumes GGG configuration and C_1 if it assumes any of the configurations TGG and TGG'. For the purpose of comparison, the e type modes in C_3 symmetry should be viewed as a type modes under C_1 symmetry (each e mode will correspond to two a type of modes). But a type modes transform to a type of modes only, when the symmetry is lowered from C_3 to C_1 .

As discussed earlier, the molecule probably assumes a single configuration in the vapour and solid phases, whereas in the liquid state it exists as a mixture of two rotational isomers. The infrared band contours suggest that the probable form of the molecule in the vapour phase is GGG (C_3 symmetry). The Raman depolarization data (as many depolarized Raman bands are present) and the number of infrared and Raman bands also favour this configuration. The presence of two rotational isomers in the liquid phase (one having C_3 symmetry and the other having C_1 symmetry) makes the depolarization data unreliable for the assignment purposes. This is because of the simple reason that though a vibration belonging to e specie under C_3 symmetry is expected to appear as depolarized band in the Raman spectrum, it may appear as polarized band if another isomer with C_1 symmetry is present as its a type of vibrations may overlap with e type vibrations in cases when the bands due to two isomers are not separated.

Assignment of Fundamentals

CH Stretchings

The CH stretching vibrations associated with the CH_3O and CH_3C groups are expected to be in the region $2800 - 3050\text{ cm}^{-1}$. It may not be unreasonable to suppose that the three CH_3 groups connected to the oxygen atom do not couple with each other as they are separated by O-C-O group, so, one may expect that the nine CH stretching modes would occur at the corresponding frequencies of the individual CH_3 group. This region may also contain overtones and combinations of the deformation

Raman counterpart of this infrared band is not available which is generally the case for this vibration. Two more infrared bands are available in the expected range for CH_3 deformation modes. They are observed at 1452 and 1472 cm^{-1} . The band at 1452 cm^{-1} could be assigned to the unsymmetric CH_3O deformation mode in analogy with the assignments for dimethyl ether and 1,2-dimethoxy ethane⁸ where the unsymmetric deformation mode is assigned at lower frequency than the symmetric mode. The unsymmetric CCH_3 and symmetric OCH_3 deformation vibrations are yet to be assigned and only one infrared band at 1472 cm^{-1} is available. However, the Raman spectrum shows two bands near here, one at 1460 cm^{-1} and the other at 1470 cm^{-1} , the latter appearing as shoulder to the former one. It is quite probable that these bands overlap in the infrared spectrum but get separated in the Raman spectrum. The depolarized Raman band at 1460 cm^{-1} and the band at 1470 cm^{-1} have been chosen for the unsymmetric CCH_3 deformation and symmetric OCH_3 deformation modes respectively.

CH_3 Rockings

The region $1100\text{--}1200\text{ cm}^{-1}$ may be highly overlapped because both the C-O stretching and CH_3O rocking vibrations are expected to fall in this region. There are certain intensity changes in the infrared bands while going from liquid to solid phase. However, there is not much change in the liquid and vapour phase spectra. The infrared band at 1255 cm^{-1} and the depolarized Raman band at 1245 cm^{-1} are assigned to the methoxy rocking mode. The liquid phase infrared band at 1244 cm^{-1} is slightly asymmetric and the solid phase spectrum shows two peaks near

here at 1240 and 1250 cm^{-1} . The appearance of the new band may be due to the sharpening of the bands at low temperatures. These bands have been assigned to OCH_3 rocking modes. The infrared band at 1222 cm^{-1} and the polarized Raman band at 1200 cm^{-1} may be attributed to the symmetric CH_3O rocking mode in analogy with trimethoxy methane where the corresponding mode has been placed at 1237 cm^{-1} ⁹. The remaining unsymmetric CH_3O rocking mode has been placed at 1182 cm^{-1} in the infrared spectrum. The Raman counterpart of this band is observed at 1175 cm^{-1} and seems to be depolarized. The unsymmetric CH_3C rocking mode may be ascribed to the perpendicular type infrared band at 1136 cm^{-1} and the depolarized Raman band at 1115 cm^{-1} . This completes the assignment of the five active rocking vibrations of the methoxy and methyl groups.

Skeletal Modes

Once the assignment of the fundamental modes related to the CH_3 groups of the molecule is achieved, it becomes possible to assign the skeletal modes of vibration. The perpendicular band at 1155 cm^{-1} in the infrared and the depolarized Raman band at 1152 cm^{-1} have been assigned to the unsymmetric C-O stretching vibration. The symmetric part of this, vibration may be assigned with considerable certainty to the weak infrared band at 736 cm^{-1} and very strong polarized Raman band at 738 cm^{-1} . The unsymmetric and symmetric $\text{CH}_3\text{-O}$ stretching vibrations are expected to show a little splitting because of the smaller coupling of these vibrations. Therefore, the close bands at 1069 and 1058 cm^{-1} have been assigned to the symmetric and unsymmetric vibrations respectively. The above assignment is based on the shape of the infrared band contours.

The Raman spectrum however, shows one broad band at 1048 cm^{-1} and seems to be polarized. The assignment of the C-C stretching mode is still left. The infrared band at 893 cm^{-1} which appears to be parallel type in nature and the polarized Raman band at 891 cm^{-1} have been attributed to the C-C stretching vibration.

The assignment of the skeletal bending modes seems to be little difficult. Two symmetric and three unsymmetric bending vibrations are expected to fall in the region $650\text{--}300\text{ cm}^{-1}$. In this region, only one band which lies at 560 cm^{-1} appears to be depolarized in the Raman spectrum while the rest of the bands are clearly polarized. However, Raman depolarization data can not always be a definite proof for the band assignment. So, some of these bands have to be assigned to the unsymmetric modes. The assignment of these bands may be guided by the intensity of the bands in the infrared and Raman spectra. A further help may be taken by looking at the spectra of similar molecules like 1,2-dimethoxy ethane⁸, trimethoxy methane and tetramethoxy methane⁹. The infrared bands at 625 and 518 cm^{-1} may be chosen for the unsymmetric and symmetric OCO bending vibrations respectively. The shape of the vapour phase infrared band contour for 518 cm^{-1} band resembles the shape of parallel type band expected for this molecule. The corresponding Raman bands are observed at 621 and 519 cm^{-1} respectively. The depolarised Raman band at 560 cm^{-1} and the corresponding infrared band at 559 cm^{-1} may be arising due to OCC rocking mode. The close doublet at 412 and 385 cm^{-1} in the solid state spectrum probably owes its existence to the unsymmetric and symmetric COC bending vibrations. The liquid phase infrared spectrum shows the lower frequency component as a shoulder

but it becomes quite clear in solid phase due to the sharpening of bands at low temperatures. The observed small splitting between the unsymmetric and symmetric COC bending modes is in accordance with the fact that the individual bending vibrations may not be much coupled with each other.

Torsional Modes

The assignment of torsional modes is highly ambiguous because of the reason that many difference bands may as well fall in the region of torsional modes. Three bands are observed in the Raman spectrum at 315, 235 and 140 cm^{-1} , whereas in total we have to assign five torsional modes. The bands at 315 and 235 cm^{-1} are in the proximity of the expected frequencies for the OCH_3 and CCH_3 torsional modes. The band at 315 cm^{-1} may be chosen for the CCH_3 torsional vibration and the remaining one at 235 cm^{-1} may be ascribed to the OCH_3 torsional modes. The symmetric and unsymmetric torsional modes may not show much splitting and hence they may be assigned to the same band (235 cm^{-1}). As the bands which could be assigned to the skeletal torsions are not available, their assignments have not been attempted.

All the other bands could be satisfactorily interpreted as overtone or combination bands. Their assignments have been listed in Table 5.3.

REFERENCES

1. K. Nukada, J. Chem. Soc. Japan, 81, 1028 (1960).
2. W.G. Braun, D.F. Spooner and M.R. Fenske, Anal. Chem., 22, 1074 (1950).
3. S.L. Gerhard and D.M. Dennison, Phys. Rev., 43, 197 (1933).
4. W.A. Seth-Paul and G. Dijkstra, Spectrochim. Acta, 23, 2861 (1967).
5. R.M. Badger and L.R. Zumwalt, J. Chem. Phys., 6, 711 (1938).
6. P. Venkateswarlu, J. Chem. Phys., 19, 293 (1951).
7. P. Venkateswarlu, J. Chem. Phys., 19, 298 (1951).
8. R.G. Snyder and G. Zerbi, Spectrochim. Acta, 23, 391 (1967).
9. H. Lee and J.K. Wilmschurst, Spectrochim. Acta, 23, 347 (1967).

TABLE 5.1

Molecular Parameters of 1,1,1-Trimethoxy ethane

	Molecular configurations		
	TGG	TGG'	GGG
I_A ($\text{amu-}\text{\AA}^2$)	189.33	163.81	215.69
I_B ($\text{amu-}\text{\AA}^2$)	246.06	255.59	215.69
I_C ($\text{amu-}\text{\AA}^2$)	313.27	329.32	337.98
A (cm^{-1})	.0890	.1028	.0781
B (cm^{-1})	.0684	.0659	.0781
C (cm^{-1})	.0538	.0511	.0498

TABLE 5.2

Description and Symmetry of the Normal Modes of Vibration* of
1,1,1-Trimethoxy ethane Molecule Under the Point Groups C_3 and C_1 .

Symmetry species		Approximate description			
C_1	C_3				
1	2	3	4	5	6
		ν_1	CH_3O	st.	(unsym.)
		ν_2	CH_3O	st.	(unsym.)
		ν_3	CH_3C	st.	
		ν_4	CH_3O	st.	(sym.)
		ν_5	CH_3O	def.	(sym.)
		ν_6	CH_3O	def.	(unsym.)
		ν_7	CH_3O	def.	(unsym.)
		ν_8	CH_3C	def.	
a	a	ν_9	CH_3O	rock.	
		ν_{10}	CH_3O	rock.	
		ν_{11}	H_3C-O	st.	
		ν_{12}	H_3C-C	st.	
		ν_{13}	$C-O$	st	
		ν_{14}	OCO	def.	
		ν_{15}	COC	def.	
		ν_{16}	CCH_3	tors.	
		ν_{17}	OCH_3	tors.	
		ν_{18}	$O-CH_3$	tors.	

Contd.

Table 5.2 (contd.)

1	2	3	4	5	6
2a	e	ν_{19}	CH_3C	st.	
		ν_{20}	CH_3O	st.	(unsym.)
		ν_{21}	CH_3O	st.	(unsym.)
		ν_{22}	CH_3O	st.	(sym.)
		ν_{23}	CH_3O	def.	(sym.)
		ν_{24}	CH_3C	def.	(unsym.)
		ν_{25}	CH_3O	def.	(unsym.)
		ν_{26}	CH_3O	def.	(unsym.)
		ν_{27}	CH_3O	rock.	
		ν_{28}	CH_3O	rock.	
		ν_{29}	C-O	st.	
		ν_{30}	CH_3C	rock.	
		ν_{31}	$\text{H}_3\text{C-O}$	st.	
		ν_{32}	OCO	def.	
		ν_{33}	OCC	rock.	
		ν_{34}	COC	def.	
		ν_{35}	OCH_3	tors.	
		ν_{36}	O-CH_3	tors	

Abbreviations : st. = stretching, def. = deformation, rock. = rocking,
 tors. = torsion, sym. = symmetric, unsym. = unsymmetric.

*The numbering of vibrations is according to C_3 symmetry.

TABLE 5.3

Infrared and Raman Spectra of 1,1,1-Trimethoxy ethane

Infrared							Raman effect in			Assignment*
Vapour			Liquid		Solid		liquid			
cm ⁻¹	Int.	Type	cm ⁻¹	Int.	cm ⁻¹	Int.	cm ⁻¹	Int.	Polzn.	
1	2	3	4	5	6	7	8	9	10	11
							140	br,w	dp?	$\nu_{3-}\nu_{34}$
							235	br,w	dp?	OCH_3 tors., ν_{35}
282	vw		303	w	315	w	315	m	p	CCH_3 tors., ν_{16}
			396	sh	385	w	400	sh		COC sym.def., ν_{15}
414	w		411	w	412	m	415	s	p	COC unsym.def., ν_{34}
			480	vw			480	m	p	OCO def.(isomer)
510	w		516	m	523	s	519	m	p	OCO sym.def., ν_{14}
518										
524										
559	vw		558	w	561	m	560	m	dp	OCC rock., ν_{33}
625	w		625	m	628	m	621	s	p	OCO unsym.def., ν_{32}
736	vw		736	w	732	w	738	vs	p	C-O sym.st., ν_{13}
			745	sh						C-O st. (isomer)
							848	w	p	$\nu_{14}^+ \nu_{16}$
893	s		890	s	890	s	891	m	p	$\text{H}_3\text{C-C}$ st., ν_{12}
900										

contd.

Table 5.3 (contd.)

1	2	3	4	5	6	7	8	9	10	11
1050 } 1058 } - }	s	⊥	1040	s	1045	s				H ₃ C-O unsym.st., \checkmark_{31}
- } 1069 } 1075 }	s		1053	s	1057	s	1048	br,s	p	H ₃ C-O sym.st., \checkmark_{11}
1090	sh		1075	m	1070	m	1078	s	p	$\checkmark_{14} + \checkmark_{33}$
~1128 } 1136 } 1145 }	m	⊥	1125	m	1121	s	1115	m	dp?	CH ₃ C rock., \checkmark_{30}
- } 1155 } 1163 }	m	⊥	1150	m	1142	s	1152	m	dp?	C-O st., \checkmark_{29}
- } 1182 } 1187 }	vs		1172	vs	1171	s	1175	m	dp?	CH ₃ O rock., \checkmark_{28}
1215 } 1222 } - }	m		1214	m	1212	s	~1200	m	p	CH ₃ O rock., \checkmark_{10}
1255	m		1244	m	1240	s	1245	w	dp	CH ₃ O rock., \checkmark_{27}
					1250	s				CH ₃ O rock., \checkmark_9
1376 } 1386 } 1395 }	s		1384	s	1383	s				CH ₃ C def.(sym), \checkmark_8
1441 } 1452 } - }	m	?	1435	m	1424	m				CH ₃ O def.(unsym), $\checkmark_3, \checkmark_6, \checkmark_7, \checkmark_{25}, \checkmark_{26}$
- } 1472 } 1481 }	m	?	1467	m	1472	m	1460	s	dp	CH ₃ C def.(unsym), \checkmark_{24}
							1470	sh		CH ₃ O def.(sym), $\checkmark_5, \checkmark_{23}$

Contd.

Table 5.3 (contd.)

1	2	3	4	5	6	7	8	9	10	11
2846	s		2833	s	2833	w	2838	s	p	CH ₃ O st.(sym), ν_4, ν_{22}
2923	w		2915	w	2888	w	~2910	w	p	CH ₃ C st., ν_3
2958	s	1								
2965			2946	s	2923	w	2950	s	p	CH ₃ O st.(unsym)
2975										$\nu_1, \nu_2, \nu_{20}, \nu_{21}$
~2970	w		2968	w	2963	w				
3002	s		2998	w	2983	m	3008	m	dp	CH ₃ C st., ν_{19}

Abbreviations : s = strong, m = medium, w = weak, vs = very strong,

vw = very weak, sh = shoulder, p = polarized,

dp = depolarized, sym = symmetric and unsym = unsymmetric.

*The numbering of vibrations has been given according to the C₃ symmetry.

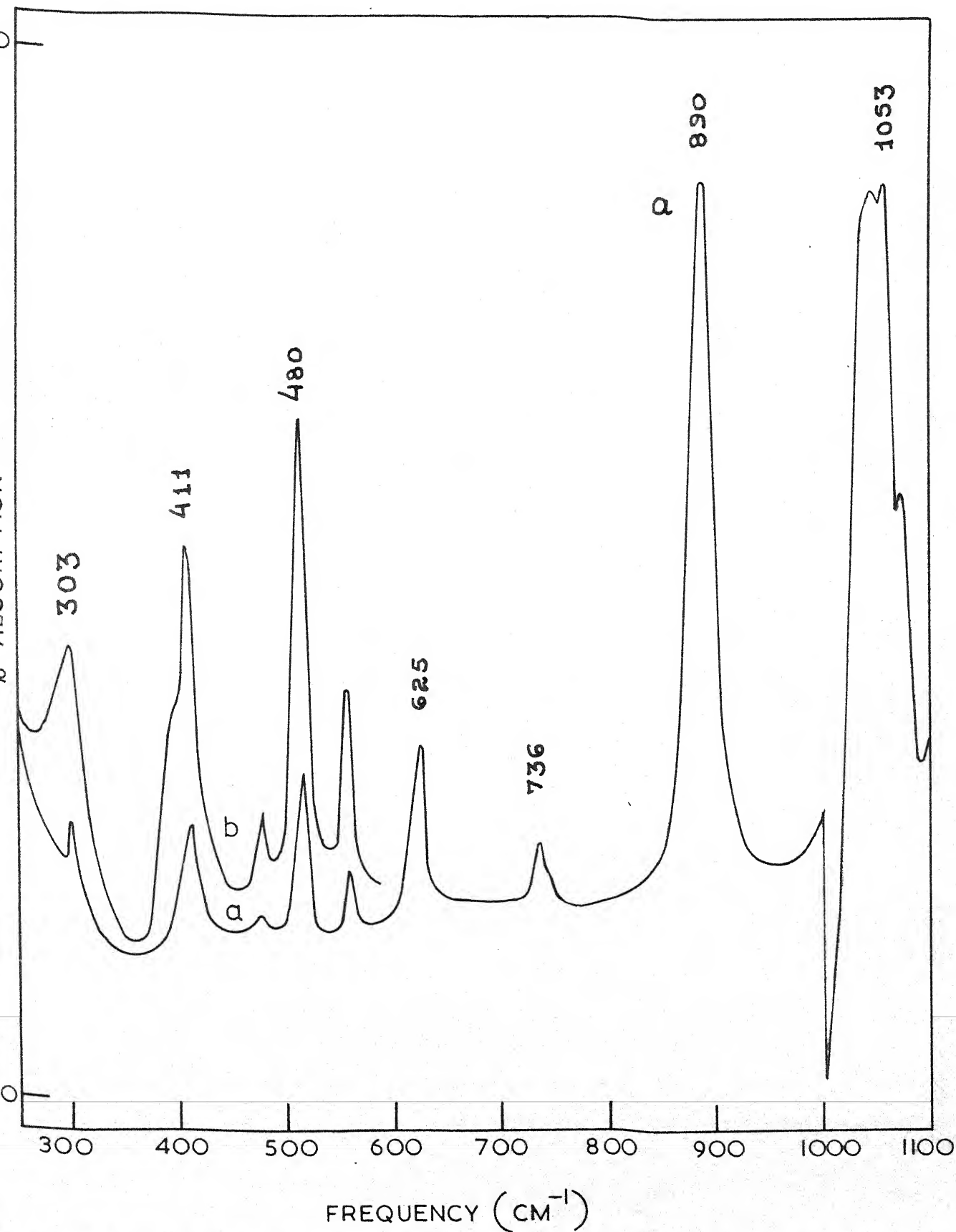


Fig.5.1(a). The infrared spectrum of liquid 1,1,1-trimethoxy ethane in the region 250-1100 cm^{-1} ; (a) thin film (b) .025 mm thick cell.

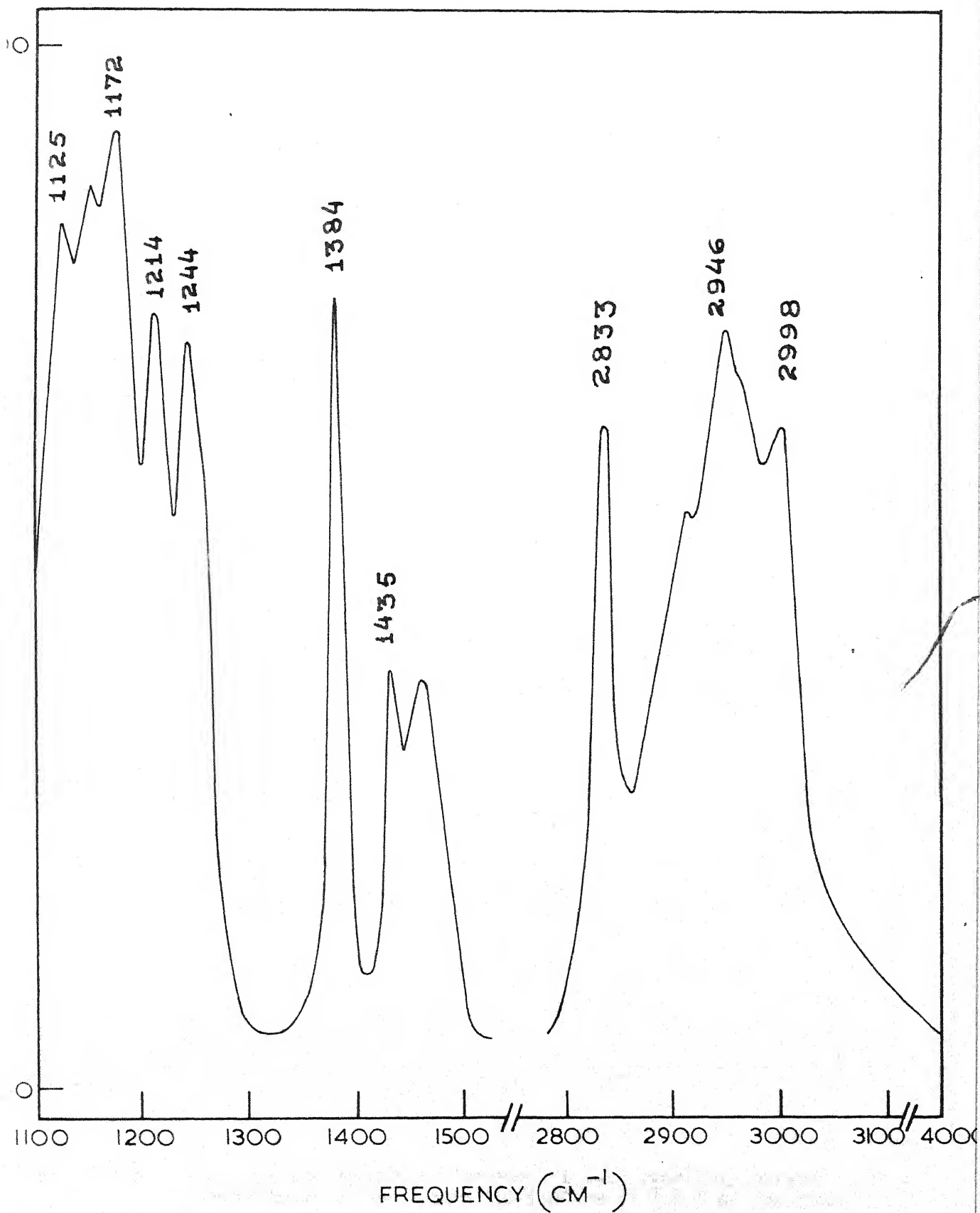


Fig.5.1(b). The infrared spectrum of liquid 1,1,1-trimethoxy ethane in the region 1100-4000 cm^{-1} ; thin film.

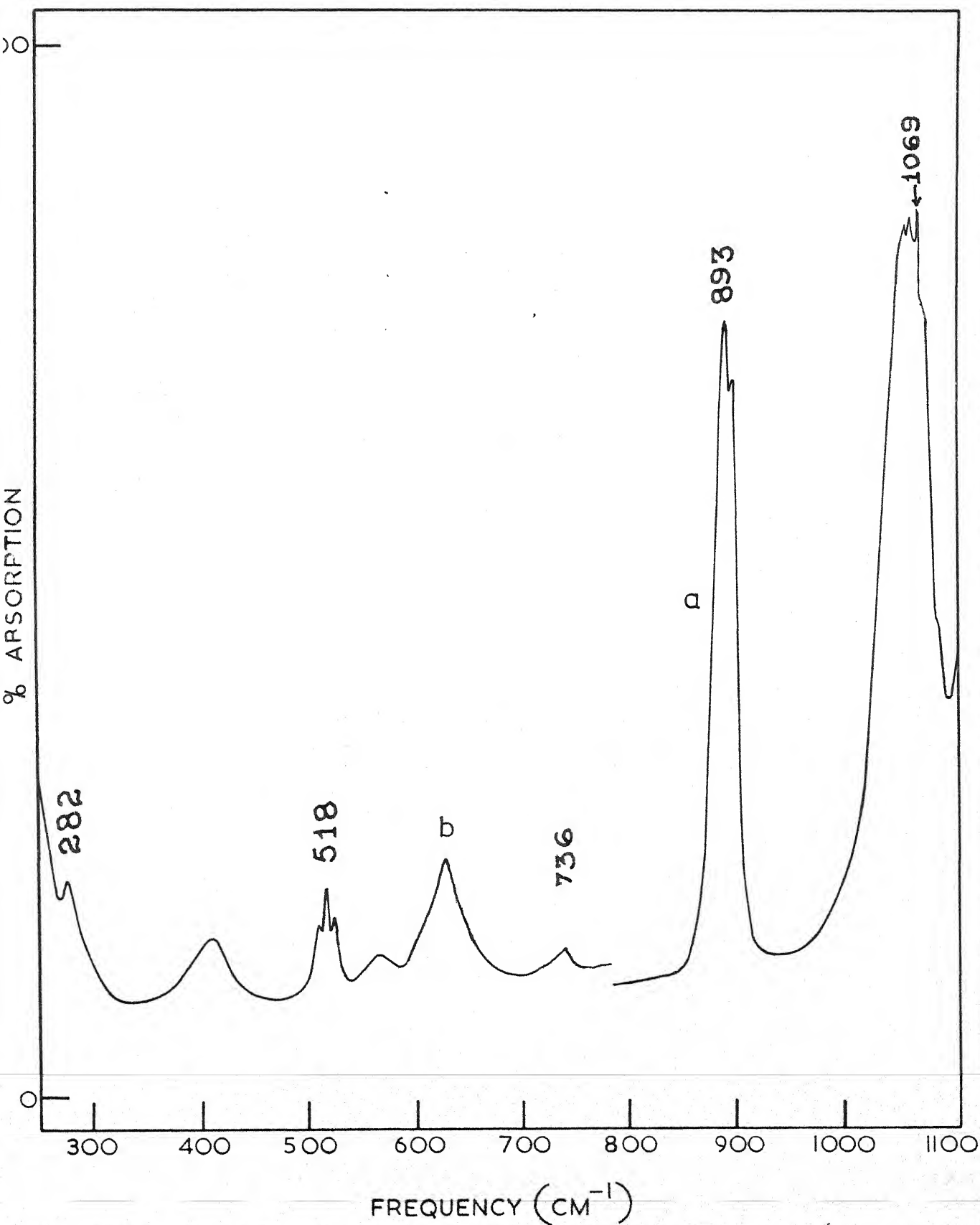


Fig. 5.2(a). The infrared spectrum of gaseous 1,1,1-trimethoxy ethane at room temperature in the region 250-1100 cm⁻¹: (a) 5 cm gas cell, (b) 10 cm gas cell.

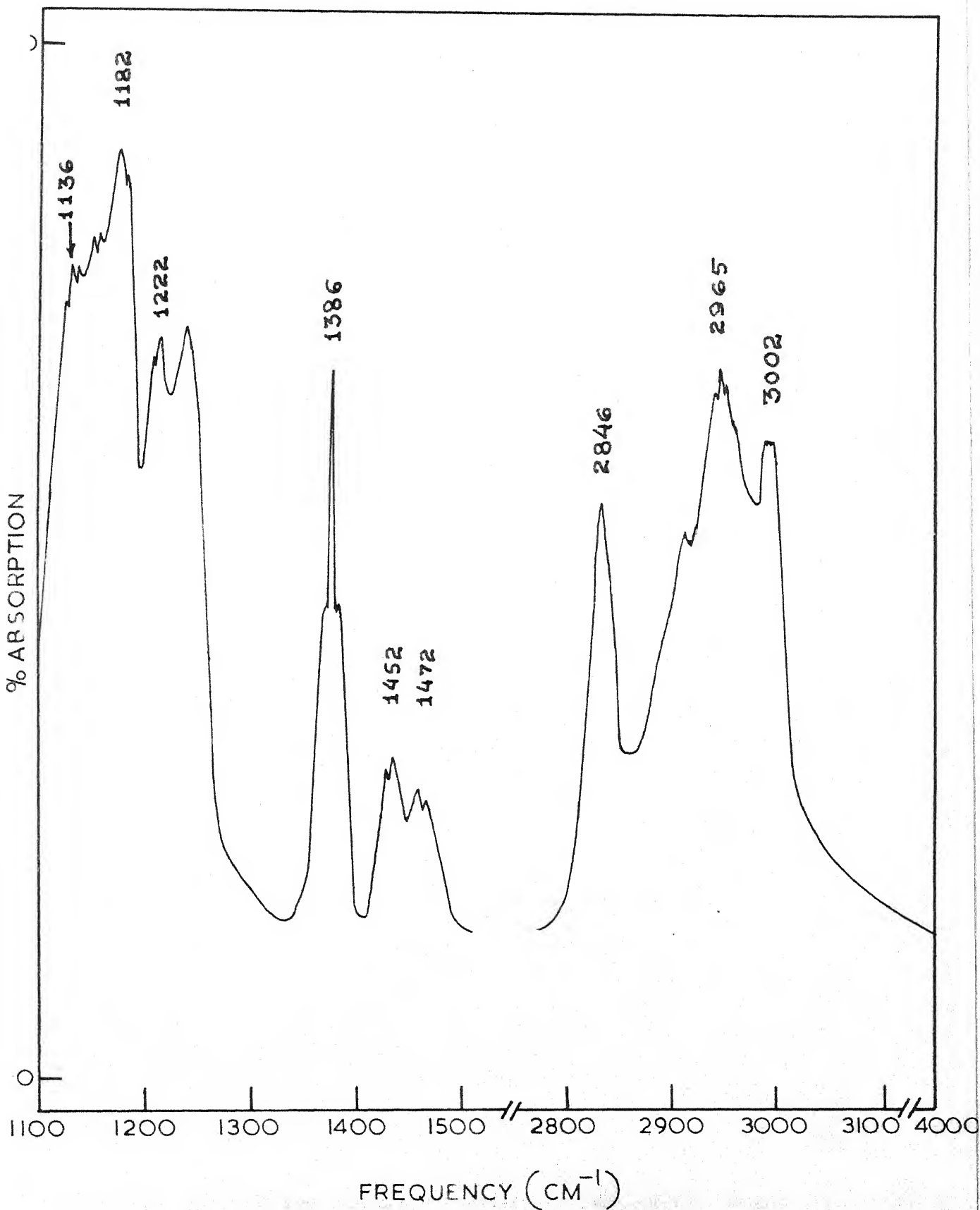


Fig.5.2(b). The infrared spectrum of gaseous 1,1,1-trimethoxy ethane at room temperature in the region 1100-4000 cm⁻¹: 5 cm gas cell.

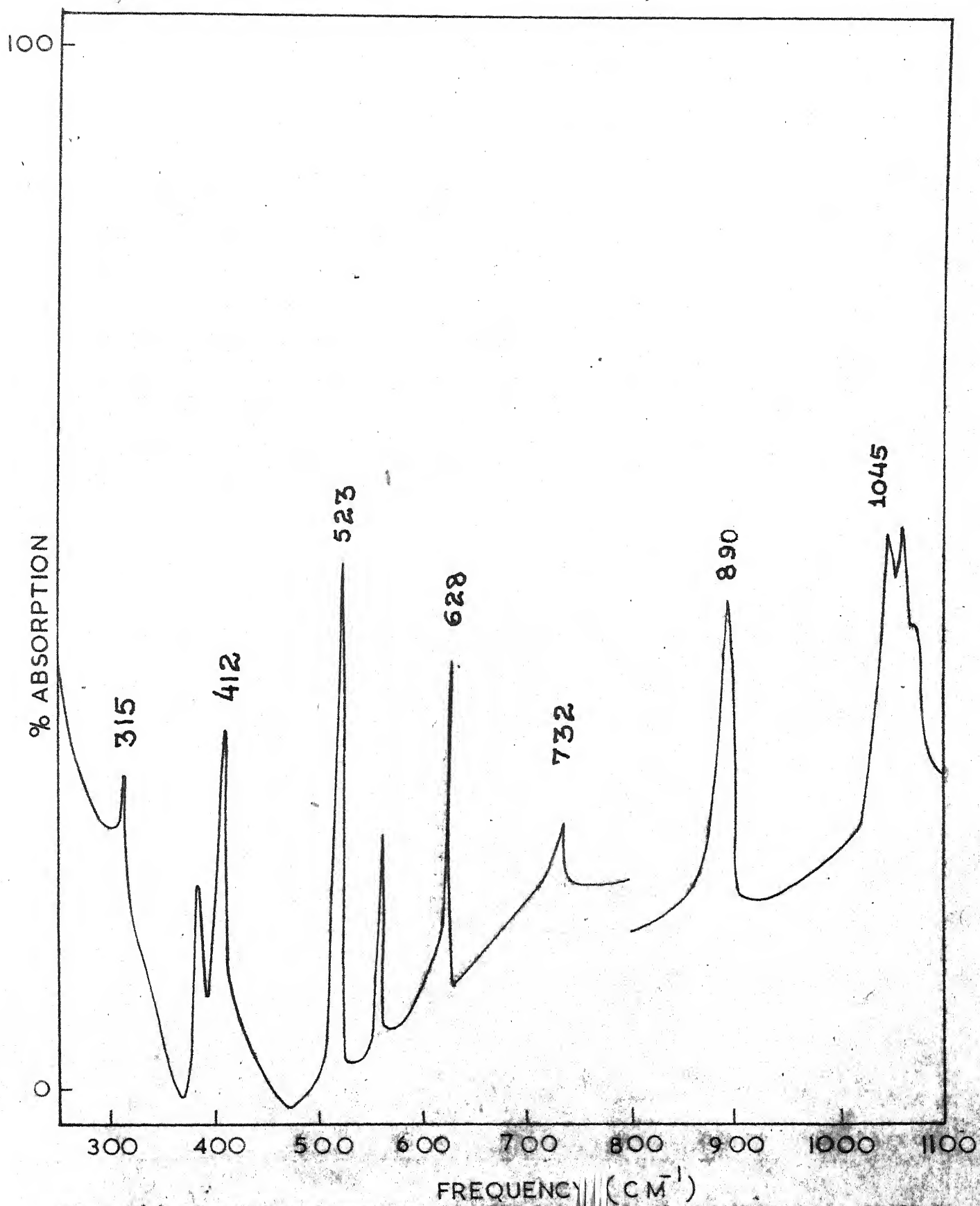


Fig. 5.3(a). The infrared spectrum of solid 1,1,1-trimethoxy ethane near -196°C in the region $250-1100\text{ cm}^{-1}$.

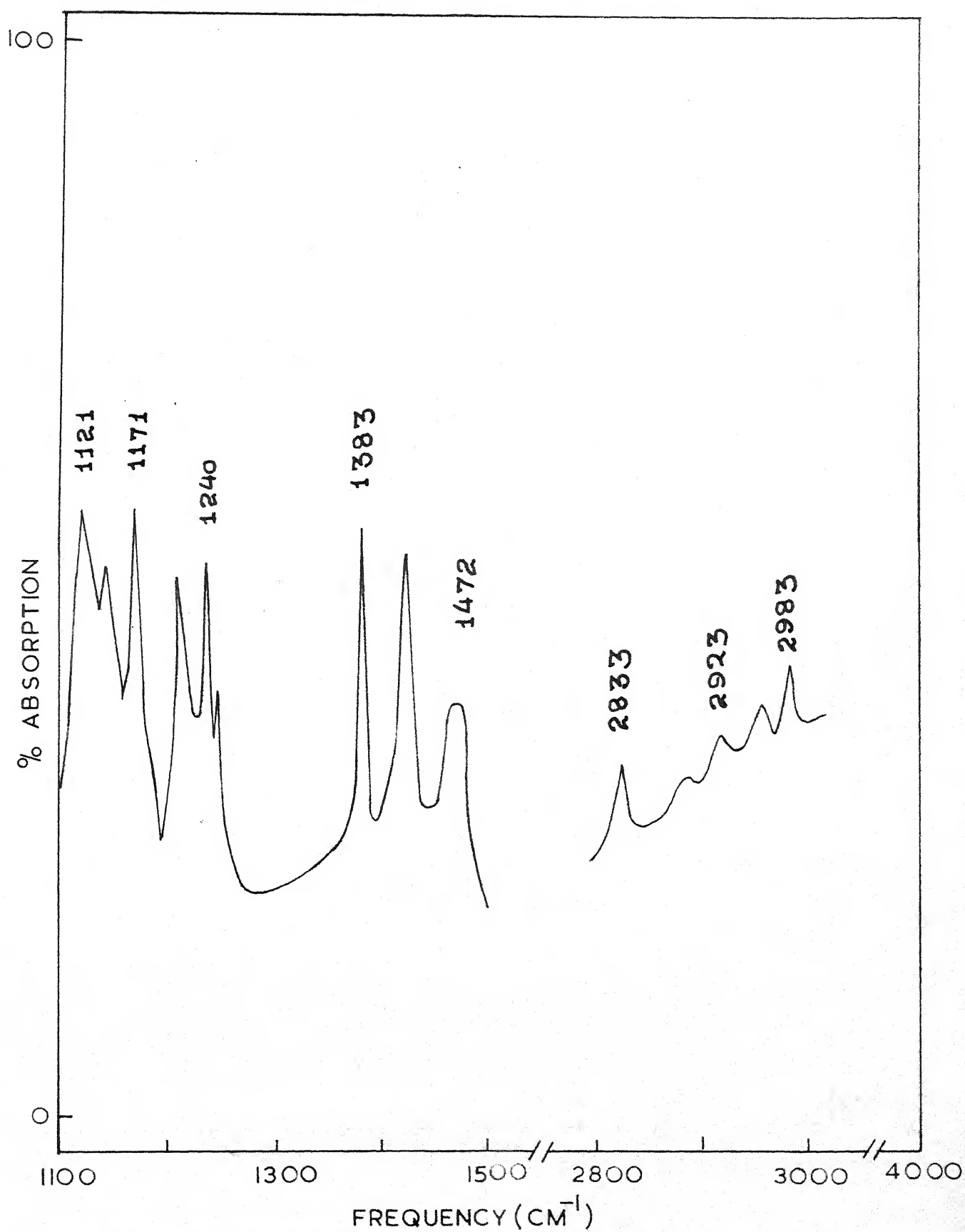


Fig.5.3(b). The infrared spectrum of solid 1,1,1-trimethoxy ethane near -196°C in the region 1100-4000 cm⁻¹.

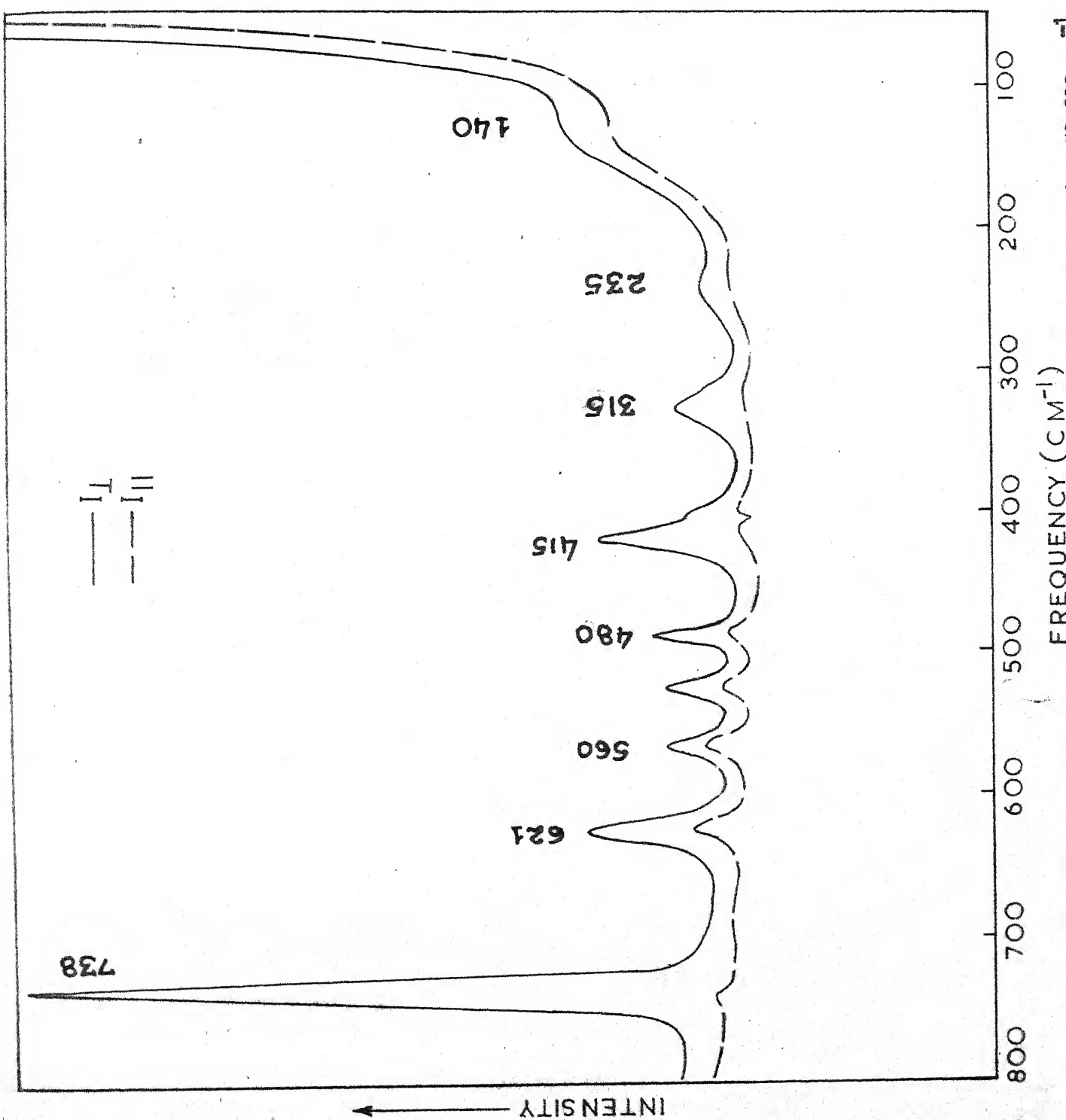


Fig. 5.4(a). The Raman spectrum of liquid 1,1,1-trimethoxy ethane in the region 50-800 cm^{-1} .

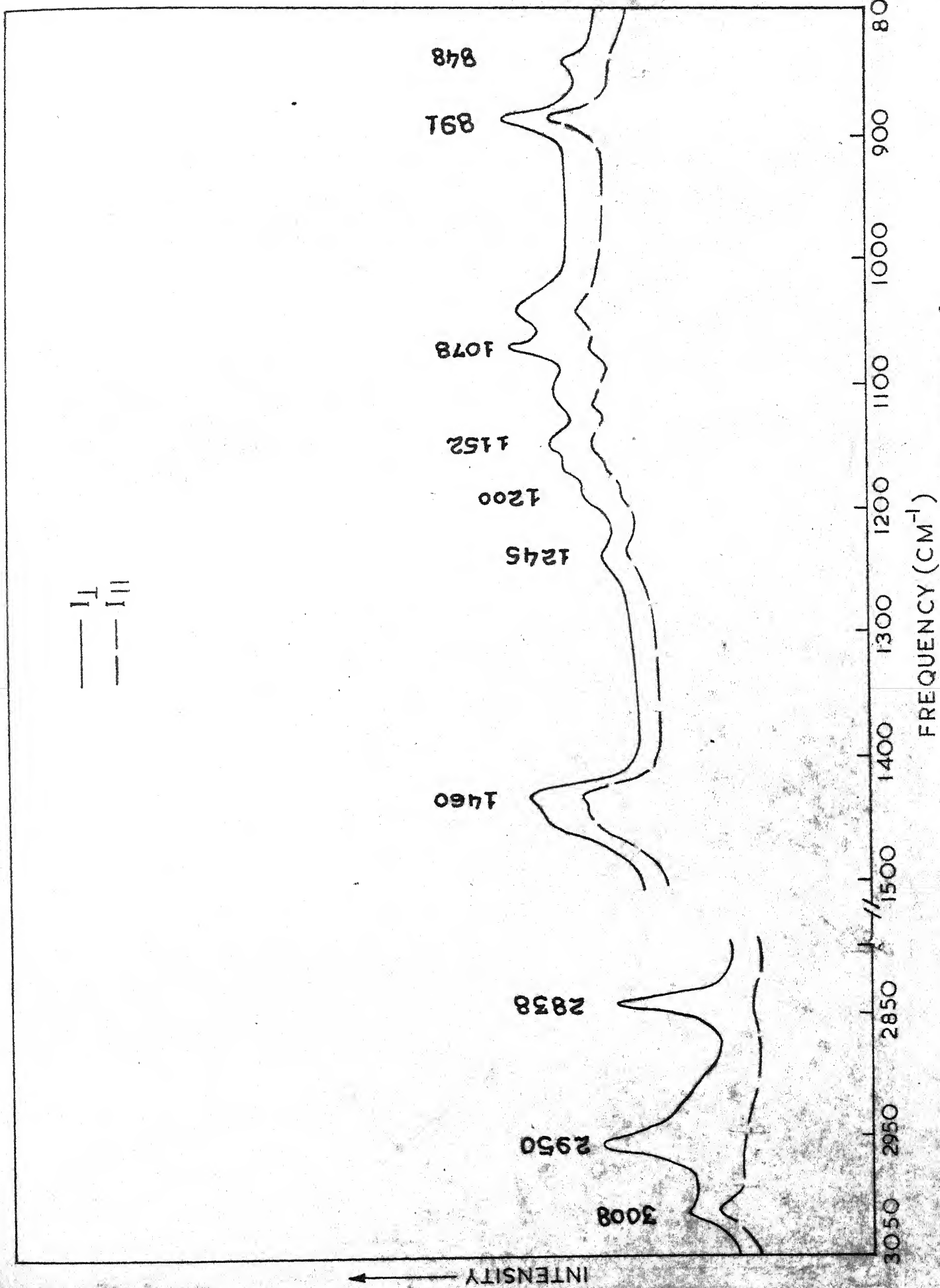


Fig. 5.4(b). The Raman spectrum of liquid 1,1,1-trimethoxy ethane in the region 800-3050 cm⁻¹.

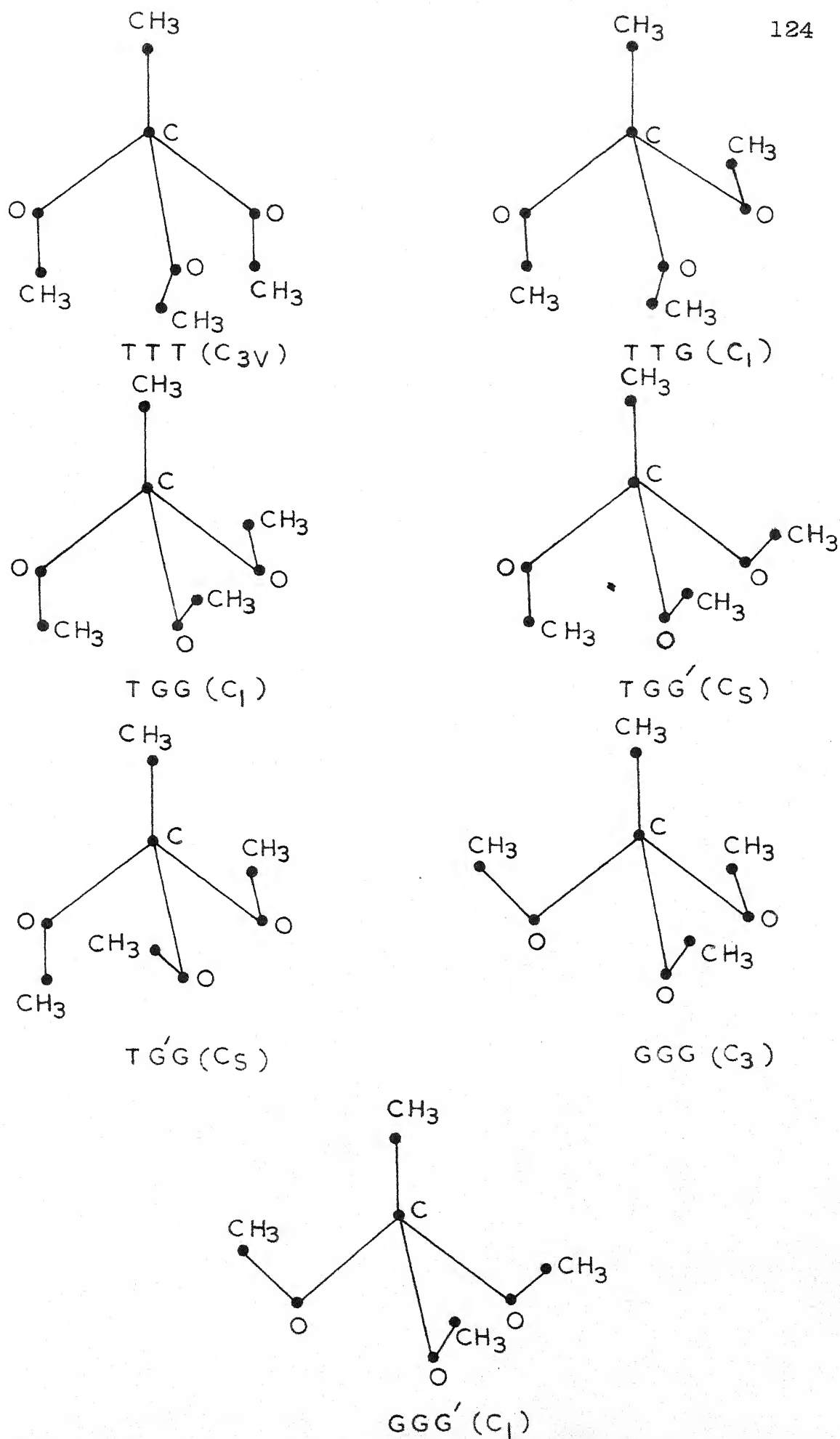


Fig.5.5. The spectroscopically distinguishable configurations of 1,1,1-trimethoxy ethane molecule.

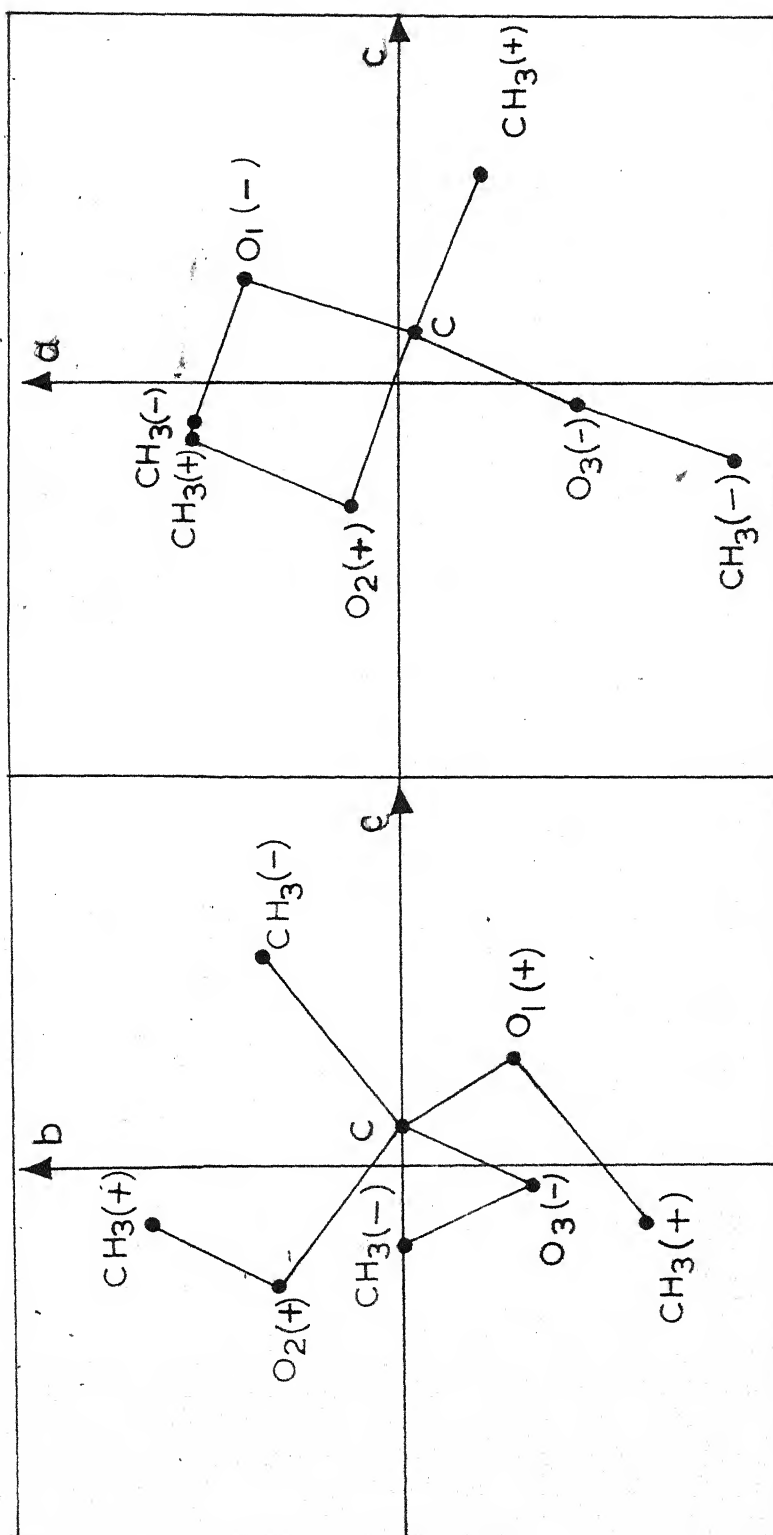


Fig. 5.6. The projections of TGG configuration of 1,1,1-trimethoxy ethane molecule on ab and bc planes of the principal axes system.

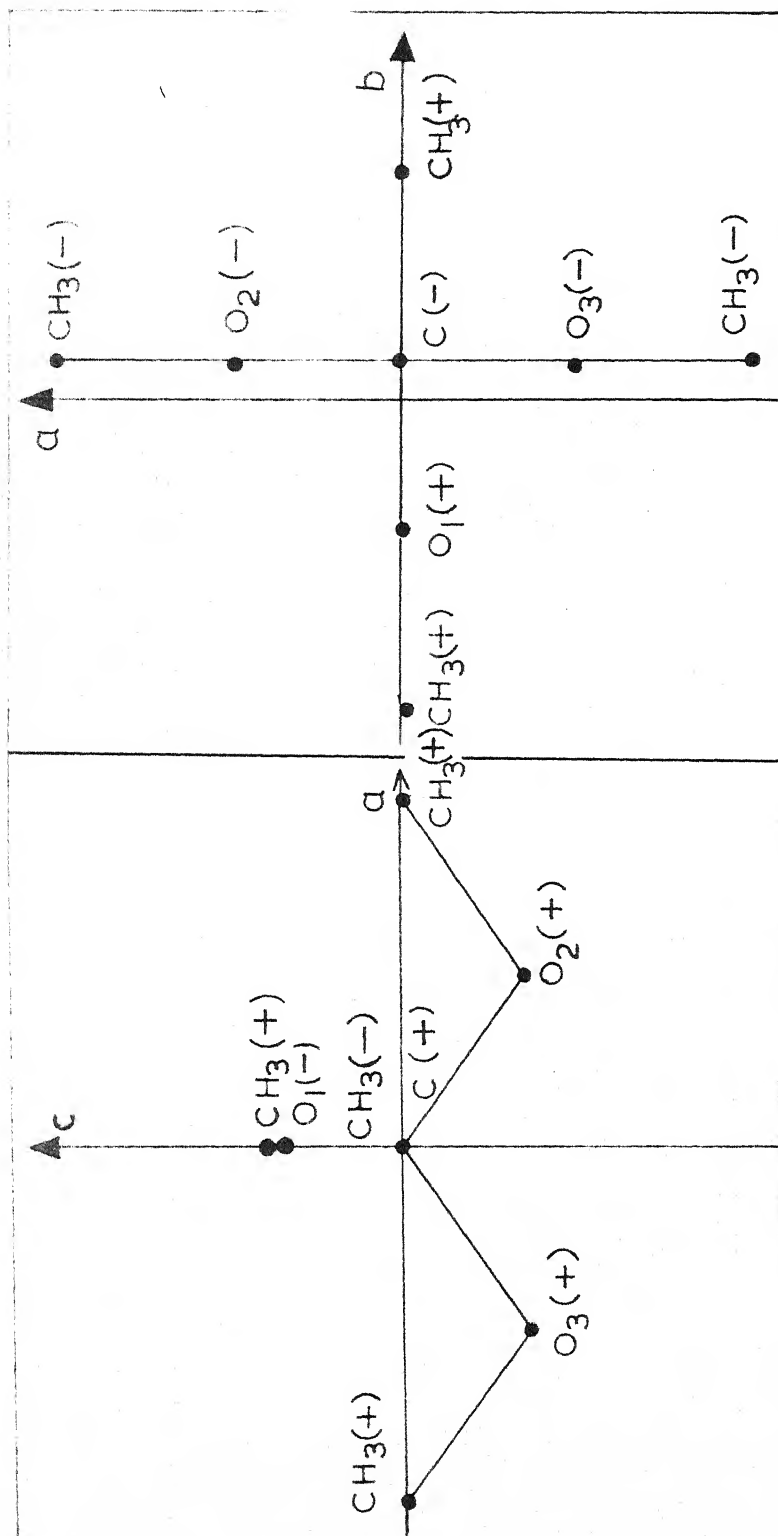


Fig.5.7. The projections of TGG' configuration of 1,1,1-trimethoxy ethane molecule on ab and ac planes of the principal axes system.

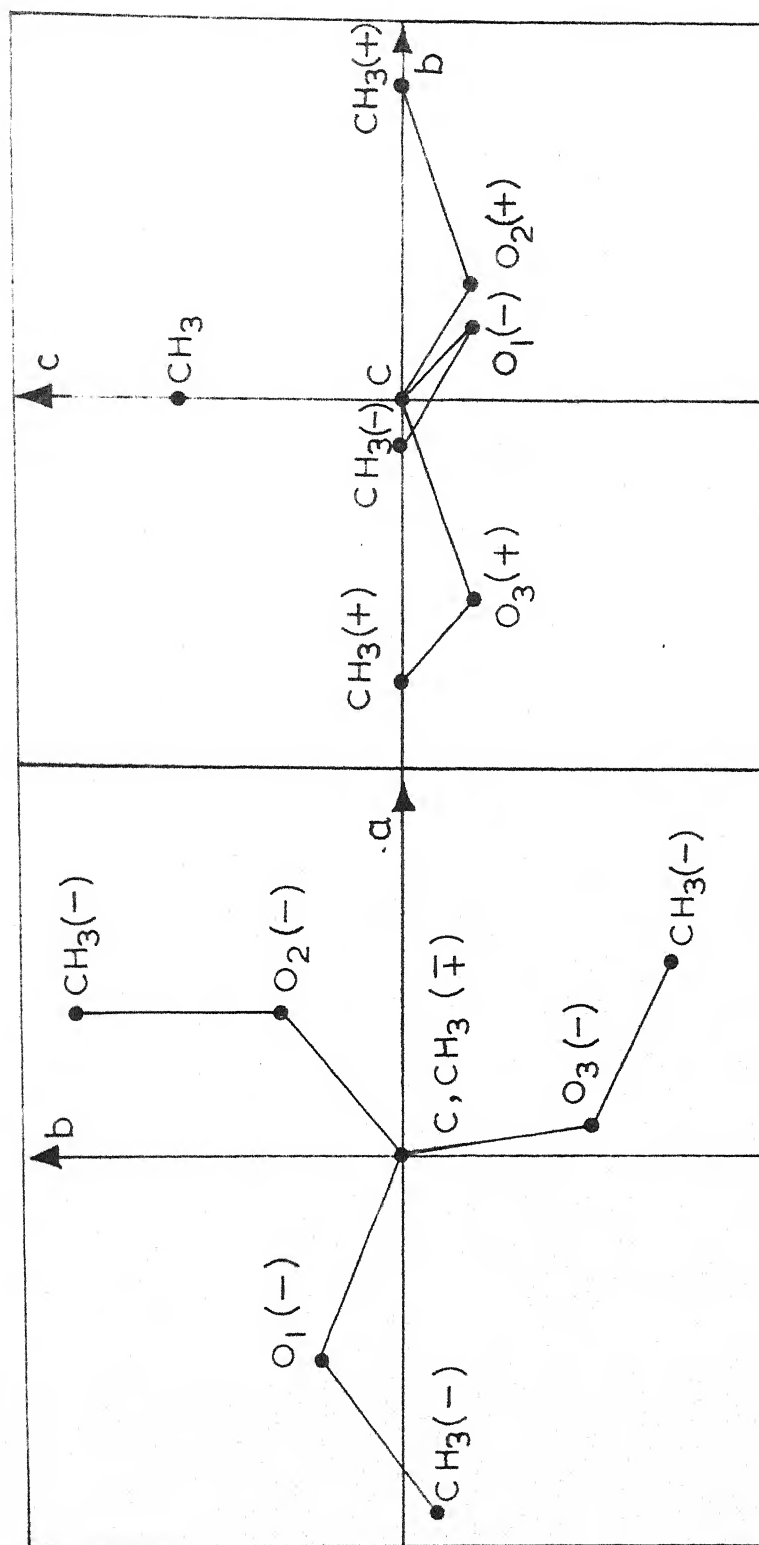


Fig. 5.8. The projections of GGG configuration of 1,1,1-trimethoxy ethane molecule on ab and bc planes of the principal axes system.

CHAPTER VI

VIBRATIONAL SPECTRA AND ROTATIONAL
ISOMERISM OF TRIETHYLAMINEABSTRACT

The infrared spectra of triethylamine in liquid, vapour and solid phases were recorded in the range $250\text{--}4000\text{ cm}^{-1}$ and the laser-Ramanspectrum of liquid was investigated, together with the depolarization data. The presence of atleast two rotational isomers is suggested in the liquid and solid phases. However, it is not clear whether the molecule exists as a mixture of two rotational isomers or assumes a single configuration in the vapour phase. A vibrational assignment is attempted for the observed bands keeping in view the presence of two rotational isomers.

INTRODUCTION

The triethylamine (TEA) molecule has been the subject of several investigations¹⁻³ from structural point of view. Brown and coworkers^{1,2} suggest that the stable form of the TEA molecule is the one in which two ethyl groups are removed to the "rear" of the nitrogen atom and the third is projected in the region of the lone pair electrons of nitrogen atom. Heasell and Lamb³ investigated the absorption of ultrasonic waves in liquid TEA over the range 25° to 70°C. The absorption results show the existence of an equilibrium mixture of at least two rotational isomers. They have, however, not predicted the form playing important part in the ultrasonic relaxation processes.

The infrared and Raman spectra have been widely used to study the rotational isomerism in the molecules and determine their structure. There does not seem to have been any infrared study in the gaseous and the solid phases of this molecule though the liquid phase spectrum has been reported upto 650 cm^{-1} ^{4,5}. The Raman spectrum in the liquid phase has also been investigated by many workers⁶⁻⁸ but a complete vibrational assignment of the bands is not attempted. It was therefore thought worthwhile to make a systematic study of the vibrational spectrum of this molecule in various phases and to get information regarding its structure.

EXPERIMENTAL

The sample used for recording the infrared and Raman spectra was obtained commercially and was distilled before use.

The infrared spectrum of the liquid was studied in cells having fixed spacers .025 mm and .5 mm thick. The spectrum in the vapour phase was obtained using 10 cm and 2 cm gas cells at room temperature. The liquid, vapour and solid phase spectra are shown in Figs. 6.1, 6.2 and 6.3 respectively.

The laser Raman spectrum of liquid only was recorded and is shown in Fig. 6.4. The details of the experimental procedure and the instruments used are given in Chapter II.

The results obtained are listed in Table 6.2 along with the frequency assignments. The Raman bands observed in the present work along with the results of previous workers are listed in Table 6.3.

DISCUSSION

The triethylamine molecule is a complex one. It may assume several conformations depending upon the relative orientations of the three methyl groups. This molecule may be regarded structurally similar to trimethylamine except that here one hydrogen atom of each methyl group is replaced by the methyl group. Recent microwave studies⁹ of several isotopic species of trimethylamine have established its structure as the one in which the hydrogen atoms are in staggered position relative to the two C-N bonds. One may then expect that these methyl groups occupy the positions of the replaced hydrogen atoms which leads to the conclusion that only trans or gauche conformations can exist relative to the lone pair electrons of the nitrogen atom. Twenty seven molecular conformations may be expected due to internal rotation about each of the

three N-Et bonds. Many of them can not be spectroscopically distinguished. The distinguishable forms are TTT, TTG, TGG, TGG', TG'G, GGG and GGG' (Fig. 6.5). The steric considerations do not favour the TTT, TTG, TG'G and GGG' as the low energy conformations. The remaining three molecular forms TGG, TGG' and GGG may then be considered as the probable configurations of the TEA molecule.

The GGG conformation belongs to C_3 point group symmetry, therefore, the sixty fundamental vibrations will divide as

$$\Gamma_{\text{vib}} = 20 \underline{a} + 20 \underline{e}$$

both the \underline{a} and \underline{e} vibrations will be infrared and Raman active with the former appearing as polarized bands in the Raman spectrum.

The moments of inertia and rotational constants of TEA were calculated assuming $r_{\text{C-N}} = 1.47$, $r_{\text{C-C}} = 1.54$ and all angles tetrahedral and are given in Table 6.4.

The calculation of the Gerhard and Dennison parameter gives $\beta = - .467$ and hence the infrared gaseous spectrum is expected to give rise to two types of bands, parallel bands having a strong Q branch with a PR spacing* of $\sim 19 \text{ cm}^{-1}$ and perpendicular type bands having a medium weak Q branch and PR spacing of $\sim 14 \text{ cm}^{-1}$.

The TGG conformation has no element of symmetry and hence all the sixty fundamental vibrations should appear in both the Raman and infrared spectra with all Raman bands being polarized. The

*The PR separations were calculated using the formulas of Gerhard and Dennison Phys. Rev., 43, 197 (1933) and Seth-Paul and Dijkstra, Spectrochim. Acta, 23, 2861 (1967) .

calculation of the Badger and Zumwalt parameters gives $K = -0.145$ and $\rho^* = .743$ and hence the infrared spectrum of the vapour may be expected to show three types of band contours, type A having a medium Q branch with a PR spacing* of $\sim 14 \text{ cm}^{-1}$, type B having a PQQR type structure with a PR spacing of $\sim 11 \text{ cm}^{-1}$ and type C having a strong Q branch with a PR spacing of $\sim 21 \text{ cm}^{-1}$.

The TGG' conformation should have one plane of symmetry and therefore possess $32a'$ and $28a''$ type of vibrations the former appearing as polarized bands in the Raman spectrum. The Badger and Zumwalt parameters for the TGG' conformation are $K = -.67$ and $\rho^* = 1.25$ and hence the infrared spectrum of the vapour should exhibit three types of band contours, type A having a PR separation of $\sim 13 \text{ cm}^{-1}$ with not well separated P, Q and R branches, type B bands having a PR structure with a separation of $\sim 10 \text{ cm}^{-1}$ and type C having a PQR structure with medium Q branch and PR separation of $\sim 20 \text{ cm}^{-1}$.

A study of the Raman depolarization data indicates that quite a large number of Raman bands are depolarized. This is consistent with the presence of either GGG or TGG' (or both) forms of the molecule but of course does not rule out the existence of another isomer TGG. The inference one can draw from this datum is that either the GGG or TGG' or both of these forms are present in the liquid phase, the third form TGG may or may not be present there.

*The PR separations were calculated using the formulas of Badger and Zumwalt, J. Chem. Phys., 6, 711 (1938) and Seth-Paul and Dijkstra spectrochim. Acta, 23, 2861 (1967).

A study of the infrared band contours shows that the band contours are mainly of the type expected for the TGG' conformation. This inference is based on the shape of the band contours rather than the PR separations as they are virtually the same for all the three conformations.

A comparative study of the infrared spectra in the liquid and solid phases indicates that there are some changes in the intensity of the infrared bands in going from liquid to solid state. The pairs of bands at $(737, 746) \text{ cm}^{-1}$ and $(1137, 1145) \text{ cm}^{-1}$ are of special interest as they show a reversal in intensity of the bands in the solid phase at low temperature. The intensities of the higher frequency components of both the doublets are less than the lower frequency components in liquid phase whereas, just the reverse happens in the solid phase. Their explanation as summation or overtone bands is not satisfactory as they are not likely to exhibit such a behaviour. The probable explanation* seems to be that these pairs arise due to two different forms of the molecule whose relative abundances are different in the liquid and solid phases. It is, however, difficult to predict whether the molecule exists as a mixture of two rotational isomers or assumes a single configuration in vapour phase, the reason being that in the vapour phase infrared bands get resolved and the P, Q and R branches may overlap with the nearby bands thus making it difficult to recognise the bands separately.

The temperature dependence of the doublet at $737/746 \text{ cm}^{-1}$ in liquid phase demonstrates convincingly that TEA molecule exists as a mixture of two rotational isomers. As the temperature is lowered the

*The presence of rotational isomers even in solid phase was also found for methyl nitrite (Spectrochim. Acta, 23, 2957 (1967)).

intensity of the higher frequency component increases markedly relative to that of the lower frequency component which indicates that the higher frequency component is due to the more stable form of the molecule.

The ratio of the two isomers present should change with the change of the polarity of the solvents. The ratio (more polar)/(less polar) of isomers should increase when the solvent is changed from non-polar to polar type. In order to study these effects, the triethylamine was dissolved in the non-polar solvent carbon disulphide and polar solvent acetone. The band pairs at $(737, 746) \text{ cm}^{-1}$ and $(1137, 1145) \text{ cm}^{-1}$ were studied. Though the bands in these pairs are not well separated from each other the changes in intensity could be seen clearly. The intensity of the 746 and 1145 cm^{-1} bands increases relative to the 737 and 1137 cm^{-1} bands respectively in the carbon disulphide solution whereas, in acetone solution the changes are just other way round and a decrease in the intensity of the bands at 746 & 1145 cm^{-1} is noted. This behaviour means that the 746 and 1145 cm^{-1} bands correspond to the less polar form of the molecule.

As the bands due to both the molecular forms persist in the liquid and solid phases and the features are not very clear in the vapour phase, the assignment of the bands on the basis of any particular symmetry of the molecule is not feasible. We shall, therefore, assign a band to only a particular type of vibration without going into the details of the symmetry species to which it may belong.

Assignment of Fundamentals

One of the basic difficulties in the assignment of CH stretching modes is that many absorption bands of the methyl and methylene groups are highly overlapped. In addition to this, several combinations or overtones of methyl or methylene bending vibrations may give rise to strong bands in this region due to Fermi resonance with CH stretching modes. The assignment of the fundamental modes of vibration, therefore, becomes quite ambiguous.

The assignment of the CH_2 stretching vibrations may be carried out by comparison with tripropargylamine¹⁰ in which no CH_3 group is present and all the bands are only due to methylene group vibrations. Two strong bands have been observed in the liquid phase at 2928 and 2817 cm^{-1} and are associated with the $\nu_{\text{asym.CH}_2}$ and $\nu_{\text{sym.CH}_2}$ vibrations respectively¹⁰. The triethylamine molecule exhibits two infrared bands near these frequencies and ^{they} may be associated with the CH_2 stretching vibrations. The infrared bands at 2936 and 2799 cm^{-1} and the corresponding Raman bands at 2937 and 2805 cm^{-1} may then be assigned to $\nu_{\text{asym.CH}_2}$ and $\nu_{\text{sym.CH}_2}$ vibrations respectively. The remaining two prominent Raman bands at 2965 and 2876 cm^{-1} and the corresponding infrared bands at 2973 and 2875 cm^{-1} may be attributed to $\nu_{\text{asym.CH}_3}$ and $\nu_{\text{sym.CH}_3}$ vibrations. The infrared band at 2895 cm^{-1} is probably a combination band and has borrowed the intensity from nearby fundamental due to Fermi resonance. This completes the assignment of the CH stretching vibrations of methyl and methylene groups.

In the region of methyl and methylene group bending vibrations, four bands are observed at 1384, 1451, 1468 and 1477 cm^{-1} in the liquid phase infrared spectrum. The Raman spectrum, however, shows only two bands at 1377 and 1466 cm^{-1} which probably correspond to 1384 and 1468 cm^{-1} infrared bands. The bands at 1468 and 1384 cm^{-1} may be associated with the asymmetric and symmetric deformation modes of the CH_3 group respectively. The remaining ones could be attributed to the deformation modes of the CH_2 groups.

The assignment of one of the CH_2 wagging modes to the strong infrared band at 1296 cm^{-1} is quite certain but the other mode has been tentatively placed at 1311 cm^{-1} . The weak infrared band at 1268 cm^{-1} in solid phase has been chosen for the twisting modes of the CH_2 groups. All the CH_2 twisting modes have been assigned coincidentally as no other bands were available in the region of CH_2 twisting vibrations.

There is considerable overlapping of the absorption bands in the region of C-N st., CH_3 rocking and C-C stretching vibrations, thus rendering the assignment of the bands quite difficult. Further, the rocking and skeletal vibrations may be highly coupled hence the bands cannot be associated with any particular mode of vibration. An approximate assignment for these bands has however, been attempted. The infrared bands at 1137, 1072 and 920 cm^{-1} and the corresponding Raman bands at 1141, 1065 and 922 cm^{-1} have been selected for the methyl group rocking modes in analogy with t-butylhalides^{11,12}. As discussed earlier, the bands at 1137 and 1145 cm^{-1} probably arise due to two different rotational isomers. Therefore, the band at 1145 cm^{-1} has also been attributed to the

fundamental vibration but of different isomer. The 920 cm^{-1} infrared band also has a band in its neighbourhood at 903 cm^{-1} which gets much weaker in the vapour spectrum as compared to 920 cm^{-1} band. But there is not much change in the relative intensities of these bands in the solid state spectrum. This band is probably a combination band which appears with increased intensity due to Fermi resonance with nearby fundamental.

In the region of CH_2 rocking vibrations, two infrared bands are observed at 802 and 784 cm^{-1} in the liquid phase. In the solid phase, however, four bands appear in this region. The bands at 781 and 799 cm^{-1} in solid state seem to correspond to 784 and 802 cm^{-1} liquid state bands. The remaining two bands at 771 and 816 cm^{-1} are probably some combination bands. They appear in the solid phase due to the sharpening of the bands at low temperature but were otherwise obscured by nearby bands in the liquid phase. The bands at 784 and 802 cm^{-1} may be associated with the CH_2 rocking vibrations. The Raman spectrum shows only one band at 810 cm^{-1} (vw) which may correspond to 802 cm^{-1} infrared band.

Once the assignment of the CH_3 and CH_2 rocking modes is achieved, it becomes easy to attempt an assignment for the skeletal vibrations. In the region where C-N stretching vibrations may be expected to fall, close doublets are observed in both the liquid and solid phases but in the vapour phase spectrum only one broad band seems to be present. In the liquid phase the band at 1215 cm^{-1} appears as a shoulder to the 1207 cm^{-1} band. The solid phase spectrum, however, shows two clear peaks at 1202 and 1213 cm^{-1} the latter being weaker in intensity than the

former. Both of these bands probably arise due to the C-N stretching vibrations. The above assignments have been made in analogy with trimethylamine where the corresponding mode has been assigned at 1270 cm^{-1} in the solid phase¹³. A little lowering in the frequency is expected in the case of TEA molecule because of the heavier ethyl group attached to the nitrogen atom as compared to the methyl group in case of trimethylamine. The C-N stretching frequencies for ethylamine and diethylamine molecules are observed at 1085 and 1140 cm^{-1} respectively¹⁴. We thus see that there is an increase in the frequency of this mode as we go from ethylamine to triethylamine. The remaining C-N stretching mode may be assigned at 737 cm^{-1} in the liquid phase. The nearby band at 746 cm^{-1} has also been assigned as C-N stretching vibration arising due to different isomer.

The C-C stretching vibrations of the three ethyl groups may not be very much separated from the C-C stretching vibration of the individual ethyl group due to the less interaction of these vibrations. Several bands are observed in the infrared spectrum in the region of C-C stretching vibrations which makes the selection of bands arising due to C-C stretching modes really difficult. However, the Raman spectrum is somewhat simpler. The bands at 1082 and 997 cm^{-1} in the Raman spectrum and the corresponding infrared bands at 1086 and 999 cm^{-1} have been chosen for the C-C stretching modes. The infrared band at 1020 cm^{-1} is probably a combination band appearing with enhanced intensity due to Fermi resonance with the nearby fundamental at 999 cm^{-1} .

In the region of the skeletal bending vibrations four prominent bands are available in the infrared spectrum of the liquid at 534, 485, 438 and 294 cm^{-1} with the corresponding Raman bands at 535, 470, 439 and 290 cm^{-1} . An unambiguous and clearcut assignment of these modes to some specific bending modes is not feasible as the CCN and CNC bending modes are likely to couple with each other. However, an approximate assignment for these bands is given here. The two bands at 534 and 485 cm^{-1} are associated with the CCN bending vibrations and the remaining two bands at 438 and 294 cm^{-1} are assigned to the CNC bending vibrations.

The assignment of the skeletal twisting and methyl torsional modes is not attempted as sufficient bands are not available for making the assignments. In addition to this the difference bands may also arise in the region where the torsional modes are expected to fall.

Apart from the bands discussed above there are some more bands in the infrared and Raman spectra of triethylamine molecule. These bands could be easily interpreted as the overtones or combinations of the fundamentals discussed above. Their assignments have been included in Table 6.2 and will not be discussed in detail here.

REFERENCES

1. H.C. Brown and M.D. Taylor, J. Amer. Chem. Soc., 69, 1332 (1947).
2. H.C. Brown and S. Sujishi, J. Amer. Chem. Soc., 70, 2878 (1948).
3. E.L. Heasell and J. Lamb, Proc. Roy. Soc., A237, 233 (1956).
4. W.W. Coblentz "Investigations of Infrared Spectra" (Carnegie Institute Publication, 35, Pt. I, Washington 1905).
5. R.J. Pace, J. Williams and R.J. Williams, J. Chem. Soc., 2197 (1961).
6. B.K. Chaudhuri, Indian J. Phys., 11, 203 (1937).
7. J.K. Syrkin and M.W. Wolkenstein, Acta Physico Chimica, 2, 303 (1935).
8. A. Dadieu and K.W.F. Kohlrausch, Monatshefte Fur Chemie, 57, 225 (1931).
9. J.E. Wollrab and V.W. Laurie, J. Chem. Phys., 51, 1580 (1969).
10. A.L. Verma and Putcha Venkateswarlu (Private Communication).
11. D.E. Mann, N. Acquista and D.R. Lide, Jr., J. Mol. Spectry, 2, 575 (1958).
12. J.C. Evans and G.Y.S. Lo, J. Am. Chem. Soc., 88, 2118 (1966).
13. T.D. Goldfarb and B.N. Khare, J. Chem. Phys., 46, 3379 (1967).
14. J.E. Stewart, J. Chem. Phys., 30, 1259 (1959).

TABLE 6.1

The Fundamental Modes of Vibration of Triethylamine
Molecule under the Point Group Symmetries C_3 , C_s and C_1

Symmetry species			No.	Skeletal	CH_2 vibrations	CH_3 vibrations
C_1	C_s	C_3				
1	2	3	4	5	6	7
a	a'	a	✓ 1			CH_3 st.(asym.)
a	a''	a	✓ 2			CH_3 st.(asym.)
a	a''	a	✓ 3		CH_2 st.(sym.)	
a	a'	a	✓ 4			CH_3 st.(sym.)
a	a'	a	✓ 5		CH_2 st.(sym.)	
a	a'	a	✓ 6		CH_2 def.	
a	a'	a	✓ 7			CH_3 def.(asym.)
a	a''	a	✓ 8			CH_3 def.(asym.)
a	a'	a	✓ 9			CH_3 def.(sym.)
a	a'	a	✓ 10		CH_2 wag.	
a	a''	a	✓ 11		CH_2 twist.	
a	a'	a	✓ 12			CH_3 rock.
a	a'	a	✓ 13	C-C st.		
a	a''	a	✓ 14			CH_3 rock.
a	a''	a	✓ 15		CH_2 rock.	
a	a'	a	✓ 16	C-N st.		

Contd.

Table 6.1 (contd.)

1	2	3	4	5	6	7
a	a', a''	e	✓ 37	CCN bend.		
a	a', a''	e	✓ 38	CNC bend.		
a	a', a''	e	✓ 39			CH ₃ tors.
a	a', a''	e	✓ 40	N-C-C tors.		

Abbreviations : syn. = symmetric, asym. = asymmetric, st. = stretching,
 def. = deformation, wag. = wagging, twist. = twisting,
 rock. = rocking, bend. = bending, tors. = torsion.

* The numbering of vibrations has been done according to C₃ symmetry.

TABLE 6.2

Infrared and Raman Spectra of Triethylamine

Infrared						Raman			Assignment*
Vapour		Liquid		Solid		Liquid			
cm ⁻¹	Int.	cm ⁻¹	Int.	cm ⁻¹	Int.	cm ⁻¹	Int.	Depol.	
1	2	3	4	5	6	7	8	9	10
						~ 200	vw	p	$\nu_{16}^- \nu_{37}$
		294	vvw	300	w	290	vw	p	CNC bend.(1), ν_{18}
						340	w	p	$\nu_{34}^- \nu_{16}$
		414	sh	420	w				$\nu_{18}^+ \nu_{20}^?$
435	w	438	w	435	w	439	s	p	CNC bend.(2), ν_{38}
481	w	485	w	480	m	470	m	p	CCN bend.(1), ν_{17}
534	w	534	w	531	m	535	w	p	CCN bend.(2), ν_{37}
737	C m	737	m	737	m	735	s	p	C-N st.(1), ν_{16}
747		746	m	744	m				C-N st.(isomer)
~755									
				771	w				$\nu_{17}^+ \nu_{18}$ (F.R.)
~785	sh	784	w	781	w				CH ₂ rock.(1), ν_{15}
793	A w								
802		802	w	799	w	810	w	dp?	CH ₂ rock.(2), ν_{36}
810									
				816	w				$\nu_{37}^+ \nu_{18}$ (F.R.)
905	sh	903	w	900	w	898	m	dp	$\nu_{17}^+ \nu_{38}$ (F.R.)
920	w	920	w	916	w	922	w	dp	CH ₃ rock.(3), ν_{14}, ν_{35}

Contd.

Table 6.2 (contd.)

1	2	3	4	5	6	7	8	9	10
1002 } 1007 }	B w	999	w	999	m	997	m	p	C-C st.(1), \checkmark_{13}
1022	w	1020	w	1017	m	1018	m	p	$\checkmark_{17} + \checkmark_{37}$ (F.R.)
				1043	w				$\checkmark_{16} + \checkmark_{18}$
		1055	sh	1053	w				2x \checkmark_{37}
1071 } 1079 } 1096 }	C s	1072	s	1068	s	1065	s	p	CH ₃ rock.(1), \checkmark_{12}
		1086	s	1083	s	1082	ms	dp?	C-C st.(2), \checkmark_{34}
		1096	sh	1094	m				$\checkmark_{15} + \checkmark_{18}$
~1106	sh	1106	sh	1105	w				$\checkmark_{18} + \checkmark_{36}$
1142 } 1152 }	B m	1137 } 1145 }	m sh	1143 } 1150 }	m m	1141	w	dp?	CH ₃ rock.(2), \checkmark_{33}
1213	s	1207 } ~1215 }	s sh	1202 } 1213 }	s s	1205	w	dp	CH ₃ rock.(isomer)
		1271	sh	1268	w				C-N st.(2), \checkmark_{32}
1298 } 1309 }	s	1296	s	1291	s				CH ₂ twist.(3), $\checkmark_{11}, \checkmark_{31}$
		1311	sh	1308	sh	1295	w	dp	CH ₂ wag.(3), $\checkmark_{10}, \checkmark_{30}$
		1336	sh	1329	w				$\checkmark_{36} + \checkmark_{37}$
1348	sh	1347	w	1340	w				2x $\checkmark_{18} + \checkmark_{16}$
~1357	sh	1357	w	1356	m				$\checkmark_{14} + \checkmark_{38}$
		~1368	sh	1370	sh				2x $\checkmark_{37} + \checkmark_{18}$

Contd.

Table 6.2 (contd.)

1	2	3	4	5	6	7	8	9	10
1379									
1385	C	s	1384	s	1380	s	1377	vw	p?
1391									CH ₃ sym.def.(3), γ_9, γ_{29}
1456	m	1451	m	1445	s				CH ₂ def.(1), γ_6
1470	m	1468	m	1468	s	1466	vs	dp	CH ₃ asym.def.(6), $\gamma_7, \gamma_8, \gamma_{26}, \gamma_{27}$
1479	sh	1477	sh	~1472	sh				CH ₂ def.(2), γ_{28}
1652	vw	1650	vw	1650	vw				$\gamma_{14} + \gamma_{16}$
1817	vw	1812	vw						$\gamma_{34} + \gamma_{16}$
1954	vw	1947	vw						$\gamma_{32} + \gamma_{16}$
2292	vw	2272	vw						2x γ_{33}
2387	vw	2384	vw						$\gamma_{10} + \gamma_{12}$
2432	vw	2425	vw						2x γ_{32}
2581	vw	2573	vw	2570	vw				$\gamma_9 + \gamma_{32}$
2617	sh	2613	sh	2610	vw				$\gamma_{28} + \gamma_{33}$
2658	sh	2643	sh	~2640	vw				$\gamma_6 + \gamma_{32}$
2683	sh	2677	sh	~2665	vw				$\gamma_{32} + \gamma_7$
~2720	sh	~2710	sh	~2710	sh				2x $\gamma_{34} + \gamma_{37}$
2731	m	2723	m	2723	m	2718	vw	p	$\gamma_6 + \gamma_{10}$
2758	sh	2757	sh	2753	m	2760	vw	p	$\gamma_7 + \gamma_{10}$
-									
2806	? s	2799	s	2794	vs	2805	m	p	CH ₂ sym.st.(3), γ_5, γ_{25}
2816									

contd.

Table 6.2 (contd.)

1	2	3	4	5	6	7	8	9	10	
2887	s	2875	s	2873	s	2876	m	p	CH ₃ sym.st.(3), ν_4, ν_{24}	
		2895	s	2895	m	~2900	m	p	$\nu_6 + \nu_7$ (F.R.)	
2946	s	2936	s	2935	s	2937	s	p	CH ₂ asym.st.(3), ν_3, ν_{23}	
2975	} ?	vs	2973	vs	2969	vs	2965	m	dp	CH ₃ asym.st.(6), $\nu_1, \nu_2, \nu_{21}, \nu_{22}$
2982										
-										

Abbreviations : s = strong, m = medium, w = weak, vs = very strong,
 vw = very weak, vvw = very very weak, sh = shoulder,
 p = polarized, dp = depolarized, st. = stretching,
 bend. = bending, def. = deformation, wag. = wagging,
 twist. = twisting, rock. = rocking, sym. = symmetric,
 asym. = asymmetric, F.R. = Fermi Resonance.

* For convenience the numbering of vibrations has been done according to C₃ symmetry. The numbers in the paranthesis denote the number of modes of vibration.

TABLE 6.3

Raman Spectrum of Triethylamine

Chaudhuri cm ⁻¹		Syrkin and Wolkeinstein cm ⁻¹	Dadien and Kohlrausch cm ⁻¹	Present Results cm ⁻¹ Int. ρ		
1	2	3	4	5	6	7
		170 (0)		~200	vw	p
		279 (0)				
		302 ($\frac{1}{2}$)		290	vw	p
		335 (1b)		340	w	p
435 (2)	.5	435 (4b)	433 (2)	439	s	p
		479 (2b)		470	m	p
		534 (1b)		535	w	p
		602 (1)				
736 (4)	.3	739 (6b)	739 (4)	735	s	p
		809 (1b)	812 (1br)	810	vw	dp?
		902 (4b)		898	m	dp
915 (4br)	.9	915 (3b)	916 (3br)	922	m	dp
997 (1)	.68	948 (3)	1000 (1)	997	m	p
		1020 (2)		1018	m	p
1069 (6)	.9	1065 (5b)	1070 (2)	1065	s	p
		1084 (2)		1082	ms	dp?
		1138 (2)	1148 ($\frac{1}{2}$)	1141	w	dp?
		1202 (2b)		1205	w	dp

contd.

Table 6.3 (contd.)

1	2	3	4	5	6	7
1286 (1)	.72	1291 (3b)	1288 (2)	1295	m	dp
		1378 (2)		1377	vw	p?
1433 (8)	.86	1452 (12b)	1452 (7br)	1466	vs	dp
				2718	vw	p
				2760	vw	p
		2795 (8b)	2795 (4br)	2805	m	p
2874 (4)	.4	2873 (8)	2874 (4br)	2876	m	p
				~ 2900	m	p
2932 (8br)	.3	2931(15b)	2932 (10br)	2937	s	p
2966 (4)	.8	2967 (12b)	2966 (10br)	2965	m	dp

Abbreviations : p and dp mean polarized and depolarized respectively.
 b or br indicate broad. The numbers in the bracket
 indicate intensity. m = medium, s = strong, w = weak.
 vw = very weak, ms = medium strong.

TABLE 6.4
Molecular Parameters

	GGG	TGG	TGG'
I_A ($\text{amu-}\text{\AA}^2$)	192.04	153.68	123.38
I_B ($\text{amu-}\text{\AA}^2$)	192.04	219.17	253.45
I_C ($\text{amu-}\text{\AA}^2$)	360.92	321.23	317.31
A (cm^{-1})	.0877	.1096	.1032
B (cm^{-1})	.0877	.0768	.0664
C (cm^{-1})	.0466	.0524	.0531

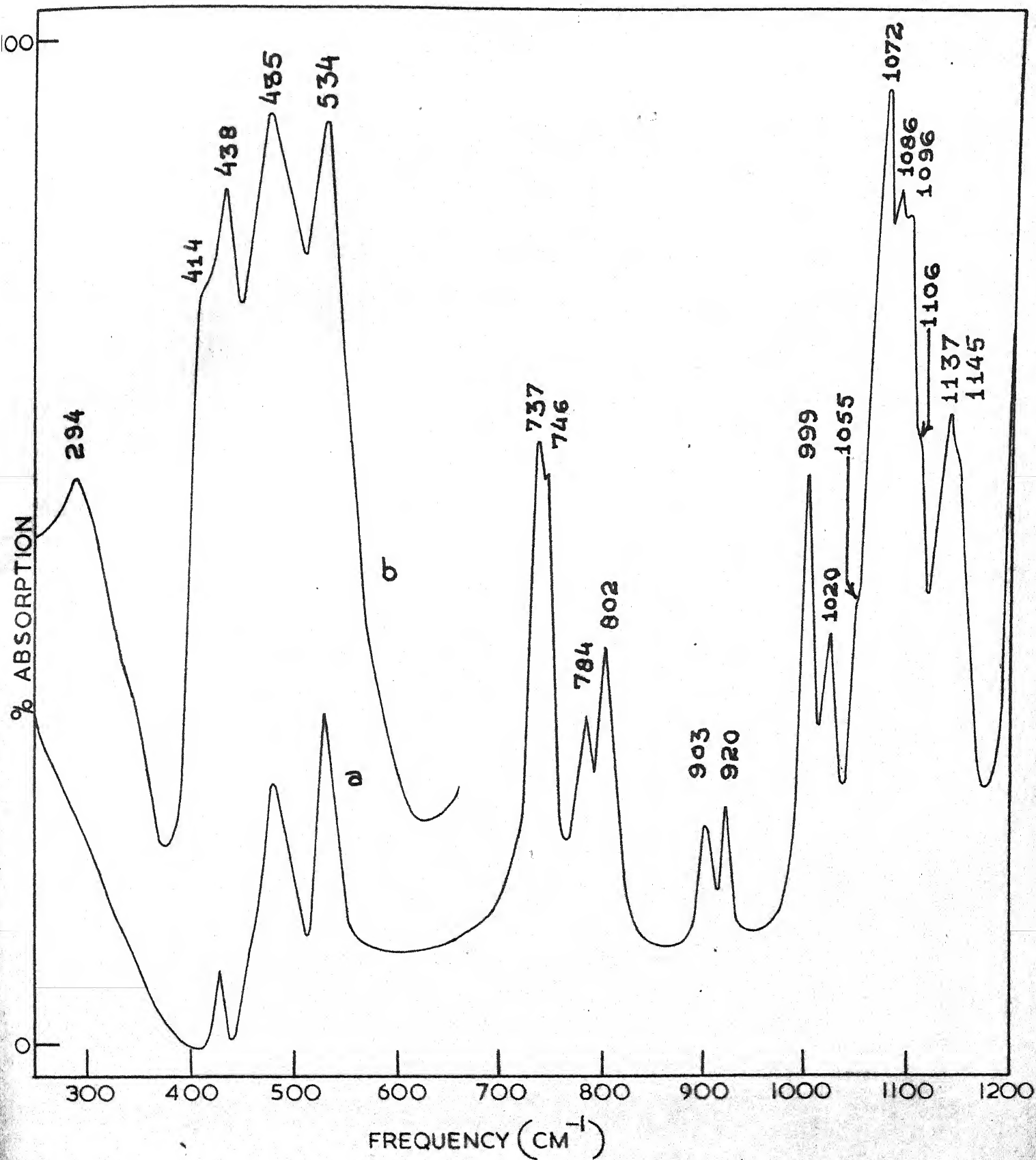


Fig.6.1(a). The infrared spectrum of liquid triethylamine in the region 250-1200 cm^{-1} ; (a) .025 mm CsBr cell, (b) .5 mm CsBr cell.

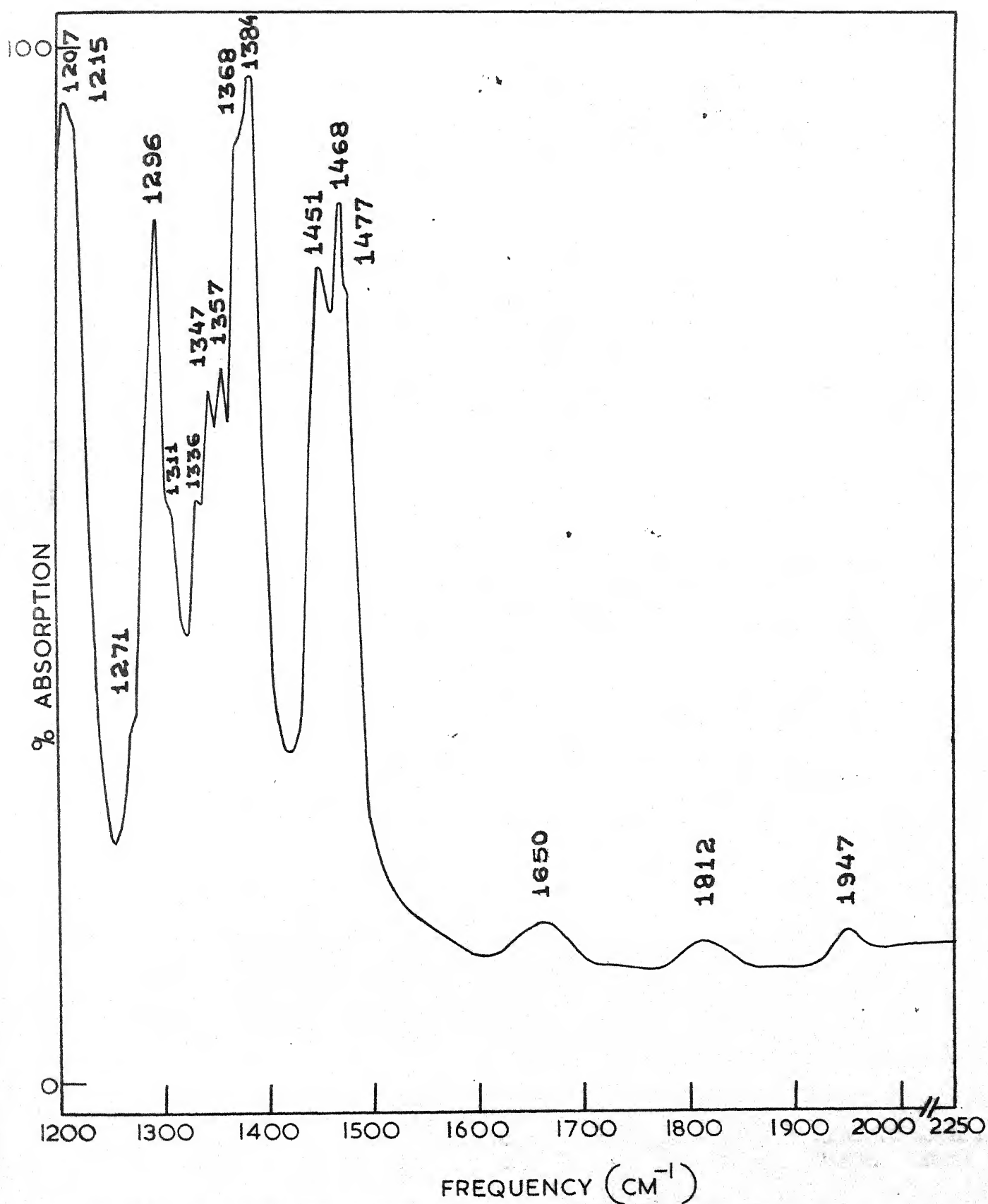


Fig. 6.1(b). The infrared spectrum of liquid triethylamine in the region 1200-2250 cm⁻¹; .025 mm CsBr cell.

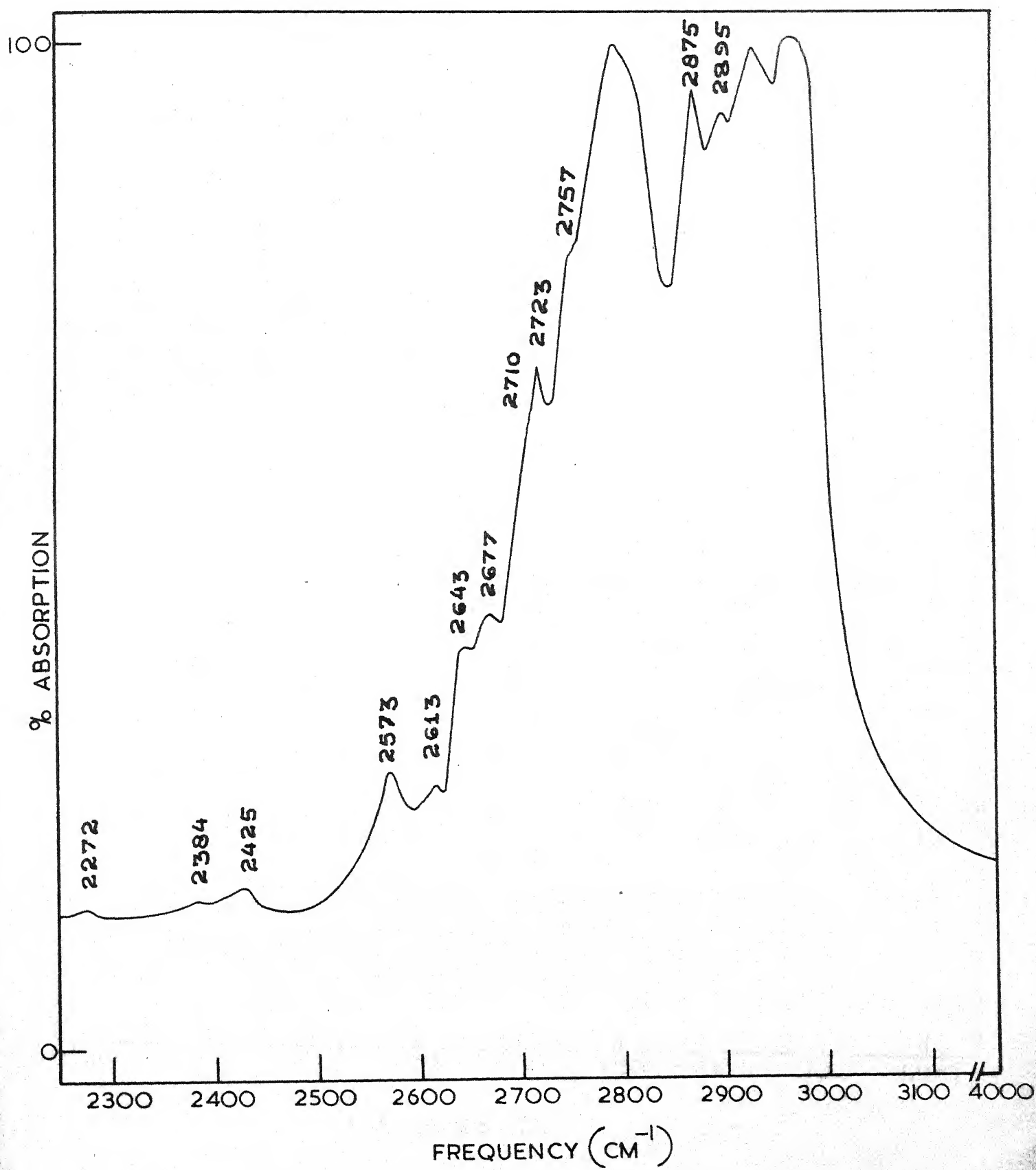


Fig. 6.1(e). The infrared spectrum of liquid triethylamine in the region 2250-4000 cm^{-1} : .025 mm CsBr cell.

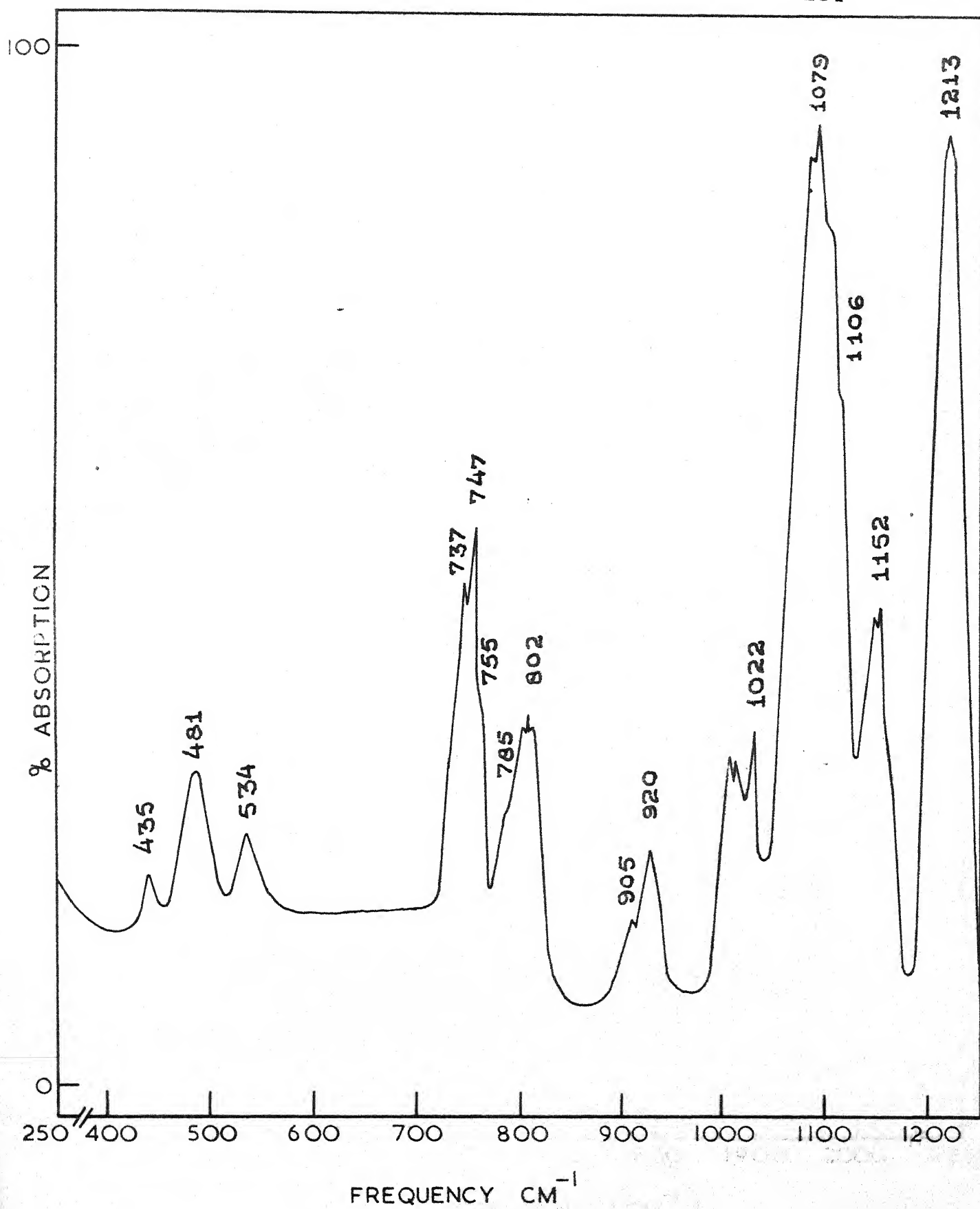


Fig. 6.2(a). The infrared spectrum of gaseous triethylamine in the 250-1250 cm⁻¹; 10 cm CsBr gas cell.

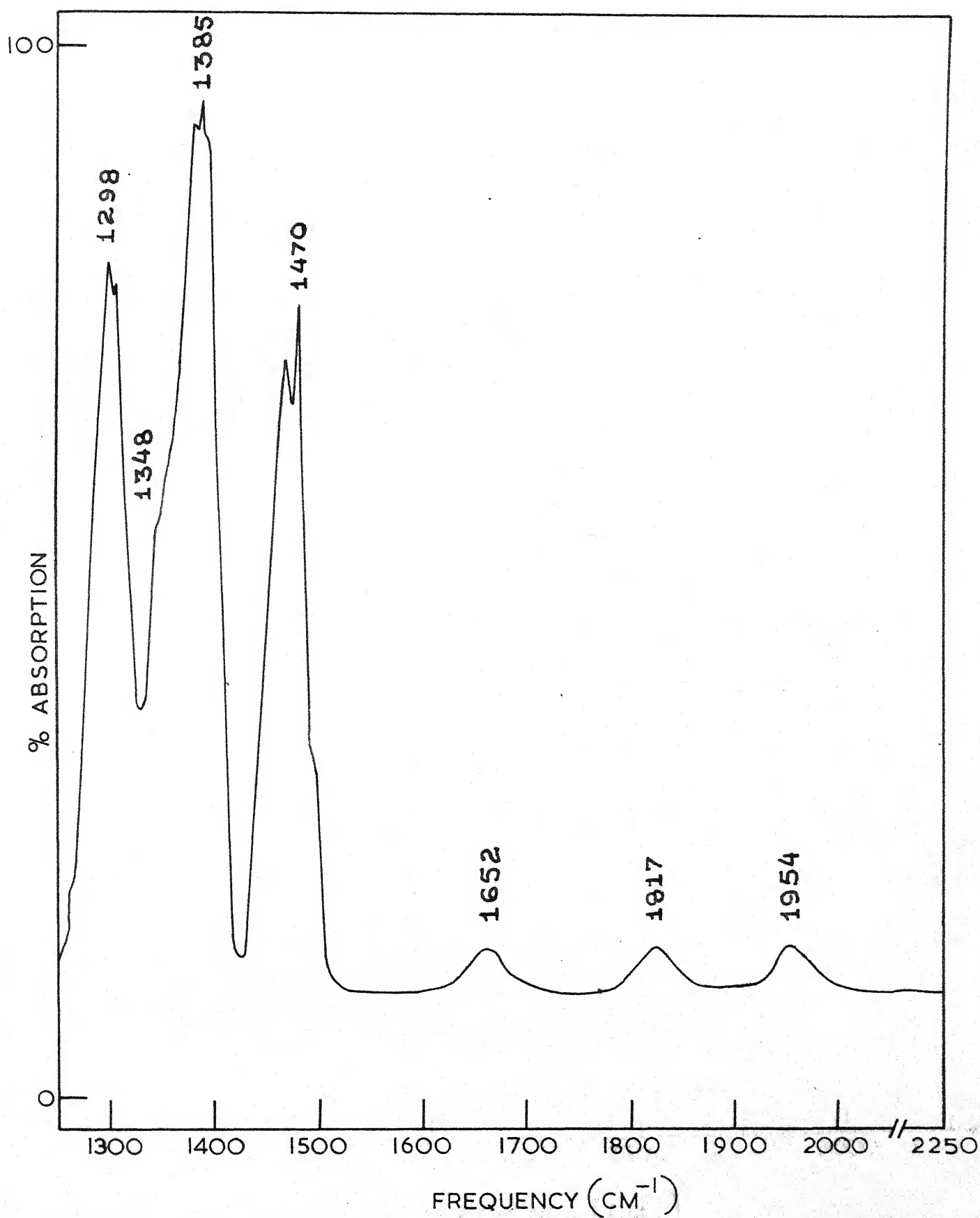


Fig.6.2(b). The infrared spectrum of gaseous triethylamine in the region 1250-2250 cm^{-1} : 10 cm CsBr gas cell.

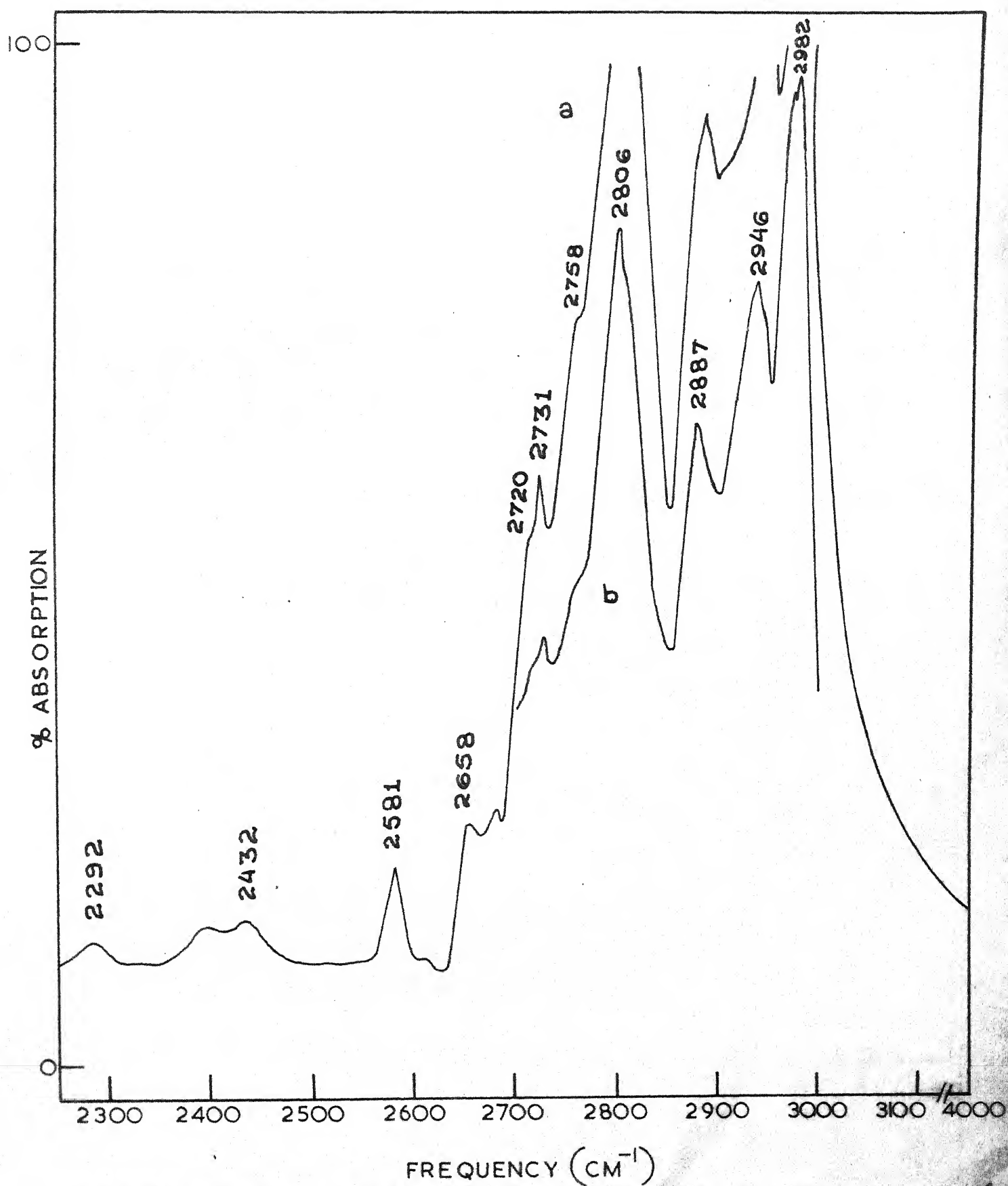


Fig.6.2(c). The infrared spectrum of gaseous triethylamine in the region 2250-4000 cm^{-1} : (a) 10 cm CsBr gas cell, (b) 2 cm CsBr gas cell.

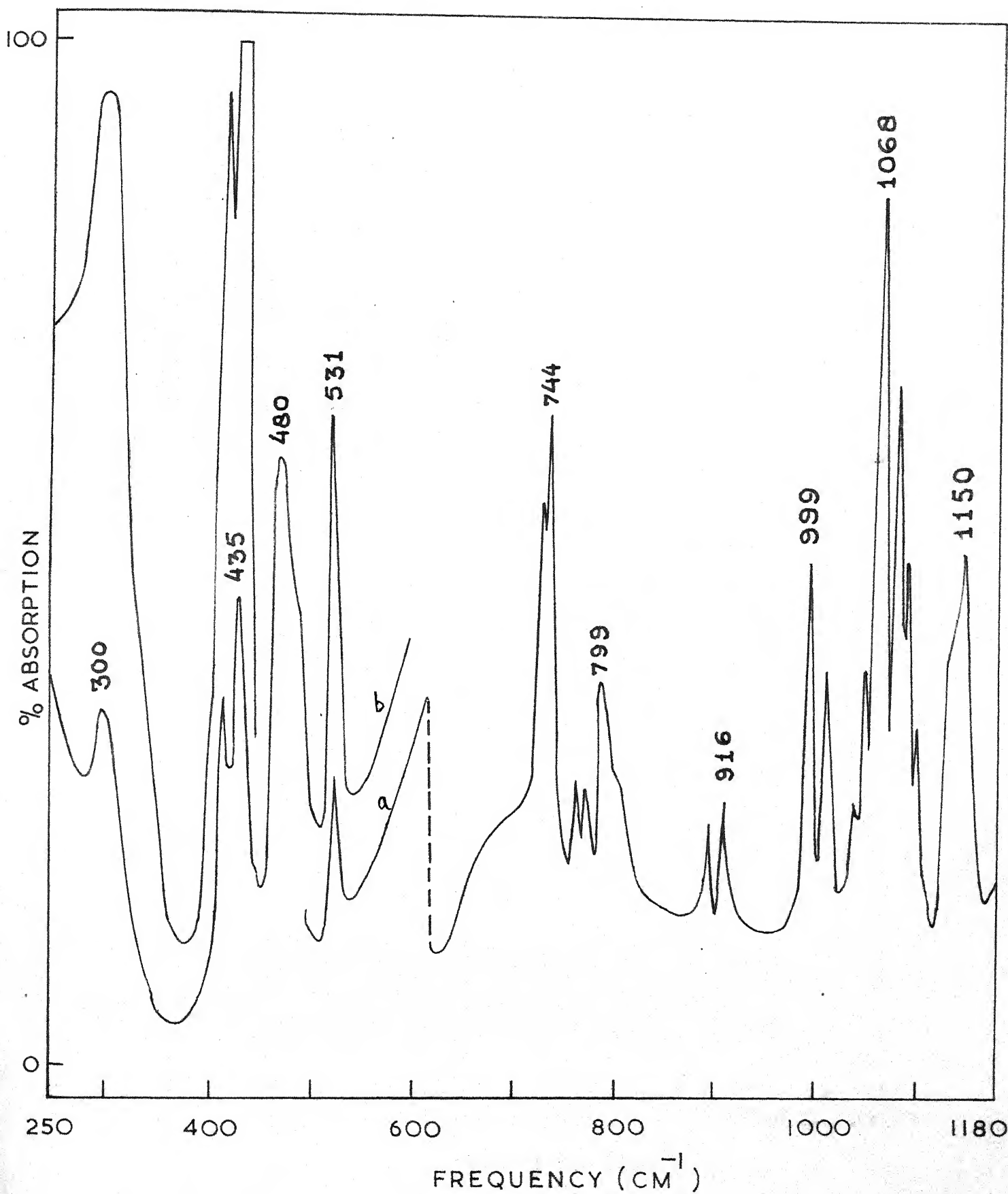


Fig.6.3(a). The infrared spectrum of solid triethylamine near -196°C in the region $250\text{--}1180\text{ cm}^{-1}$. The thickness of the deposited film is more in the case of (b) as compared to (a).

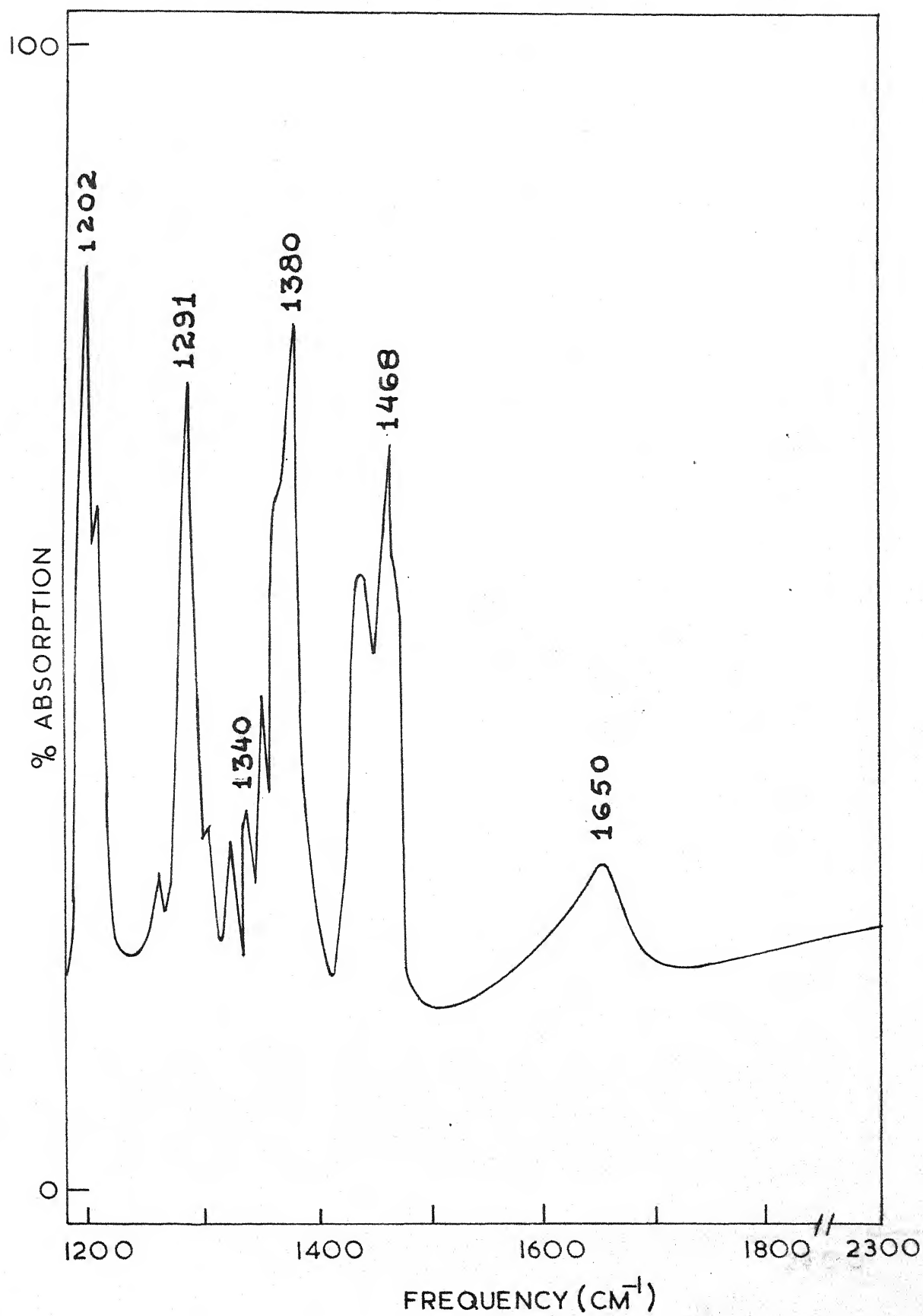


Fig.6.3(b). The infrared spectrum of solid triethylamine near -196°C in the region $1180\text{--}2300\text{ cm}^{-1}$.

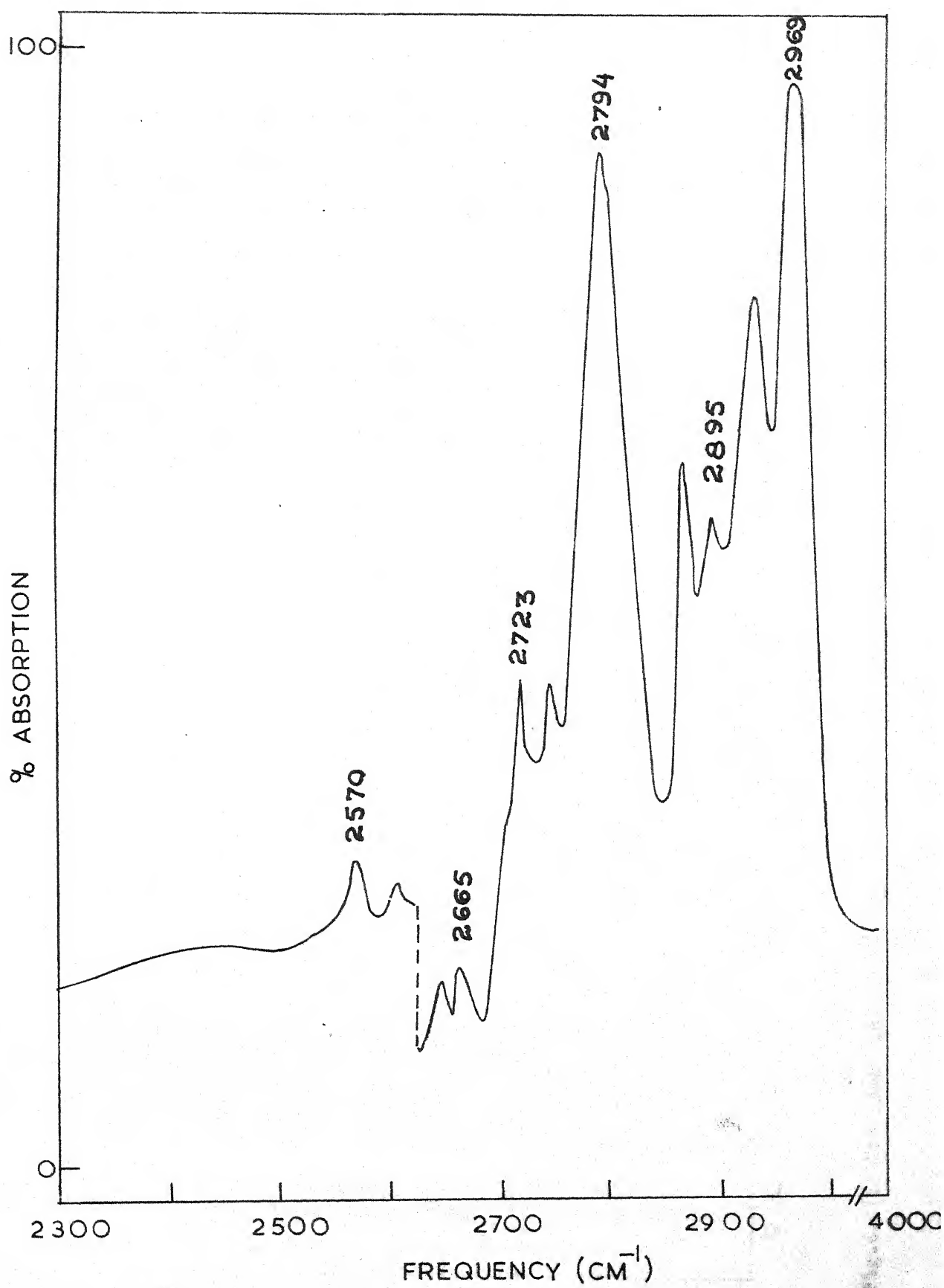


Fig.6.3(c). The infrared spectrum of solid triethylamine near -196°C in the region $2300\text{--}4000\text{ cm}^{-1}$.

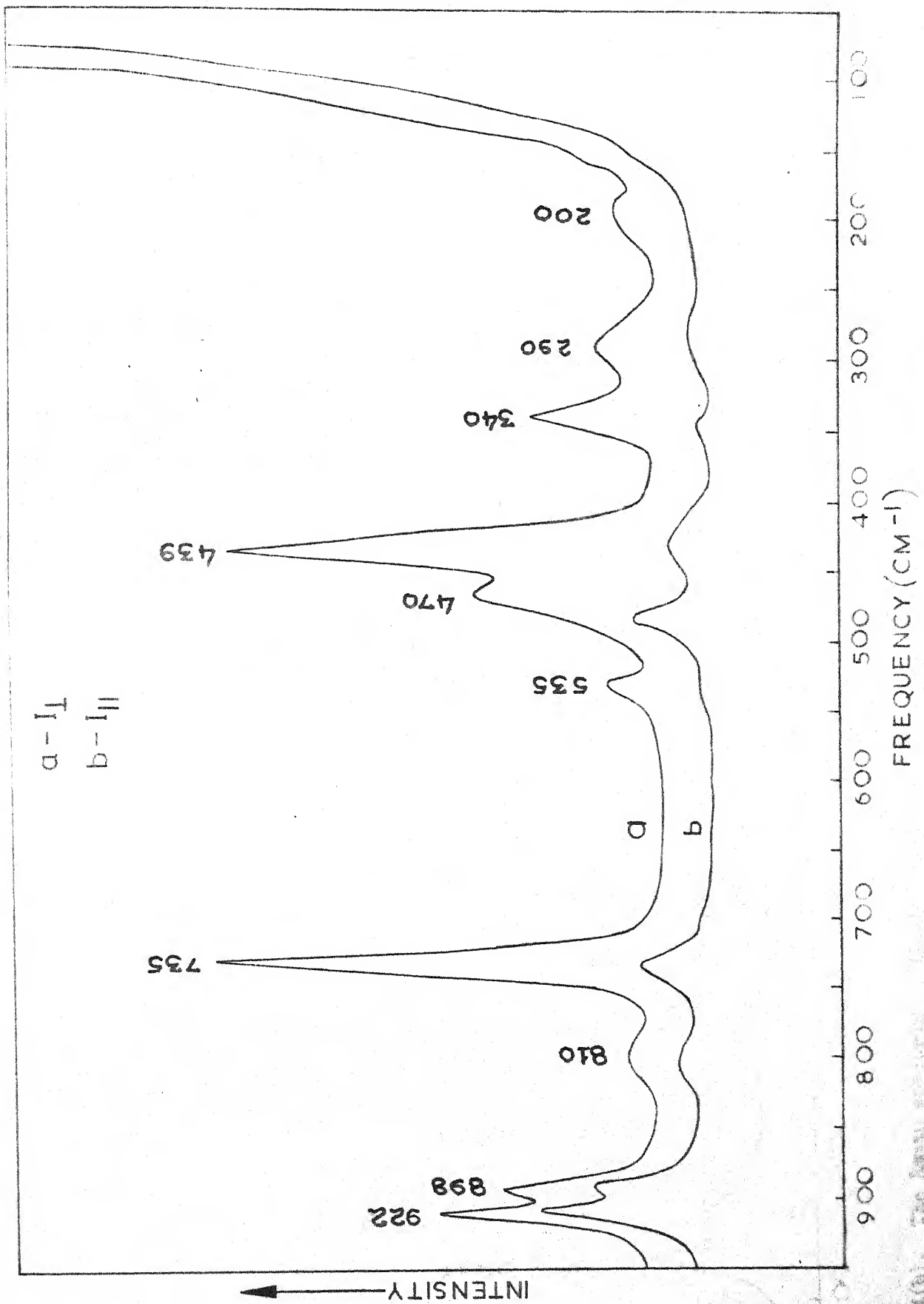


Fig. 6.4(a) The Raman spectrum of liquid triethylamine in the region 50-950 cm^{-1} .

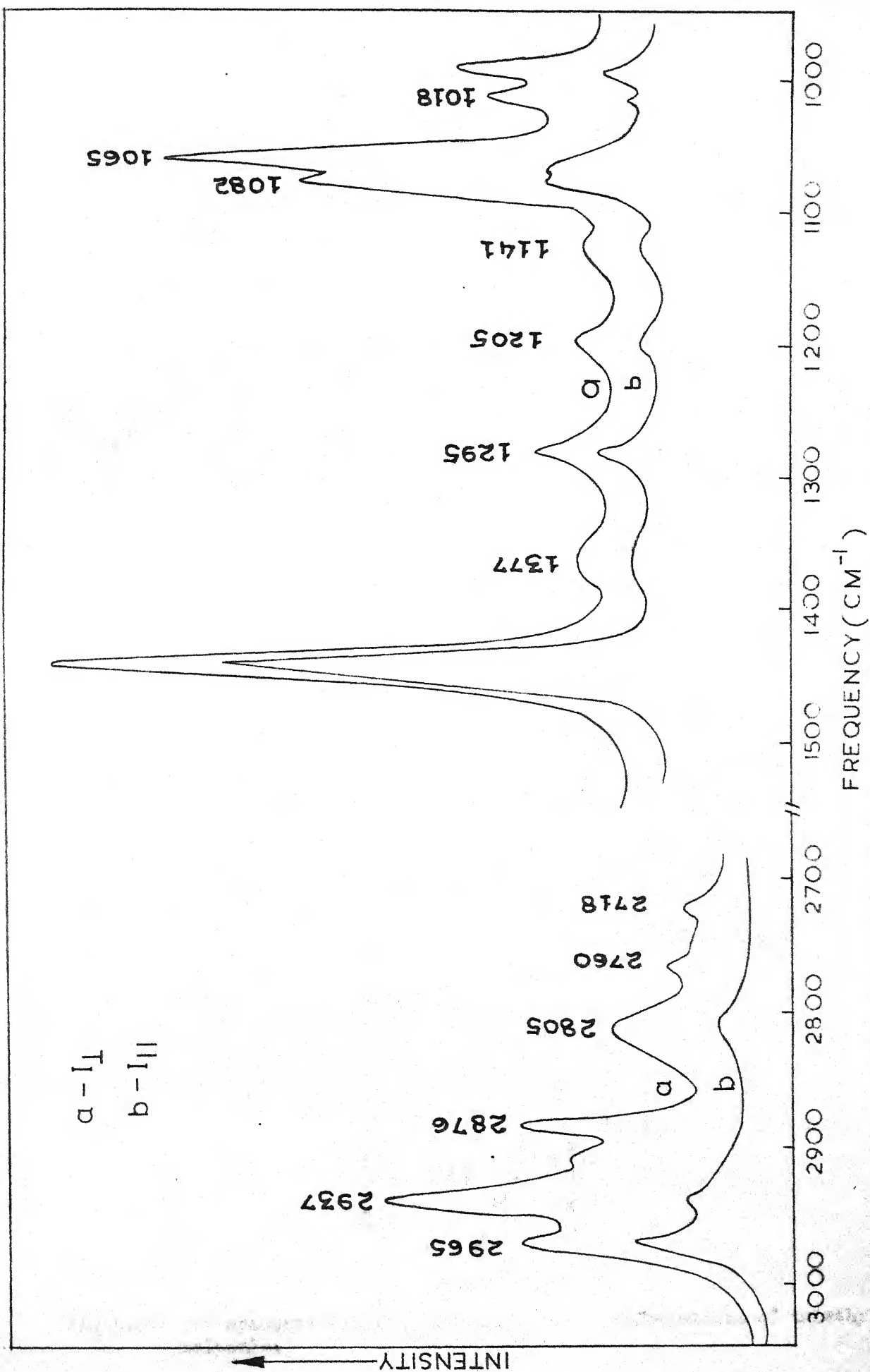
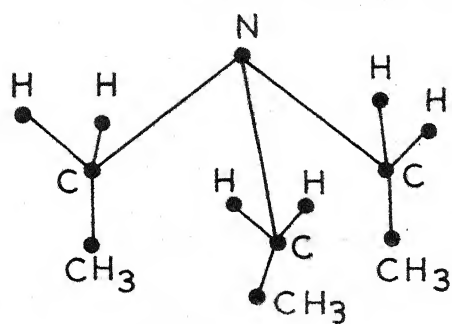
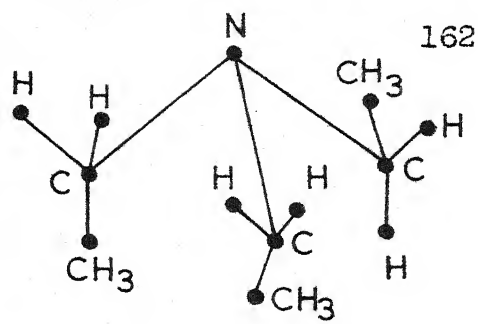


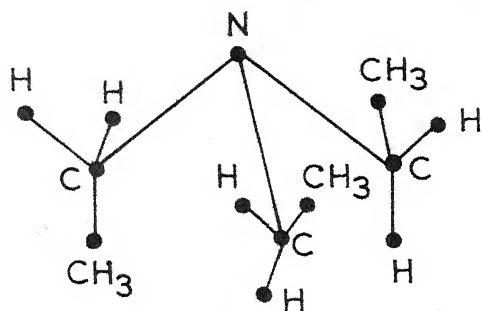
Fig. 6.4(b). The Raman spectrum of liquid triethylamine in the region 950 - 3050 cm^{-1} .



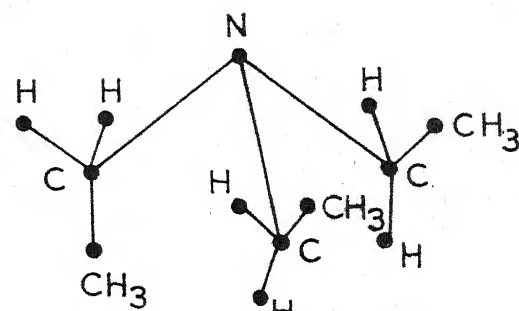
TTT (C_{3V})



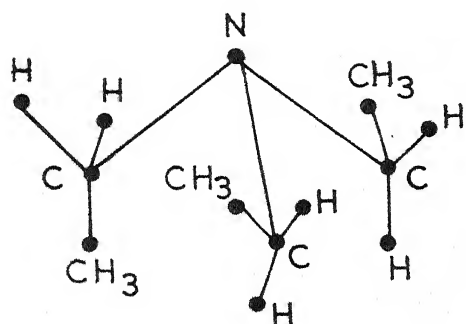
TTG (C_1)



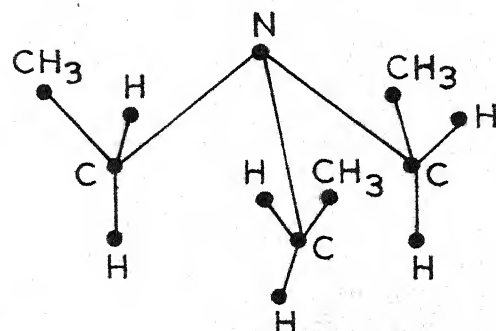
TGG (C_1)



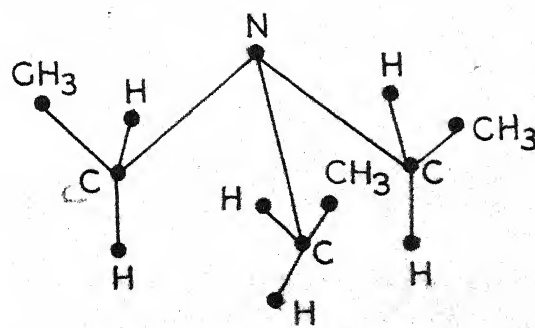
TGG' (C_5)



TGG' (C_5)



GGG (C_3)



GGG' (C_1)

Fig.6.5. The spectroscopically distinguishable conformations of triethylamine molecule.

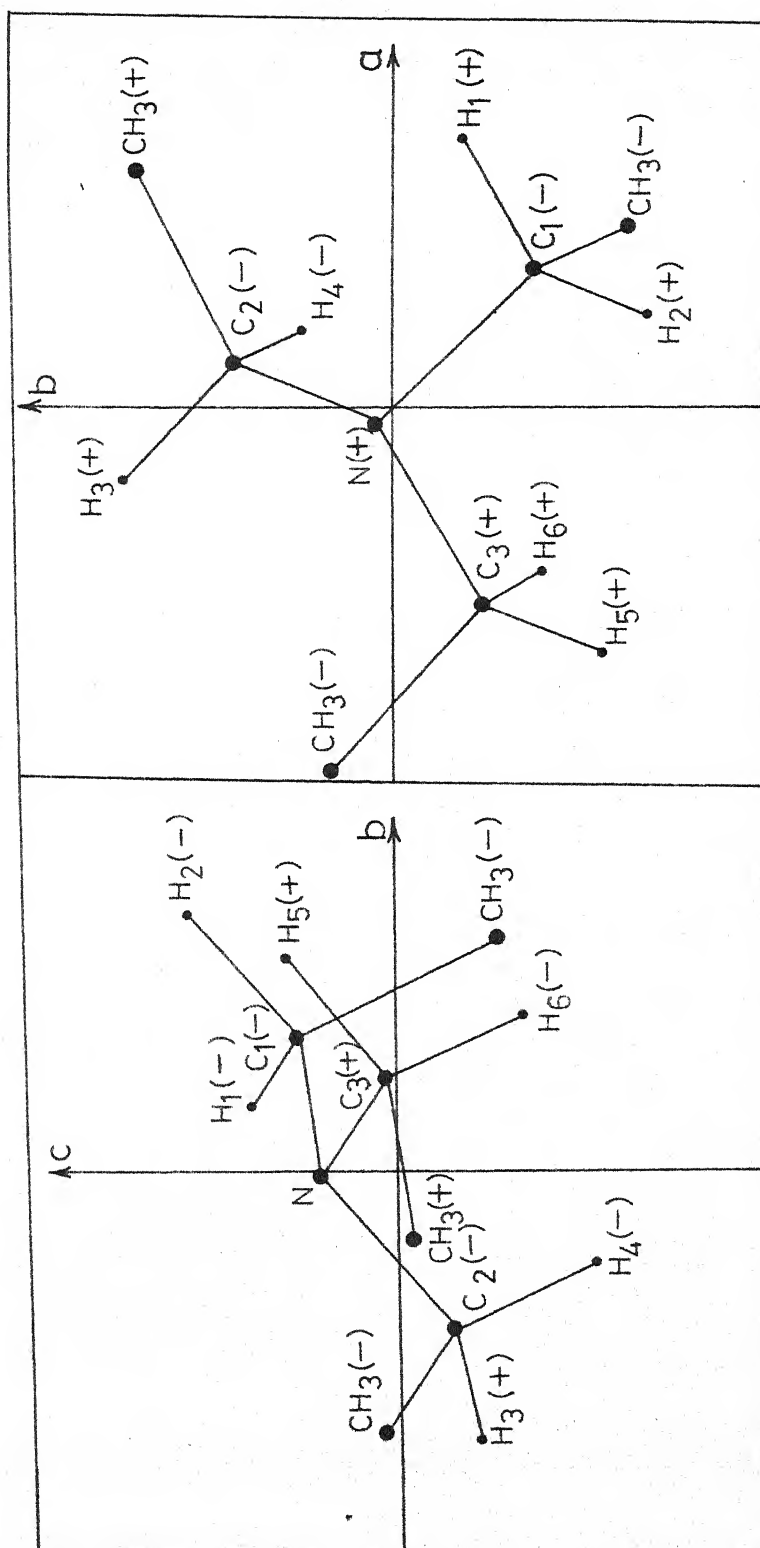


Fig. 6.6. The projections of TGG configuration of triethylamine on the ab and bc planes of the principal axes system (+ and - signs indicate the atoms above and below the plane of the paper respectively).

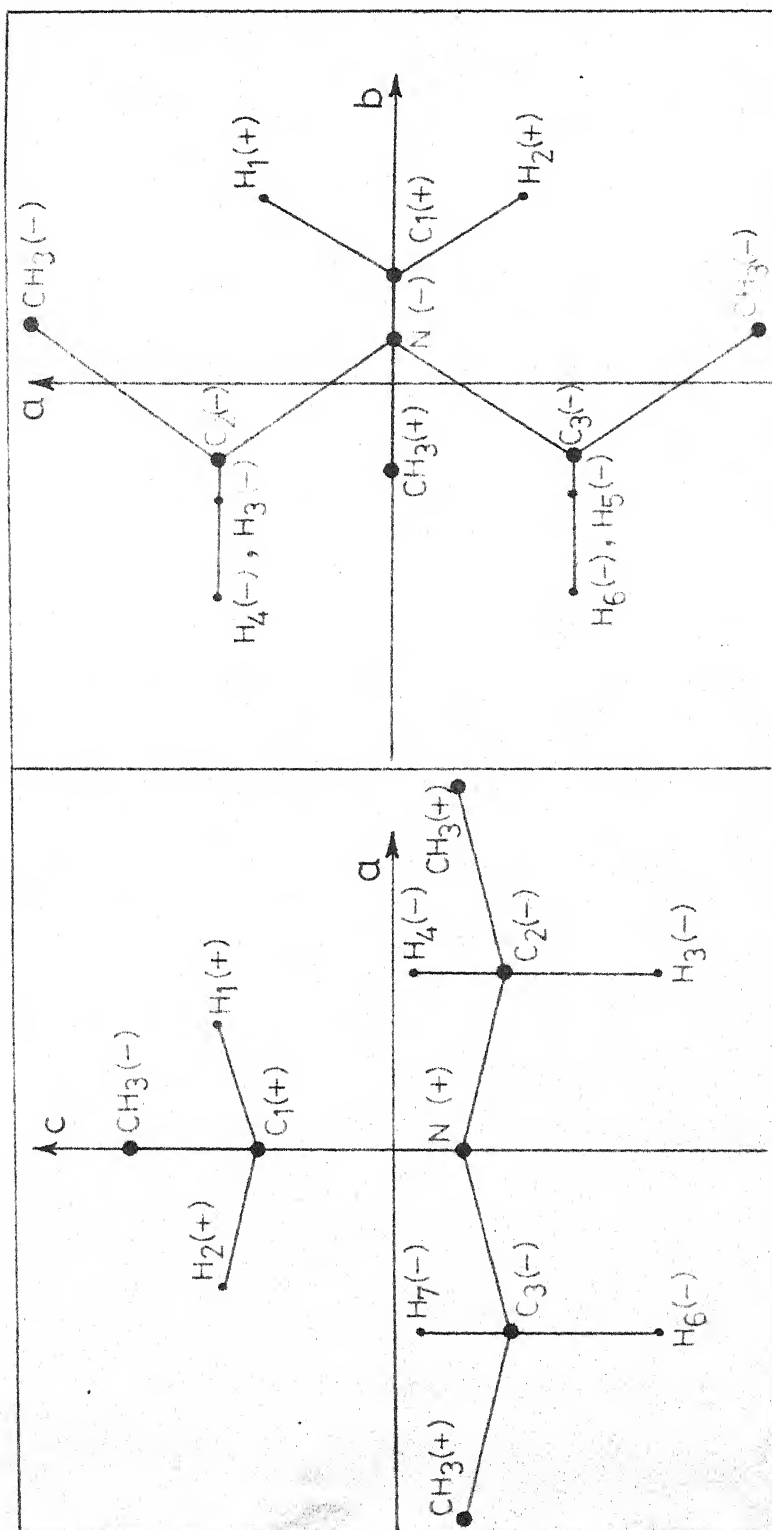


Fig. 6.7. The projections of TGG' configuration of triethylamine on ab and ac planes of the principal axes system (+ and - signs indicate the atoms above and below the plane of the paper respectively).

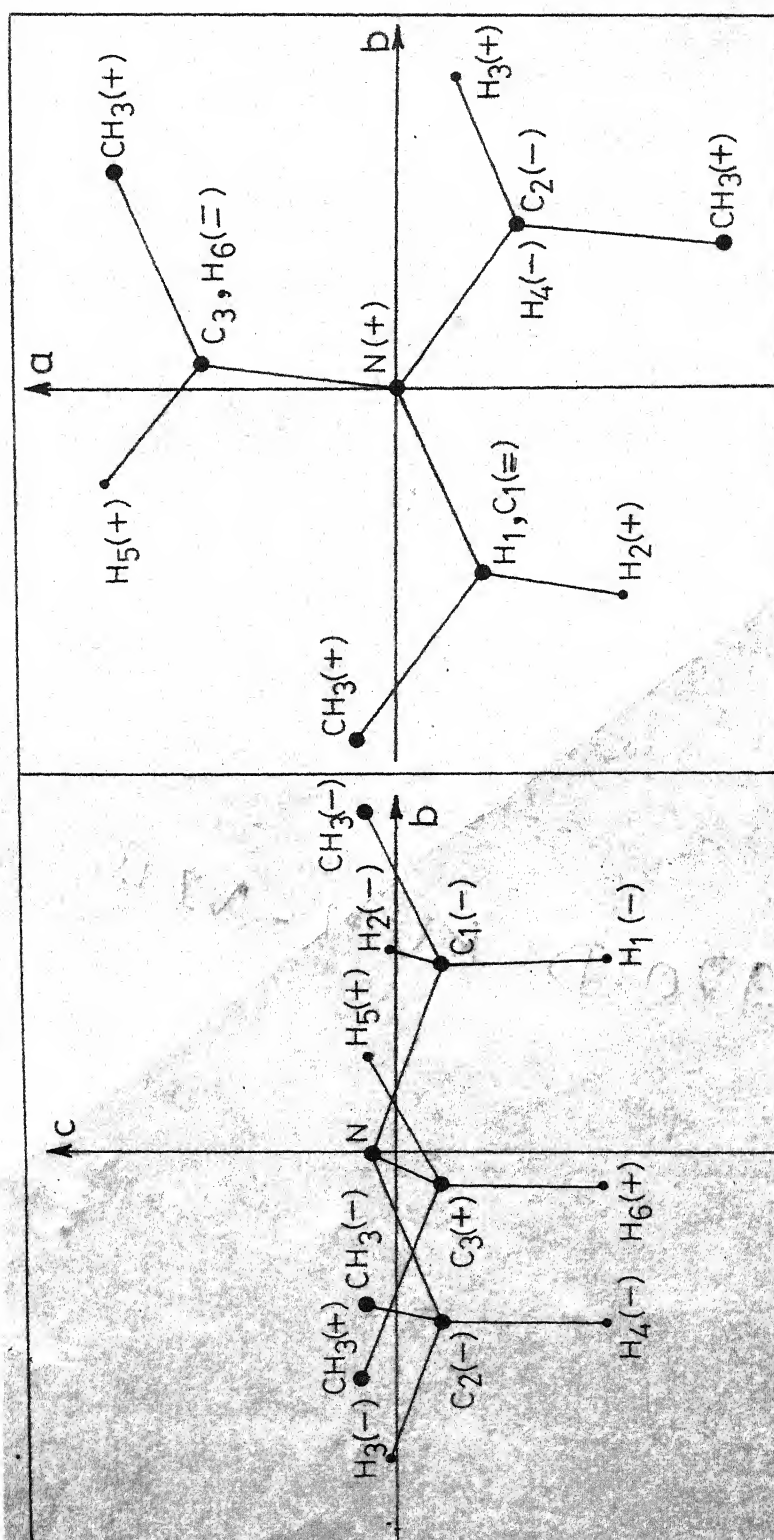


Fig. 6.8. The projections of GGG configuration of triethylamine on ab and bc planes of the principal axes system (+ and - signs indicate the atoms above and below the plane of the paper respectively).